Max-Planck-Institut für Meteorologie
Max Planck Institute for Meteorology

MAX-PLANCK-GESELLSCHAFT

Indirect Aerosol Effects Observed from Space

Olaf Krüger

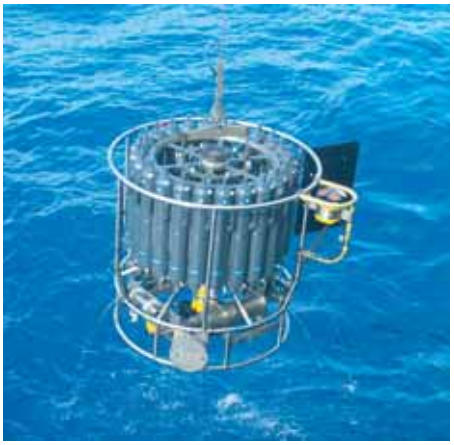

Berichte zur Erdsystemforschung 34/2006

Reports on Earth System Science

Hinweis

Die Berichte zur Erdsytemforschung werden vom Max-Planck-Institut für Meteorologie in Hamburg in unregelmäßiger Abfolge herausgegeben.

Sie enthalten wissenschaftliche und technische Beiträge, inklusive Dissertationen.

Die Beiträge geben nicht notwendigerweise die Auffassung des Instituts wieder.

Die "Berichte zur Erdsystemforschung" führen die vorherigen Reihen "Reports" und "Examensarbeiten" weiter.

Notice

The Reports on Earth System Science are published by the Max Planck Institute for Meteorology in Hamburg. They appear in irregular intervals.

They contain scientific and technical contributions, including Ph. D. theses.

The Reports do not necessarily reflect the opinion of the Institute.

The "Reports on Earth System Science" continue the former "Reports" and "Examensarbeiten" of the Max Planck Institute.

Anschrift / Address

Max-Planck-Institut für Meteorologie
Bundesstrasse 53
20146 Hamburg
Deutschland

Tel.: +49-(0)40-4 11 73-0
Fax: +49-(0)40-4 11 73-298
Web: www.mpimet.mpg.de

Layout:

Bettina Diallo, PR & Grafik

Titelfotos:
vorne:
Christian Klepp - Jochem Marotzke - Christian Klepp
hinten:
Clotilde Dubois - Christian Klepp - Katsumasa Tanaka

Berichte zur Erdsystemforschung 34/2006

Indirect Aerosol Effects Observed from Space

Habilitationsschrift
Universität Hamburg
Fachbereich Geowissenschaften

Olaf Krüger

Hamburg 2005

Reports on Earth System Science 34/2006

ISSN 1614-1199

Olaf Krüger
Max-Planck-Institut für Meteorologie
Bundesstrasse 53
20146 Hamburg
Germany

ISSN 1614-1199

Indirect Aerosol Effects Observed from Space

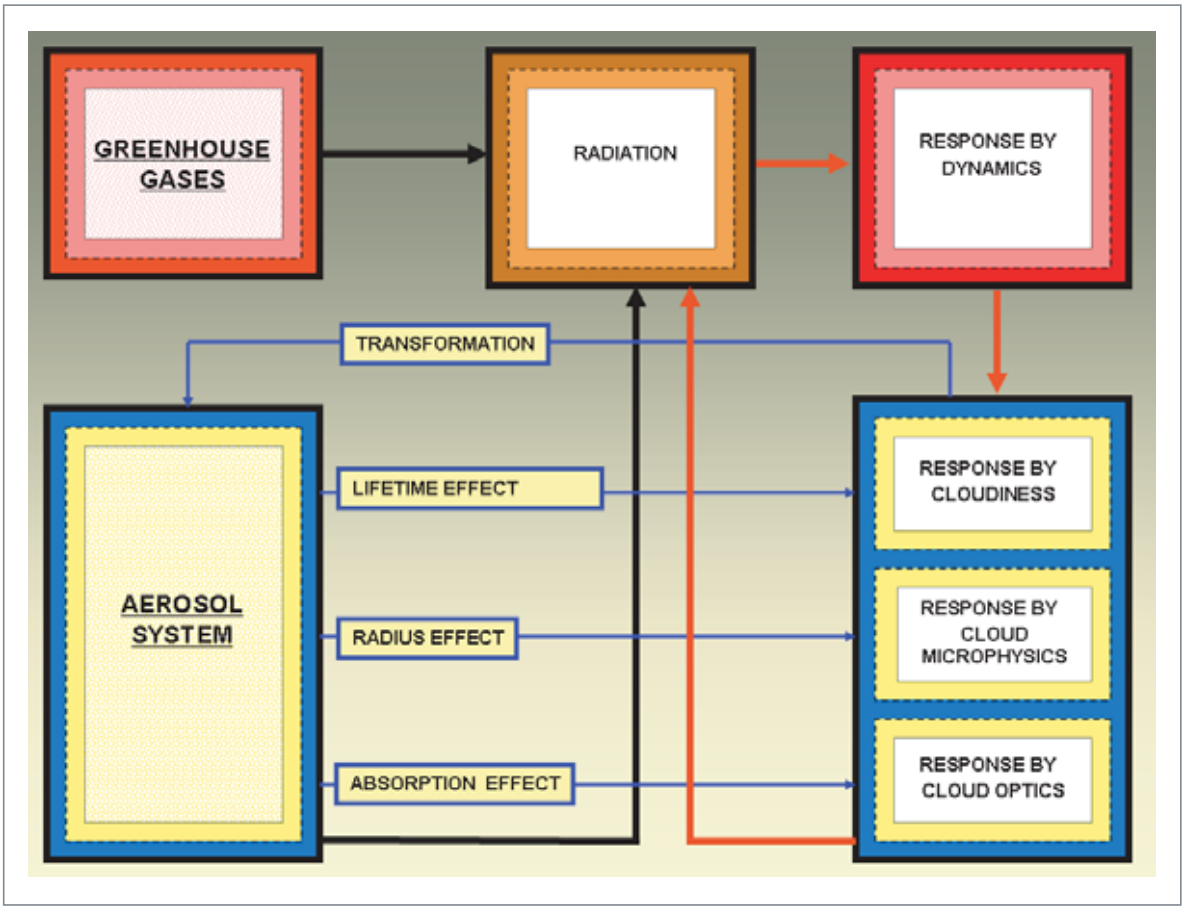

Olaf Krüger

Hamburg 2006

ABSTRACT

In order to assess the influence of anthropogenic emissions on cloud albedo over Europe a reprocessed set of satellite measurements from 1981 to 1999 was investigated. Special emphasis is given to the Central European main emission area, including the so-called 'Black Triangle', which covered parts of Germany, the Czech Republic and Poland. Due to the decrease of aerosol precursor gases the analysis reveals a pronounced decrease of cloud albedo of about 2% from the late 1980s to the late 1990s. During winter in source regions of anthropogenic particulate matter emissions the cloud reflectance is more than 5% lower referring in addition to an absorption effect caused by black carbon in clouds.

A second study over Europe is directed to investigate the variability of cloud reflectance. In the main European emission areas the high degree of air pollution generally enhanced variability of cloud reflectance during the 1980s. The variability was strongest for the early 1980s. A distinct influence of increased particle number density and increased black carbon content as well as secondary aerosol formation is detected. Towards the late 1990s, both the radius effect and the absorption effect, as the two components of the so-called first indirect aerosol effect, have declined due to the reduced particulate matter and sulphur dioxide emissions. The results indicate a pronounced influence of stability on the indirect aerosol effect over Central Europe. The analyzed frequency distributions of cloud reflectance show characteristics, which are in line with the theory of radiative transfer.

Another study is directed to evaluate the influence of pollution on the local planetary albedo over China. There, long-term observations show that absorbing aerosols have reduced the local planetary albedo from the late 1980s to the late 1990s. While the reduction of air pollution was leading to a local planetary albedo decrease in Europe, an increase of pollution in China also lowered the local planetary albedo. The strong absorption in clouds is accompanied by a cloud lifetime effect over the Red Basin and surrounding areas in southern China.

Further, first evidence is presented that an increase in aerosol particle number concentration lifts cloud top height. The analysis of satellite measurements over strongly polluted areas in China shows an indirect aerosol effect in the thermal infrared spectral range. The radiative forcing in the thermal infrared overrides the solar one.

PREFACE

The main purpose of the present manuscript is to demonstrate effects of air pollution on cloud albedo. In order to detect the influence of anthropogenic emissions on cloud optical properties from space long-term satellite measurements (1981-1999) over regions of strong air pollution have been evaluated.
This work is mainly based on the results and conclusions presented in the following papers, referred to by bold Roman figures in the text:

I. O. Krüger, H. Graßl (2002):
The Indirect Aerosol Effect over Europe.
GEOPHYSICAL RESEARCH LETTERS,
Vol. 29, No. 19, 1925, doi:10.1029/2001GL014081.

II. O. Krüger, H. Graßl (2004):
Albedo Reduction by Absorbing Aerosols over China.
GEOPHYSICAL RESEARCH LETTERS,
Vol. 31, L02108, doi:10.1029/2003GL019111.

III. O. Krüger, R. Marks, H. Graßl (2004):
Influence of Pollution on Cloud Reflectance.
JOURNAL OF GEOPHYSICAL RESEARCH,
VOL. 109, D24210, doi:10.1029/2004JD004625.

But it also contains hitherto unpublished material on indirect aerosol effects, e.g. the influence of pollution on brightness temperature:

IV. O. Krüger, A. Devasthale, H. Graßl (2005):
Pollution Lifts Clouds : A Further Indirect Aerosol Effect.

TABLE OF CONTENTS

1. INTRODUCTION

The anthropogenic release of chemicals into the atmosphere has already changed climate during the past century. A large part of the warming at the surface, which has been observed in the 20th century, can be attributed to changes in atmospheric composition [IPCC, 2001]. Observations show that the atmospheric concentrations of all long-lived natural greenhouse gases have increased from pre-industrial time (1750) until today (1998). Carbon dioxide (CO_2) increased by 85ppm to 365ppm, methane (CH_4) by 1045ppb to 0.75ppm, nitrous oxide (N_2O) by 44ppb to 0.312ppm. Also 268ppt chlorofluoro-carbon-11 ($CFCL_3$), 14ppt hydrofluoro-carbon-23 (CHF_3) and 40ppt perfluoro-methane (CF_4) have accumulated in recent decades [IPCC, 2001]. The change in concentration of the short-lived ozone (O_3), the third most important greenhouse gas, is more difficult to evaluate because of lack of global data during pre-industrial times and its high spatial variability. Estimates from numerical modelling indicate that since pre-industrial conditions the ozone concentration increased by about 9 dobson units in the troposphere [Hauglustaine et al., 1998]. Earth observation from space (Stratospheric Aerosol and Gas Experiment (SAGE) I/II and Total Ozone Mapping Spectrometer (TOMS)) and ozone-sonde profiles commonly confirm that in the lower stratosphere at high latitudes ozone concentrations decreased substantially due to ozone depletion especially in spring [Randel and Wu, 1999]. These satellite missions also revealed some important characteristics about the variability of stratospheric aerosol concentrations due to volcanic eruptions [Saxena et al., 1995].

In contrast to the rather good knowledge about greenhouse gas trends, the tropospheric aerosol particles and their resulting effects on climate are among the factors marked with very low level of scientific understanding as outlined by the Intergovernmental Panel on Climate Change [IPCC, 2001]. In particular information about regional trends in the tropospheric aerosol mass concentration or aerosol number concentration is widely missing. Moreover, the few measurement records being available do not allow a straightforward interpretation because of the very regional aerosol characteristics, which may change in a changing climate. Nevertheless, there are data from ice core analysis, which indicate changes in the aerosol system due to sulphur dioxide emissions in the Northern Hemisphere. Other than in the Southern Hemisphere the records from Greenland and the Alps show evidence for an increased sulphate concentration in air since 1900 [Döscher et al., 1995; Fischer et al., 1998]. Also the historical development of carbonaceous particle concentration could be re-constructed by the analysis of ice cores originating from a European high-alpine glacier [Lawanchy et al., 1999]. Here, the content of organic carbon in ice shows an increase by about 100µg to 300µg carbon per liter from the beginning of the 1900s to the 1980s. For elemental carbon the values are two to three times lower but show the same increase. In the Southern Hemisphere at the Cape Grim site the total number of particles increased by 0.7% per year from 1977 to 1991 [Gras, 1995].

Despite the high value of this information it must be noticed that the above data firstly are representing a local aerosol system. Since these measurements were taken in remote regions they are likely only applicable for estimating the hemispheric or global long-term trend. Because of the variability of regional source strengths and the various formation processes of aerosols these studies cannot be used to evaluate the regional trends of aerosol abundance. A larger data density is needed to achieve this.

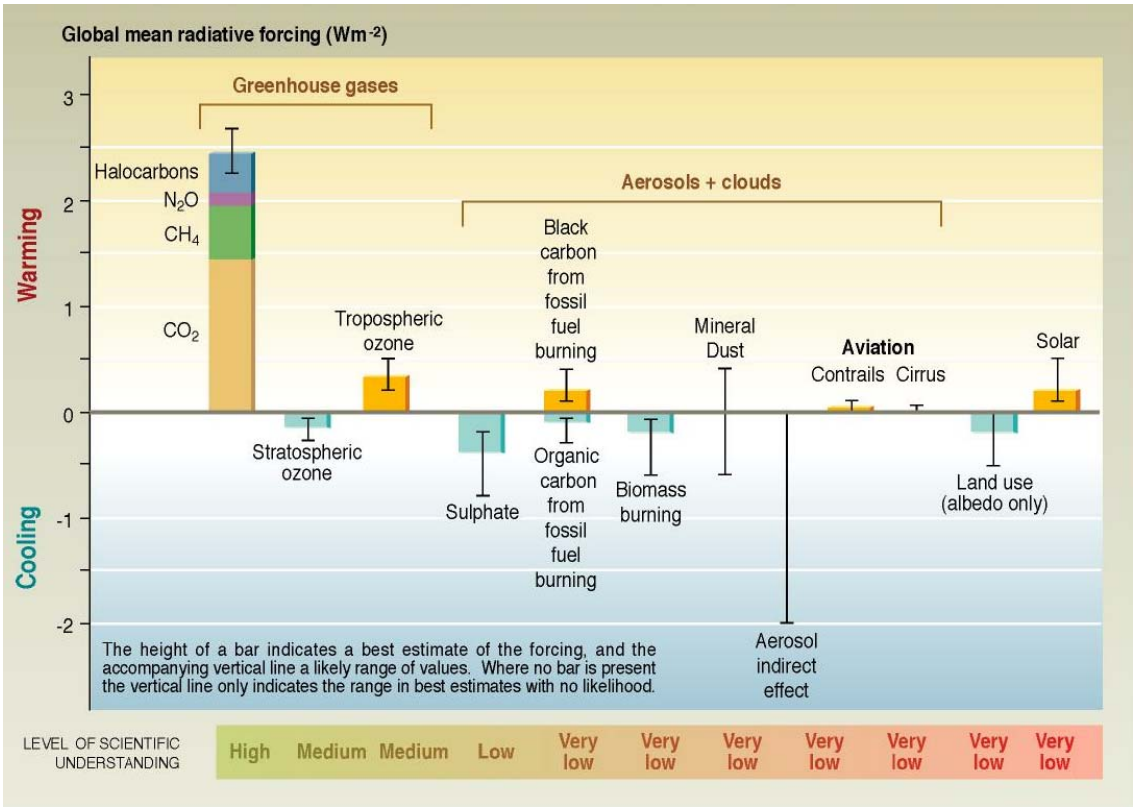

Figure 1. Anthropogenic and natural forcing of the climate for the year 2000, relative to 1750 [IPCC, 2001].

Different aerosol properties as well as surface albedo (land use), solar irradiance and aviation are very uncertain forcing agents. Aerosols are expected to have a very strong influence on climate [IPCC, 2001]. However, while the planet's additional greenhouse effect is increasing, which is well supported by the analysis of temperature and concentration records, a clear indication for climate change caused by aerosol abundance is missing. This might be mainly due to the heterogeneity of the source strengths, a short residence time and a multitude of chemical and physical processes by which aerosols are characterized. The strongest uncertainty arises from the impact of the variable aerosol particle number and aerosol composition on optical properties of clouds and on cloud cover. Theoretical investigations underline: The influence of aerosol particles on radiative fluxes in cloudless atmospheres is neither negligible in the solar nor in the terrestrial spectral region. Within clouds aerosol particles may contribute remarkably to heating rates in the solar part of the spectrum, while cloud albedo is a function of aerosol particle number and their chemical characteristics [Grassl, 1978]. Consequently, the cloud radiation field as modified by aerosol changes is an important and widely open issue, which needs to be addressed in estimates of the earth radiation budget.

In order to account for perturbations of climate, which are driven by an imbalance between incoming and outgoing energy in the earth/atmosphere system, the concept of radiative forcing is commonly used (see figure 1). The concept approximates the forcing of the slowly adjusting surface troposphere system by using the net irradiance change at the tropopause, due to a changed atmospheric composition or solar irradiance. The radiative forcing can also be computed for aerosols in numerical models after allowing stratospheric temperatures to readjust to radiative equilibrium. However, the real

behaviour of the atmosphere will be different as this concept fixes tropospheric properties at their unperturbed values.

Contrary to the well-known positive radiative forcing caused by increased concentrations of long-lived greenhouse gases, anthropogenic aerosols can have very different consequences for the radiation budget. They either can warm or cool the earth/ atmosphere system. Thereby the sign of the direct aerosol forcing for cloudless atmospheres is determined both by back-scattering and absorption, which may vary considerably in the vertical. Also the reflectance of the under-lying surface plays an important role. If the surface is non-Lambertian the bidirectional reflectance distribution function (BRDF) has to be considered [Kriebel, 1977]. The apparent reflectance, i.e. the reflectance of a natural surface modified by the Rayleigh scattering and aerosol layer(s) above, varies with optical thickness and type of the aerosol. The wavelength dependent aerosol influence ranges from an increase for low reflectance to a decrease in case of a strong absorbing component. Higher absorption is characteristic for urban aerosols usually containing clearly more black carbon (BC) than continental aerosols. A lowering of reflectance, resulting in a warming effect at the surface can preferably occur for a strongly absorbing component in the aerosol above a highly reflecting surface like white sand, snow or ice [Krüger and Fischer, 1994].

Once deposited on the surface absorbing aerosols can also alter the surface reflectance. The analysis of BC in snow water shows mean values of 30ppb (parts per billion by mass; equivalent to ng/g or μg per liter meltwater) in fresh, non-fresh, firn and windblown snow even in the Arctic indicating the relevance for global warming [Noone and Clarke, 1988]. The values at rural sites e.g. in Lithuania often exceed 100ppb with peak values of 150ppb during the cold season [Amalis, 1999]. Therefore an additional forcing mechanism so far not included in the IPCC forcing diagram (see figure 1) needs to be considered: It is the reduction of snow and ice albedo due to the dry or wet deposition of carbonaceous particles. Since data collected in arctic regions demonstrated a long-range transport of aerosol of anthropogenic origin the issue needs to be emphasized in global climate change studies. It has been pointed out that the reductions in Arctic snow albedo are leading to absorption of shortwave radiation being 5–10 % higher than that of soot-free snow [Clarke and Noone, 1985].

Based on atmospheric general circulation model (AGCM) results estimates of radiative forcing by aerosols can be found in the latest report of the IPCC (see figure 1). It is obvious that especially for the effects of aerosols on clouds there are large discrepancies in the results pointing to the need of further improved models. The Third Full Assessment Report (TAR) of the IPCC indicated that the mean global radiative forcing caused by the direct aerosol effect for pure aerosol components amounts to about –0.4 W/m^2 for sulphate, –0.1W/m^2 for fossil fuel organic carbon and +0.2W/m^2 for fossil fuel black carbon aerosols. For aerosols originating from biomass burning a value of –0.2W/m^2 is given. The indirect aerosol forcing marked with the lowest level of scientific understanding is estimated to be negative, reaching in the global mean up to –2W/m^2 [IPCC, 2001]. Here, the major present deficiency in knowledge is, however, not just the accuracy of any global mean value. The more general question is if the global radiative forcing is an adequate metric at all to describe potential effects of aerosol particle abundance.

In order to approach this question two issues need to be addressed more specifically in future assessments:

1. ***The characterization of forcing in regions experiencing distinct aerosol influence is missing. The spatial variability of indirect aerosol forcing on a regional scale needs an assessment using measurements.***

2. ***A detailed description of the changes caused by aerosol and cloud interactions is missing. The magnitude of the contribution of absorption is widely unknown and needs further investigations using measurements.***

The Third Assessment Report (TAR) made it clear: The radiative forcing mechanisms by aerosols via the water cycle even on the global scale are far from being well understood. An increasing number of modelling studies [Jones and Slingo, 1996; Hansen et al., 1997, Rotstayn, 1999; Lohmann et al., 2000, Kristjansson, 2002] substantiated that the magnitude of the calculated indirect forcing varies considerably. The reason is that changes in cloud optics, microphysics and cloudiness induced by aerosols are too complex and occur on scales far too small to be explicitly resolved in large-scale climate models. Since the magnitudes of the processes involved are not yet known sufficiently from measurements, simplified parameterizations must fail and AGCM results on aerosol influence will remain highly uncertain.

A prominent example for model uncertainty is the change in the Top of the Atmosphere (TOA) cloud radiative forcing (CFR) associated with a CO_2 doubling. Le Treut and McAvaney (2000) compared 10 models' results (Meteorological Research Institute (MIR, Japan), Laboratoire de Meteorologie Dynamique (LMD, France), Centre for Climate System Research (CCSR, Japan), Geophysical Fluid Dynamics Laboratory (GFDL), Hadley Centre (HC, UK), Max Planck Institute for Meteorology (MPI-M, Germany), the Commonwealth Scientific and Industrial Research Organization (CSIRO, Australia), the National Centre for Atmospheric Research (NCAR, USA) and the Bureau of Meteorology Research Centre (BMRC, Australia)). The models above, all coupled to a mixed layer ocean for simulations of equilibrium climate, delivered distinct results in the net cloud radiative forcing ranging from $-1 W/m^2$ to $+3 W/m^2$. The differences indicate that model output is highly sensitive to the water vapour-radiation feedback. If separated into short wave and long wave forcing the range grew to $-2 W/m^2$ to $+3 W/m^2$ and $-3 W/m^2$ to $+2 W/m^2$ respectively. The finding confirms that an extension of current knowledge on the water cycle is necessary, which gives a clear hint to global monitoring [Raschke et al., 1973]. The TAR already stated that a straightforward approach of model validation is not sufficient to constrain the models efficiently and more dedicated approaches have to be developed pointing to data from global observation systems, namely through the use of satellite data. However, it must be noticed here again feedback mechanisms in the climate system complicate the interpretation of measurements especially for long-term data records.

The indirect aerosol effect manifests itself as a cloud radiation feedback, which in turn interacts with the water vapour/radiation feedback. Basically these two feedback mechanisms in the earth/atmosphere system must be taken into account jointly for an assessment of physical and chemical processes induced by aerosols. From the dynamical point of view a complication arises for the evaluation of aerosol influences from the broad spectrum of scales in time and space involved. Already on the micro scale a variety of transformation processes continuously leads to changes within the aerosol system. Numerous chemical and physical processes are acting on characteristic time scales between seconds and hours. They include aerosol formation from the gas

phase as well as heterogeneous nucleation including growth by condensation and coagulation. Besides, the particle sinks dry and wet depositions have a pronounced influence on the aerosol system. In order to describe such a balance also the emission and transformation of aerosol precursor gases including their stability dependent deposition processes, highly variable within season and from season to season [Krüger and Tuovinen, 1997], must be taken into account. Further, chemical processes in aqueous phase also contribute to aerosol formation. The importance of clouds for the meso-scale aerosol system is exemplarily shown by the cloud-mediated production of cloud condensation nuclei [Saxena, 1996]. The latter process indicates the dominant role of clouds for aerosol transformation and finally confirms that major cloud influences on the aerosol system are by far not just limited to below cloud and in cloud scavenging.

On the other hand the aerosol system itself can affect motions, which in turn determine the transport of pollutants. A first example for an aerosol influence on the dynamics is the occasionally enhanced heating rate by aerosols within the atmospheric boundary layer. While an increased scattering process induced by aerosols mainly redistributes energy and modifies the local planetary albedo, an additional heating rate can be established through absorption. Within the shortwave spectral range it varies stronger with the complex index of refraction than with size distribution and can reach 2K per day for an optical thickness of 0.3 at 0.55um wavelength dependent on the sun zenith angle [Grassl, 1974b]. But also a cooling rate by aerosols in the long wave spectral range, which is mainly due to the radiative transfer in the 8-13μm wavelength window region, must be taken into account. These estimates are lower as compared to the absorption of solar radiation and can reach about 0.5K per day. Higher values can occur in all layers at high relative humidity when most aerosol particles grow by condensation of water vapour [Grassl, 1974a].

Increased aerosol absorption also can strengthen baroclinicity through stronger horizontal temperature gradients. In the case of continuously high aerosol optical thickness an influence on atmospheric circulation over time scales of weeks or months, e.g. expressed by shifted pressure systems via this process is conceivable. An example is given here with the emission of Saharan dust aerosol, which is accompanied by a pronounced long-range transport over the northern tropical Atlantic. The dust aerosol can reduce the insolation at the ocean surface, thereby reducing the heating of the ocean surface waters and hence surface temperatures [Prospero and Lamb, 2003]. This also influences the air-sea interaction, namely the transfer of water vapour and latent heat, which has a major influence on the intensity of Atlantic hurricanes [Landsea and Gray, 1992].

The discussion about an aerosol influence on the position of pressure systems already started during the 1970s based on the early work by Korff and Flohn [1969]. Originally Korff and Flohn [1969] investigated the relation between the latitude of the subtropical anticyclone belt and the equator to pole temperature difference. They found that for higher temperature differences the anticyclone is shifted southwards and that an increase in the temperature gradient between equator and high latitudes from 293K to 308K shifts position from 40 to 32 degree latitude. It has been argued that the shift southward being roughly linear by about 0.5 degree latitude for an increase in the gradient by 1K affects the baroclinic stability and consequently the meridional extent of the tropical Hadley Cell. Later Charlson [1979] suggested that desert dust aerosol originating from the Sahara could change the temperature gradient by enhanced heating rates which amount to 1K per day and might explain the persistence of droughts in the

Sahel by moving the ITCZ southward. However, the task to receive evidence for such an aerosol influence on precipitation is a complicated one because the high albedo in desert regions contributes to a net radiative loss relative to its surroundings, which induces circulation. The resulting sinking motion [Charney, 1975a,b] and in addition changes in evapotranspiration, which was later recognized by Charney et al. [1976] both also contribute to rainfall decrease.

An anthropogenic aerosol component, which can lead to a significant change in dynamics by sensible heating are the carbon black particles. These particles, commonly called black carbon (BC) or soot, consisting of more than 95% pure carbon, have a high absorption coefficient and a low heat capacity [Gray et al., 1973]. In contrast to the basic tropospheric aerosol components, water insoluble, soluble continental and sea-spray particles, the absorption in the visible spectral range by BC particles is much stronger. The complex index of refraction, which determines the absorption coefficient, can be by orders of magnitude higher for black carbon aerosols dependent on wavelength [WCP-55, 1983].

Once black carbon is emitted into the atmosphere it will tend to change the temperature profile by absorption of solar radiation. In the cloud free case a direct influence on stability would occur. If the heating occurs strong enough, the vertical motions would be altered. This can lead to quite different consequences for the state of the atmosphere above and below the perturbed layer. While the part below will undoubtedly be stabilized, the atmospheric layers above can become unstable. Hence it can be hypothesized that this process could favour quite different results depending on surface temperature, atmospheric stability as well as strength and height of the heating layer.

Two extreme cases of atmospheric response on this perturbation are suggested here. In the first case over a warm land surface heating of the boundary layer by aerosol particles would result in a reduction of the land-air virtual temperature difference. In this case the heating through absorption can lead to reduced convection.

In the second case cloud formation could be stimulated by a destabilization of the atmosphere. The maritime boundary layer, when the ocean is colder than the atmosphere, gives such a precondition. If in these cases the black carbon concentration becomes sufficiently high close to the surface a destabilization will result and then vertical motions strong enough for cloud formation are likely induced. Evidence for the latter effect arises from early model estimates, which basically confirm a pronounced tendency that the heating will lead to cloud formation [see Orville, 1965; Gray, et al., 1976]. In the study described by Gray et al. [1976] a boundary layer model was used to investigate the influence of artificial heating in a tropical cloud layer over the ocean. Here a rather moderate hourly heating by 0.25K was applied for 10 hours. The calculations show clear effects on mixed layer, potential temperature profile and relative humidity, which finally cause the convective cloud-level base to rise and cloudiness to increase. Also Lopez [1973] confirmed, that an increase of the boundary layer temperature by 1-2K as well as a small increase in boundary layer specific humidity can have a significant influence on the intensity and depth of cumulus convection. But among the possible effects induced by extra heating through aerosol absorption could be as well other quite different atmospheric responses. Examples are rainfall enhancement or cirrus cloud generation, which consequently would reduce the tropospheric energy loss. Even a reduction in inner-core circulation of hurricanes through heating by aerosols is possible [Gray et al., 1976]. The influence through black carbon seeding was theoretically investigated using a symmetric primitive equation model of tropical cyclones [Rosenthal, 1971]. It was concluded that a reduction of the hurricane's

intensity would occur. In the case of an extremely high black carbon concentration kinetic energy at the radius of maximum winds within the hurricane drop to 60% of its original value. It is clear that any change in energy will change the cyclone trajectory.

Another potential for an aerosol influence on the dynamics arises from the limited number of condensation nuclei (CCN) over the oceans. Here the typical values of CCN range from about 30 to 200cm^{-3} [Pruppacher and Klett, 1978], which is several times lower than over the continents. In maritime regions an increased cloud formation easily can take place through increasing the number of CCN. Depending on supersaturation and state of the atmospheric boundary layer this would alter the cloud liquid water content and increase the release of latent heat. Increased latent heat in turn could enhance the energy and life cycle of extratropical cyclones. It can be assumed that, if the diabatic heating is strong enough, low pressure systems with modified kinetic energy could finally alter mesoscale pressure patterns; which would also modify the transport and deposition of aerosols over the oceans considerably.

An increased number of aerosol particles also can have an influence on precipitation because of the suppression of coalescence [Rosenfeld, 2000]. This process could have enormous consequences for the general circulation because of the possibility to alter the release of latent heat and therefore change its vertical and horizontal transport. Especially for convective precipitation a high potential for dynamical changes with possibly global impact may arise. In the tropics where biomass burning is a major aerosol source and where convective precipitation is predominant strong changes can be expected through an aerosol influence on convective heating. However, this effect must not necessarily mean less convective precipitation in all cases. The reduction of rain initialization enhances cloud liquid water content in the lower troposphere which on principle can lead to shifted precipitation belts or to increased precipitation amounts originating from higher altitudes depending on convective mass flux. First global modelling attempts including the change in so-called warm precipitation formation also suggest that an amplification of the Walker circulation by this type of aerosol perturbation is possible [Nober et al, 2003].

The examples above demonstrate a broad spectrum of atmospheric processes linking the aerosol system, clouds and dynamics. On the other hand they elucidate that the majority of the influences by aerosols on climate are accompanied by changed cloud microphysics and cloud optical properties including cloud cover, the latter being the most important factor governing the radiation regime of the earth. After all, it can be stated that the aerosol influence on climate includes many characteristics, which considerably complicate the detection:

1. ***Aerosols affect climate indirectly on different scales. The indirect aerosol effect(s) can appear simultaneously on different scales, occasionally even interacting among each other.***

2. ***The initialization of indirect aerosol effect(s) in many cases starts in the cloudless atmosphere. The magnitude of indirect aerosol effects can change rapidly and show a strong time dependence, e.g. during the formation process of clouds.***

Both issues have direct implications for the successful detection of indirect aerosol effects. Any strategy for deriving indirect aerosol effects from measurements therefore should rely on it. Otherwise important information might be omitted. It is also reasonable firstly to investigate the aerosol influence for different scales separately. The appropriate distinction into three major groups is made with the cloud scale, the

regional scale and the global scale. On each scale characteristic atmospheric perturbations become dominant dependent on solar irradiance and on location in the earth/atmosphere system. Generally the following changes are expected being characteristic for the scale:

On the cloud scale the interaction of cloud and aerosol processes determine the initial concentration and size of the droplets. The aerosol cloud interaction is perturbed in many regions by an increasing amount of anthropogenic aerosol particles. The major influence is due to changed cloud albedo, cloud lifetime and precipitation amount.

On the regional scale pronounced indirect aerosol effects are expected to occur in areas of strong anthropogenic release of particles, i.e. the so-called polluted regions of the continents. This may modulate the additional greenhouse effect considerably. The aerosol influence on clouds could dominate other perturbations dampening or amplifying the cloud-radiation feedback, which reduces the relative importance of any other forcing agent on this scale considerably. In case of the more heterogeneous aerosol perturbation the regional radiation regime in an initial environment will react by a more variable radiation budget in contrast to the much more homogeneous warming by long-lived greenhouse gases. This heterogeneity of the aerosol effects is also due to the pronounced dry and wet deposition processes in the atmospheric boundary layer. The general influence of aerosols may be recognized in data records for albedo, solar irradiance, temperature, precipitation and cloudiness.

On the large or global scale, for example over the oceans of the northern hemisphere, indirect aerosol effects could be connected to enhanced cloudiness. Firstly, this will change the Earth's radiation budget. Further, as mentioned above, it also could modify the transport or redistribution of latent heat through the general circulation. The major influence of aerosols on the global scale therefore might be responsible for altering the zonal energy balance by a shift of the dominance of water vapour evaporation cooling the surface and precipitation heating the atmosphere.

However, any assessment of such a global climate change needs the knowledge about the seasonal or annual fluctuations of regional circulation, which drive and is driven as well by the aerosol system. It must be expected that a strong regional abundance of anthropogenic aerosols will mask the seasonal fluctuations and inferred conclusions considerably. For example albedo changes over the continents could alter the monsoon circulation by means of changed response of the hydrological cycle on the radiation regime.

The overall most important effect of aerosols however might be a change of the global planetary albedo leading to a long lasting perturbation of climate. In his work 'Pollution and the Planetary Albedo (1974)' Twomey mentioned:

The eminent Russian climatologist Budyko (1969) suggested that a reduction of perhaps as little as 2 per cent in solar radiation falling on this planet could cause an irreversible "flip" from our present apparently stable and more pleasant climate to another stable but not so pleasant state in which the earth, much whiter and colder, would be in the grip of another ice age. It would seem that an increase in the planetary albedo if not accompanied by some compensating effect, would be equally harmful.
Attention has lately been directed to the effect of pollution on a global scale on the energy balance of the earth, but most of this attention has been confined to effects outside clouds where particles reflect and absorb radiation and thereby modify the planetary albedo. The purpose of this paper is to point out that a direct connection exists between pollution and the number of drops in a cloud and hence an influence on

the optical thickness and the reflectance of the clouds (cloud albedo). There have been suggestions that pollution can lead to "dirty" clouds with lower albedo, but the volume of water cycled through the atmosphere is so much greater than of any pollutant that it is difficult to see how such effects could be significant unless there were magnifying influence by which (say) a particle absorbed very much more efficiently when immersed in a cloud drop.

The manifold radiative, microphysical and dynamical perturbations, induced by anthropogenic aerosols in the climate system, can be demonstrated with two major pathways of action. A flow chart diagram (see figure 2), where both the dynamics and the water cycle are involved, illustrates the impacts of the aerosol system within the cloud radiation feedback schematically. The influence of aerosols via the cloudless atmospheres is partly indirect because the change in the radiation fluxes can finally change cloudiness. In both cloud-free and cloudy cases the responding meteorological variables temperature, winds, density and specific humidity indicate the response of the dynamics. The changes might be expressed as a shift of the position of high-pressure systems or modified trajectories of low-pressure systems. Other changes might be seen through an induction or strengthening or weakening of thermal circulations accompanied with an effect on cloud formation through a modified stability of the boundary layer. The response of clouds on changes in the dynamics mainly is expressed in reduced or enhanced cloudiness or altered geometric thickness of clouds. Both influences in turn would have consequences for the radiation budget. The resulting net change always is determined by both the change in albedo and outgoing long wave radiation. An increase in cloudiness would cause an increase in albedo and a decrease in outgoing long-wave radiation, because of clouds´ opaqueness to the long-wave radiation. The latter is due to both an increase of the horizontal extent of the cloud coverage as well as an increase in the effective height of the cloud top, which reduces the upward flux of the long wave radiation being lost by the earth/atmosphere system.

From the flow chart diagram (figure 2) it becomes also clear that it is unfavourable to call the influence of anthropogenic aerosols on cloud albedo an indirect aerosol effect. Rather the so-called direct aerosol effect in the cloudless atmosphere is in parts an indirect effect on climate, since it can change cloudiness through thermal stability change. Thus the notation above only makes sense as long as one considers the subdivision of aerosol effects into cloudy and cloudless atmospheres and neglects the influence of aerosols on circulation. However, if any perturbation in circulation induced by aerosols causes a change in cloudiness then just this would be rather the indirect than the direct influence of aerosol particles on cloud optical properties. The latter definition 'direct' was already used in early studies in context with the cloud-radiation feedback mechanism. There a direct effect of aerosols on clouds and an indirect via a changed radiation budget or humidity budget caused by a higher CO_2 level was discussed [see e.g. Schneider, 1972]. Here, in this work the notation follows the definition by the TAR where the majority of aerosol effects on cloud properties are called indirect.

The most serious complication for the detection of aerosol effects on cloudiness and cloud microphysics is given by the fact that global warming and consequently atmospheric circulation always has an influence on clouds. On any scale one must expect both effects being involved, which just means that the quantification of the indirect aerosol effects is hampered by long-term changes in atmospheric water path and in cloudiness caused by greenhouse gases.

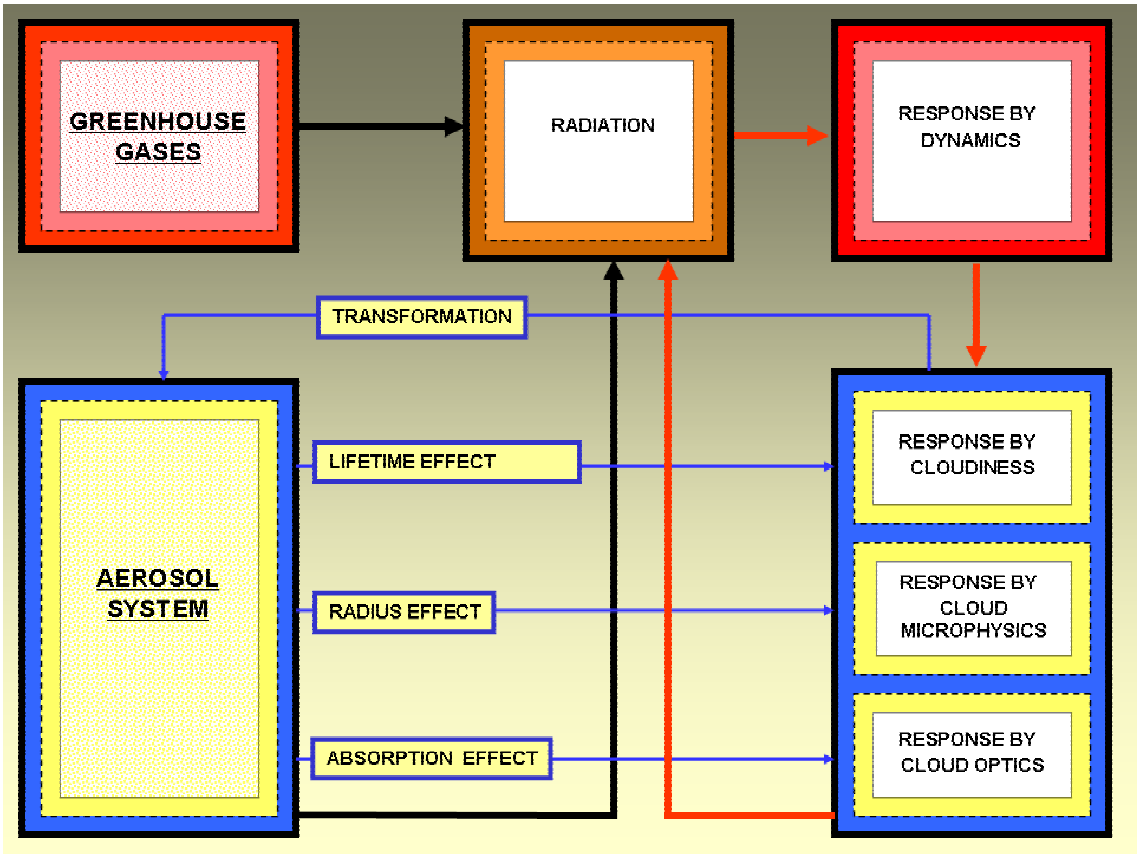

Figure 2. Flow chart illustrating the role of aerosols and clouds as a climate feedback on the local (dotted), regional (dashed) and global scales (solid). The earlier scheme suggested by Stephen Schneider (1972) is extended for indirect aerosol effect(s). Also contained are the effects of increased lifetime, decreased droplet size and increased absorption of clouds due to anthropogenic aerosol particles. The transformation includes the source and sink processes after emission, such as condensation nuclei production by clouds, as well as particle deposition through rainout, i.e. in-cloud and below cloud scavenging. It is important to note that all indirect aerosol effects on cloud radius, absorption and lifetime, can lead at the same time to a response of cloud microphysics, cloud optics as well as cloudiness (see also table 1).

This seems to be an insurmountable barrier already for the detection. However, since polluted clouds show special optical signatures a way out of this dilemma is possible.

Generally the interaction of electromagnetic radiation with gases, aerosols and hydrometeors is described through the wavelength dependent absorption and scattering coefficients. These optical properties vary with the thermodynamic state of the atmosphere as expressed by air temperature and pressure. Therefore the changes in the fraction of incident solar radiation diffusively reflected by clouds, in reality caused by scattering, is a suitable indicator for the anthropogenic influence by aerosols. Any anthropogenic perturbation of the tropospheric aerosol system will lead to changes in cloud droplet scattering which leads to a changed cloud albedo if the droplet spectrum changes.

The scattering of solar radiation by cloud droplets varies with angle, droplet size and wavelength. The individual photons entering from the top of a cloud always have followed quite different paths within the cloud dependent on the cloud droplet spectrum. On their pathways the photons do meet several drops, i.e. easily 20 [Twomey, 1974]. This multiple scattering finally leads to the so-called isotropic reflectance, only a slow variation with angle is left.

A comparison of calculated optical and physical properties reveals that in the visible and near infrared the cloud parameters which strongly affect the cloud albedo are concentration of large droplets, mode radius, maximum drop size, and range of the drop size distribution [Carrier et al., 1967]. Since these parameters are highly variable the albedo of clouds alters considerably with the state of the atmosphere or cloud lifetime. As a rough first estimate a few values from the literature are presented here. Typical values amount to about 65% for stratocumulus and stratus, 30% for altostratus and higher than 70% for cumulonimbus [see Linke and Bauer, 1962]. There is also a strong dependency on geometrical thickness and water content. For example the albedo of stratus clouds varies from 35% for a thickness of 100m to 76% for 800m. These numbers demonstrate that independently from cloud type the cloud albedo can approach the albedo values of snow. The relatively high albedo of clouds is a consequence of the nearly negligible absorption by water in liquid or solid phase within the visible and parts of the near infrared spectral range. Air pollution can potentially become visible through clouds if strongly absorbing aerosols lower cloud albedo substantially.

In his work ‘Albedo Reduction and Radiative Heating of Clouds by Absorbing Aerosol Particles (1975)’ Graßl pointed out the importance of absorbing aerosol particles for the Earth climate:

Another important aspect of the physical properties of absorbing aerosol particles within clouds is shown ... namely the change in albedo; this plays a decisive role in controlling the climate of the earth. Climate model computations have led to the conclusion that a change in the planetary albedo by a mean of 1% affects the climate more directly than does a noteworthy increase of the CO_2 concentration.

Further Graßl (1975) concluded:

The effectiveness of absorbing aerosol particles in the visible will not be reduced in case of cloud formation; it does not matter whether the aerosol particle turns into a cloud droplet or continues to be suspended as an absorbing small particle in the cloud air or is caught by droplets. The comparison between cloudless and overcast sky reveals that within clouds the effectiveness of the aerosol is enhanced. For the investigation into man made climatic changes a reduction in albedo has a bearing if there is evidence for the fact that the absorption rate due to atmospheric aerosol particles in industrial areas strongly deviates from that in unpolluted areas. According to Fischer this is true in many cases: he found higher absorption rates in industrial areas than in the country side; thus it can be assumed that clouds of equal optical thickness undergo a reduction in albedo over industrial areas. This would exercise a decisive influence on the climate of the Earth.

The cloud albedo, or the isotropic reflectance of clouds, can be represented by so-called bulk-averaged quantities such as cloud optical thickness, the single scattering albedo and the asymmetry factor [Twomey, 1974]. Among these properties, which already are well suitable for describing the influence of pollution on cloud albedo, the cloud optical thickness becomes dominant.

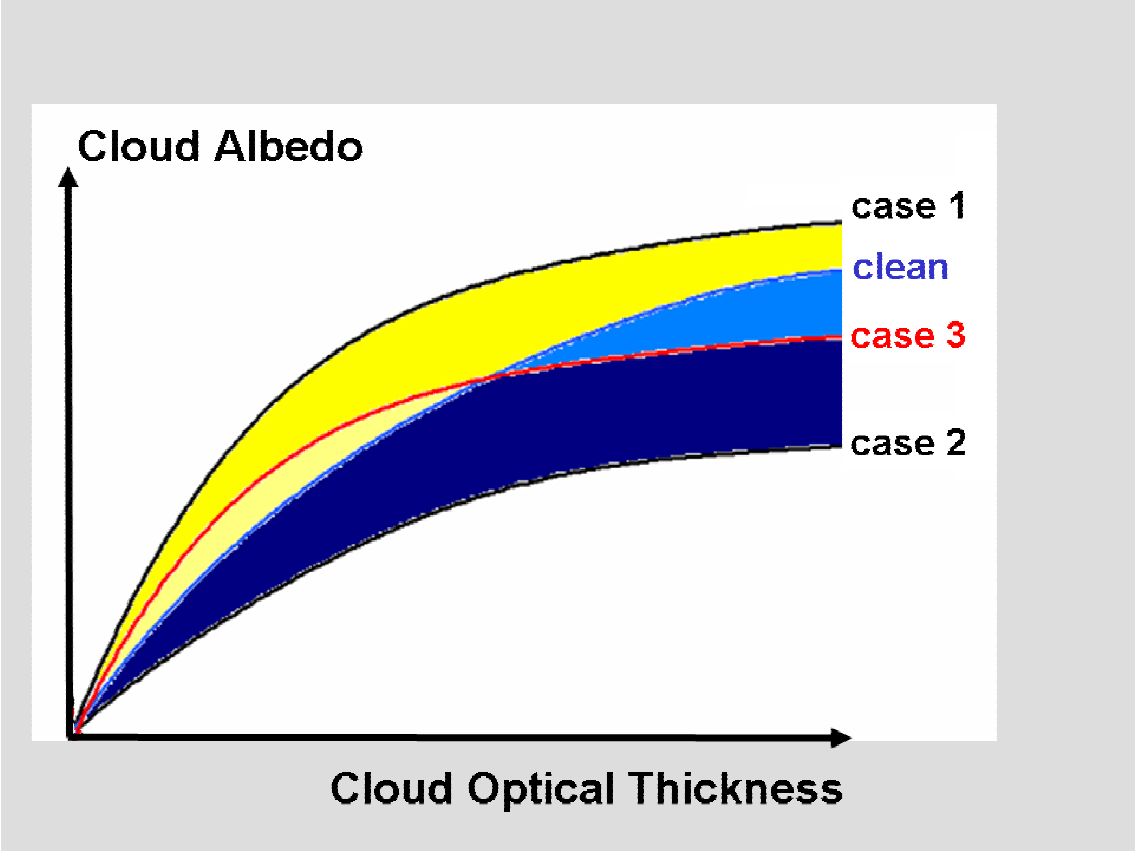

Figure 3. Schematic illustrating the changes of cloud albedo by anthropogenic aerosol particles. Three major cases of polluted clouds as compared to the clean case (blue curve) can occur. Case 1 shows the sulphur rich case (upper black curve) without absorbing aerosols, where more aerosol particles lead to more cloud droplets and consequently to an albedo increase. In case 2 all aerosol particles are absorbing (lower black curve), without increasing the number of droplets, which lowers albedo. In reality, represented by case 3 (red curve) the albedo can also show both characteristics: It can increase due to increased number of cloud droplets for optically thin clouds and decrease for optically thicker clouds due to stronger absorption.

Therefore the overall influence of air pollutants on cloud albedo, which has been formulated in the theoretical studies by Twomey (1974) and Grassl (1975), can be well described using a cloud albedo versus optical thickness diagram. Such a diagram is shown in figure 3 including exemplarily the competing processes. The first example considered here (see case 1 in figure 3) is the abundance of anthropogenic particles, which are only weakly absorbing. In reality this could be due to a sulphur rich case where aerosol precursor gas emissions are dominating the aerosol system and leading to increased aerosol and cloud droplet number concentrations. In that case the albedo will be clearly increased for optically thin clouds while the optically thick clouds show only a very weak increase.

The second extreme case considered as an example here is the strong aerosol particle absorption case at same cloud droplet number. This black carbon rich case leads to lower albedo for any cloud optical thickness. However, if at the same time the number of droplets would be increased, then often for optically thin clouds the net effect would still be an albedo increase (as shown by case 3 in figure 3). Therefore in polluted regions on could observe a paradoxon: As long as the cloud vertical extent, or more precisely, cloud optical thickness is small the brightness is increased; when clouds become optically thicker they will appear darker than unpolluted clouds. Grassl (1978)

in his theoretical work has shown, that three processes generally must be considered, one albedo decreasing and two albedo increasing, which can affect the cloud albedo in polluted regions considerably:

- Albedo reduction through absorption increase.
- Albedo increase through increased scattering caused by a higher number of cloud droplets.
- Albedo increase through increased backscattering caused by smaller cloud droplets at unchanged liquid water content.

In reality one should expect a combination of the competing effects in each cloud case. On the other hand the distinct characteristics, both the albedo increase for optically thin clouds and the albedo decrease for optically thick clouds are suitable for detecting indirect aerosol effects. The critical cloud optical thickness, i.e. the point without any change in albedo, will depend on the aerosol type.

Early experimental evidence for indirect aerosol effects was received in 1966 when Conover [1966] detected the “anomalous cloud lines”, which typically occurred as 500km long and up to 25km wide lines of brighter clouds, in TIROS VII satellite scenes over the ocean. He rejected that these lines involve aircraft condensation trails or missile trails. He concluded that this could also not be convection induced at the edges of major currents in sea. The most likely explanation for Conover was a general influence of ship emissions on cloud albedo; however, he also excluded that the lines are the smoke screens from ships.

It is still an open question whether the albedo increase Conover [1966] found was due to a decrease in droplet size or to an increase in cloud liquid water path through additional droplets. Radke et al. [1989] pointed out that the latter process could well explain the finding because over the ocean other than over land the number of condensation nuclei is generally limited. Since large numbers of Aitken nuclei can be formed in the exhaust, the ocean going vessels could easily contribute to the anomalous formation of Aitken nuclei. In the earlier work Conover specified the critical conditions. Especially convectively unstable situations from the surface up to a low level stable layer, slight supersaturation at the top of the convective layer, presumably deficient in cloud nuclei, are favouring the observed anomalous cloud lines. These commonly called “ship tracks” widely have been used together with Twomey’s theoretical work [e.g. Twomey 1977] to manifest the high importance of indirect aerosol effects in the climate system. Later field experiments in marine stratocumulus clouds supported the conclusions above on the occurrence of the indirect aerosol effects [Coakley et al., 1987].

In 1989, Albrecht [1989], also influenced by the finding of Radke et al. [1989], in his theoretical work formulated the basis for the so-called second indirect aerosol effect. He postulated that a reduction in drizzle increases the cloud lifetime over the ocean because this process regulates the liquid water content and energetics of shallow marine clouds. This in turn would contribute to a cooling of the earth’s surface and could have enormous consequences for climate. Consequently a special focus were investigations whether drizzle is suppressed in ship tracks. In 2000 this second indirect effect, often

Parameter	Process	Effect	Theory	Detection
Scattering	Increased number of cloud droplets via increased number of condensation nuclei - at unchanged cloud water - increases cloud albedo.	First indirect aerosol effect (radius effect)	Warner and Twomey (1967) Grassl (1978)	Conover (1966) (cloud scale) Krüger and Graßl (2002) (regional scale)
Absorption	Absorption, i.e. black carbon, haematite (Fe_2O_3) or fly ash, in cloud droplets or interstitial aerosol reduces cloud albedo.	First indirect aerosol effect (absorption effect)	Grassl (1975)	Krüger and Graßl (2004) (regional scale)
Cloudiness	Increased number of cloud droplets via suppressed or reduced coalescence regulates precipitation and cloud lifetime.	Second indirect aerosol effect (cloud lifetime effect)	Albrecht (1989)	Ferek et al. (2000) Rosenfeld (2000) (cloud scale) Krüger and Graßl (2004) (regional scale)
	Aerosol absorption reduces relative humidity and cloudiness.	Semi-direct aerosol effect (cloud burning)	Ackerman et al. (2000)	INDOEX Ackerman et al. (2000) Ramanathan et al. (2001) (cloud scale)

Table 1. The modification of cloud properties by anthropogenic aerosols.

called cloud lifetime effect, was detected by both a field experiment and satellite measurements. Ferek et al. [2000] were able to show by radiometric measurements and radar observations that increased droplet concentrations in ship tracks, accompanied by smaller droplet sizes, significantly alter the liquid water path. In observations of the Tropical Rainfall Measuring Mission (TRMM) over South Australia Rosenfeld [2000] found the same result on the cloud scale: The drop growth by collision is very effectively suppressed by anthropogenic aerosol particles originating from power plants, lead smelters and oil refineries. The same effect of cloud droplet size reduction together with a delay in the onset of precipitation has been found over the Amazon during the Large-scale Biosphere-Atmosphere Experiment in Amazonia subproject on Smoke, Aerosols, Clouds, Rainfall, and Climate (LBA-SMOCC), where it was shown in detail which enormous influence heavy smoke fires can have on cloud microphysics [Andreae et al., 2004].

Other comprehensive field experiments which contributed considerably to the knowledge about aerosol cloud interactions were the Smoke, Clouds, Radiation-Brazil (SCAR-B) experiment [Kaufmann et al. 1998], the Tropospheric Aerosol Radiative

Forcing Experiment (TARFOX), the Indian Ocean Experiment (INDOEX), the Aerosol Characterization Experiments (ACE-1) [Bates et al., 1998] and ACE-2 [Raes et al., 2000] and the Aerosol Characterization Experiment in Asia (ACE-Asia). The planning of these field campaigns was stimulated by the presence of global fields of aerosol optical thickness derived from satellite [e.g. Husar et al. 1997] as well as by global model results [e.g. Langner and Rodhe, 1991], which depicted some regions of conspicuously enhanced aerosol concentrations.

One of those regions is the Indian Ocean. Here, INDOEX discussed another aspect of indirect aerosol effects: Highly absorbing aerosol particles and their long-range transport over the ocean. Trade wind cumuli were moving within deep layers of dark haze. Based on these observations Ackermann et al. [2000] suggested that the reduction of tropical cloudiness by soot could represent another major effect of aerosols on clouds. By model calculations it was shown that the typical decrease of relative humidity during daytime driven by solar heating with a maximum around noon is enhanced by the presence of absorbing haze in the boundary layer. As compared to the influence by the "white" non-absorbing aerosol the absorbing haze leads to increased temperature, lowered relative humidity and shorter anvil lifetime. The process, which shows a clear diurnal cycle, is called the semi-direct effect or cloud burning.

In this study, which is already included in table 1, long-term measurements by the AVHRR instrument onboard the NOAA operational satellite series are investigated for the changing effects of anthropogenic aerosols on regional scale. The overall hypothesis for the study can be formulated as follows:

The anthropogenic influence on cloud albedo in industrial or rapidly developing areas is both driven by the aerosol particle density increase and enhanced soot content of the aerosol particles and influences regional or continental scale climate.

Since, as pointed out above, measurements from satellites have contributed strongly to the knowledge on indirect aerosol effects it was expected that the analysis of a very large number of measurements over roughly two decades would lead to major progress. However, there was firstly the major question how to reduce and to separate the number of data into samples, which include pronounced indirect aerosol effects. There was also some concern whether the resulting samples would include contradicting processes, which finally would result in a net effect to be zero. Further, there was the question what region would be the most promising to analyse: Would it be better to look over the ocean, where the surface conditions are much more homogeneous with regard to interactions with the atmosphere? Or, would there be an advantage if the evaluation would be restricted to areas nearer to strong point sources such as power plants, which sometimes with high stacks can approach the cloud level?

Finally it was decided to analyze not only one polluted region. The idea was, as the flow chart diagram in figure 2 indicates, that the indirect aerosol effects should become visible through albedo changes. These albedo changes within the polluted region can result from a pronounced radius, absorption or lifetime effect. Since the effects may alter with distance from the sources a spatial heterogeneity in addition should become visible on the regional scale with a signature within hundreds of kilometres.

Therefore the major scientific objectives for this study are formulated as follows:

1. ***Is it possible to detect the indirect aerosol effect(s) on regional scale?***

2. ***How do the processes of scattering and absorption contribute to the overall effect? Is there dominance by scattering or even by absorption on regional scale?***

3. ***Is it possible to derive a trend for the indirect aerosol effect(s) on a regional scale due to changes in anthropogenic emissions?***

In order to realize the detection of aerosol processes satellite measurements from 1981 to 1999 were evaluated. The areas chosen are strongly polluted regions in Central Europe (5^{o}W to 28.5^{o}E longitude and 48.5^{o}N to 57.5^{o}N latitude) and Eastern Asia (100^{o}E to 150^{o}E longitude and 20^{o}N to 55^{o}N latitude). The motivation for Europe was to investigate, if the collapse of the former East Block, which was accompanied by a sudden reduction of industrial activities and a consequent slow down in anthropogenic emissions, becomes visible through changes in cloud properties. It was expected that this change should have a major influence on cloud albedo. The area in Europe in its centre includes the so-called 'Black Triangle', an area with strong air pollution covering parts of Germany, the Czech Republic and Poland.

The investigation over China was motivated by the fact that China is one of the most rapidly developing countries. Despite the limited knowledge about air pollution in China it was expected that pollution originating from large fast growing cities, i.e. in the Pearl River Delta, the lower Jangtze river and the Red Basin, must have an influence on cloud albedo. Also the so-called Asian brown haze, which was observed in South East Asia during INDOEX, stimulated the study over China.

2. ANALYSIS OF SATELLITE MEASUREMENTS

The studies presented in the **papers I**, **II**, **III, IV** [Krüger and Graßl, 2002, Krüger and Graßl, 2004, Krüger et al., 2004, Krüger et al., 2005] are based on long-term data of cloud reflectance over Central Europe and South East Asia. All three studies are making use of the reprocessed global NOAA/NASA Pathfinder data set [James and Kalluri, 1994] from the Advanced Very High Resolution Radiometers (AVHRR) on board the afternoon-viewing NOAA series satellites (NOAA-7, 9, 11, and 14). All investigations in **papers I**, **II**, **III, IV** are based on data within the time period from 1981 to 1999.

The Pathfinder data set, which is a further development of the complete AVHRR Global Area Coverage (GAC) archive, has been processed by NASA [James and Kalluri, 1994] using best available methods for building up a consistent time series of unprecedented quality. Methods used in reprocessing include cross-satellite calibration, application of a precision navigation system and correction for Rayleigh scattering. The radiometric calibration, i.e. the converting of the detected counts for the five channels (at 0.58-0.68um, 0.7-1.1um, 3.5-3.9um, 10.3-11.3um, 11.5-12.5um) into reflectance or brightness temperatures, includes four major steps. The first two steps are the determination of the spectral response function [Kidwell, 1991] and the pre-launch calibration of all channels [Rao, 1987]. The others are the in-flight calibration of the thermal infrared channels and a post-launch calibration.

Except for the channels 1 and 2, which are calibrated before launch, in-flight calibration is possible. The in-flight calibration bases on two measurements: One looking to deep space and the other onto the Internal Calibration Target (ICT) of the AVHRR instrument. Since the conditions in the satellite orbit are differing from ground pre-launch conditions for the channels 1 and 2 a post-launch calibration has been established. That post-launch calibration can generally be achieved by statistical methods or numerical calculations or in-situ measurements. The Pathfinder data set bases on the first possibility using data from the Libyan desert site, assumed to be radiometrically stable. Aircraft measurements confirmed the validity of the procedure [Rao, 2000].

The Pathfinder data also include corrections for three uncertainties due to the lifetime of the instruments and satellites. Considered are the sensor degradation [Rao and Chen, 1994]. The orbital drift [Jin et al., 2003], which affects the anisotropy, and the solar contamination of the ICT measurements [Cao et al., 2001] are still under investigation.

After calibration the filtered radiances in channel 1 and 2 are converted into a bi-directional reflectance, sometimes called effective isotropic albedo [Gutman, 1988], which is dependent on solar zenith angle, satellite zenith angle and satellite azimuth angle [Kriebel, 1976]. The conversion, whereby the filtered radiance is divided by the filtered solar irradiance and normalized by the cosine of the solar zenith angle, assumes the radiation field being isotropic. In this study the parameter is referred to hereafter as cloud reflectance or cloud albedo.

Since the AVHRR instrument measures both reflected solar and emitted terrestrial radiation in the five spectral channels, which take advantage of maximum transmittance in the atmospheric windows, the instrument enables a detailed classification into cloudy pixels. In **papers I, II** and **III**, for delineating optical characteristics of clouds, the NOAA/NESDIS algorithm, the technique suggested by Stowe et al. [1999] was used. The method, termed Clouds from AVHRR (CLAVR), utilizes the five-channel AVHRR

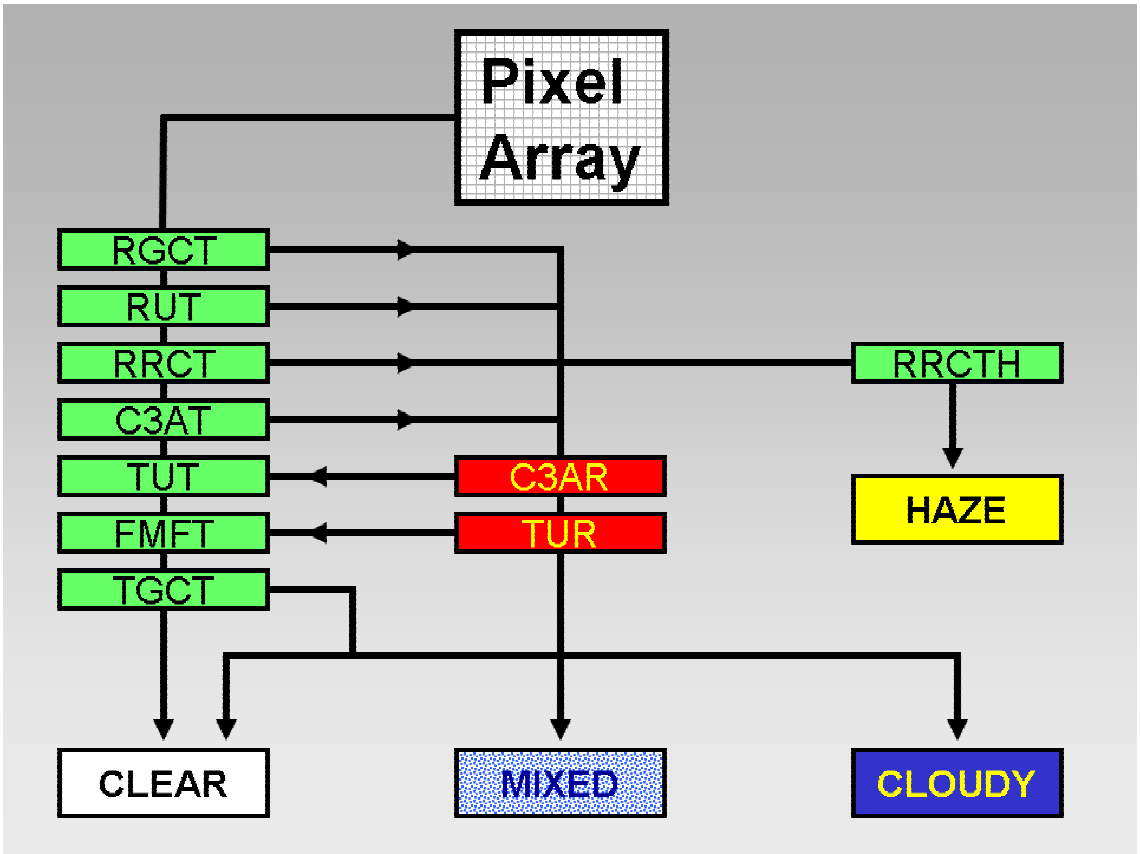

Figure 4. The cloud classification scheme based on the method suggested by Stowe et al. (1999). Cloud tests are represented in green and red boxes. The method is designed to test a 2x2 pixel array sequentially for being clear (cloud-free array), mixed (partly cloudy array) and cloudy (all pixels of an array are classified as cloudy). An array is classified clear or cloudy in case all pixels in the array are clear or cloudy. Since the first four tests RGCT, RUT, RRCT and C3AT (green boxes) can misclassify some data into cloudy, the so-called restoral tests C3AR and TUR (red boxes) are applied (depending on latitude) to classify the arrays into clear.

multi-spectral information, individual values, as well as spatial differences, in series of sequential decision-tree type tests and includes established or empirically optimized thresholds. Through the sequence of contrast, spectral and spatial signature tests the procedure allows the identification of cloud-free, mixed and cloudy situations (figure 4). The cloud detection is based on the intensity of emitted and reflected radiation, the wavelength dependence and spatial variability. The classification includes the following sequence of tests and thresholds [see Stowe et al., 1999]:

The Reflective Gross Cloud Test **RGCT**: The RGCT is the first daytime test, which uses the observed bidirectional reflectance from AVHRR channel 2 normalized by the solar zenith angle. In order to avoid misclassification of high aerosol loading in the cloud-free atmosphere as cloudy the threshold value given here is clearly higher than in other suggestions [see the Multi Channel Sea Surface Temperature Algorithm (MCSST), McClain et al., 1985].

The Reflectance Uniformity Test **RUT**: The RUT compares an array of pixels for identifying so-called mixed pixels. These mixed pixels with a high probability are not fully cloud covered. Over the ocean the test is performed through calculating the difference between the maximum and minimum reflectance for channel 2 and its

comparison to a threshold value. Very low differences occur for uniform cloud-free ocean satellite scenes. Over land channel 1 is chosen because of the highly variable reflectance in channel 2, which is due to the influence of vegetation. Generally the RUT, in a conservative manner, minimizes the possibility for a misclassification into cloudy pixels. However, if the array shows a heterogeneous reflectance also totally cloud-covered pixels could be classified into this mixed category.

The Reflectance Ratio Cloud Test **RRCT**: The spectral signature test RRCT makes use of the wavelength dependency of cloud reflectance. Since the wavelength dependence is rather weak in the visible and near infrared part of the spectrum the channel 2 to channel 1 reflectance ratio is approaching 1. The RRCT demands this ratio to be in the range within 0.9 to 1.1 to classify the corresponding pixel as cloudy. Saunders and Kriebel [1987] found values typically to be lower than 0.75 for a cloud-free ocean.

The Channel 3 Albedo Test **C3AT**: The C3AT is used for detecting weakly reflecting clouds such as cirrus or thin water clouds as well as sub-pixel cloudiness. The idea is to make use of the higher signal in channel 3 related to reflected solar radiation originating from hydrometeors as compared to aerosol particles [Deirmendjian, 1969]. Since the information in channel 3 is a combination of emitted and reflected radiation, during daytime a separation of the two distinct contributions is needed. This is performed through estimating the emitted portion from the signals in channel 4 and 5 [Stowe et al., 1999]. In the procedure the reflected radiance is estimated. The empirically derived C3AT thresholds are about a factor of two higher over land than over the ocean [Stowe et al., 1999].

The Thermal Uniformity Test **TUT**: The TUT is a spatial signature test, which employs the channel 4 brightness temperature. The TUT requires that the difference in brightness temperature within the 2x2 array exceeds a given threshold for the array to be classified cloudy. These differences over land are several times higher than over the ocean and much more variable, because of the much higher spatial heterogeneity of the emissivity.

The Four Minus Five Test **FMFT**: The FMFT is used to detect thin cirrus clouds [Prabhakara, 1988]. The physical principle of the test is based on the fact that the signal in channel 4 in atmospheres containing ice crystals or humid atmospheres generally originates from a higher temperature level than in channel 5. The reason is that water vapor and ice crystals absorb stronger in the spectral range of channel 5. The presence of a layer of ice particles, which have a lower emissivity or higher transmittance at 10.8 um wavelength, can lead to a much higher channel difference than for the water vapor attenuation alone. However, it should be mentioned here that this test also rather effectively might detect aerosols of volcanic origin. The threshold for the FMFT is chosen to be the maximum value for a cloud-free atmosphere that is attributable to high water vapour content.

The Thermal Gross Cloud Test **TGCT**: The TGCT is a contrast signature test based on an emission threshold. Since the idea is to prevent snow and ice covered areas to be classified as cloudy the threshold has been chosen as a minimum temperature for ocean and land. These temperatures are defined by the freezing point of seawater and a zonally averaged cloud-free land temperature equator-ward of 60 degrees latitude [Stowe et al., 1999].

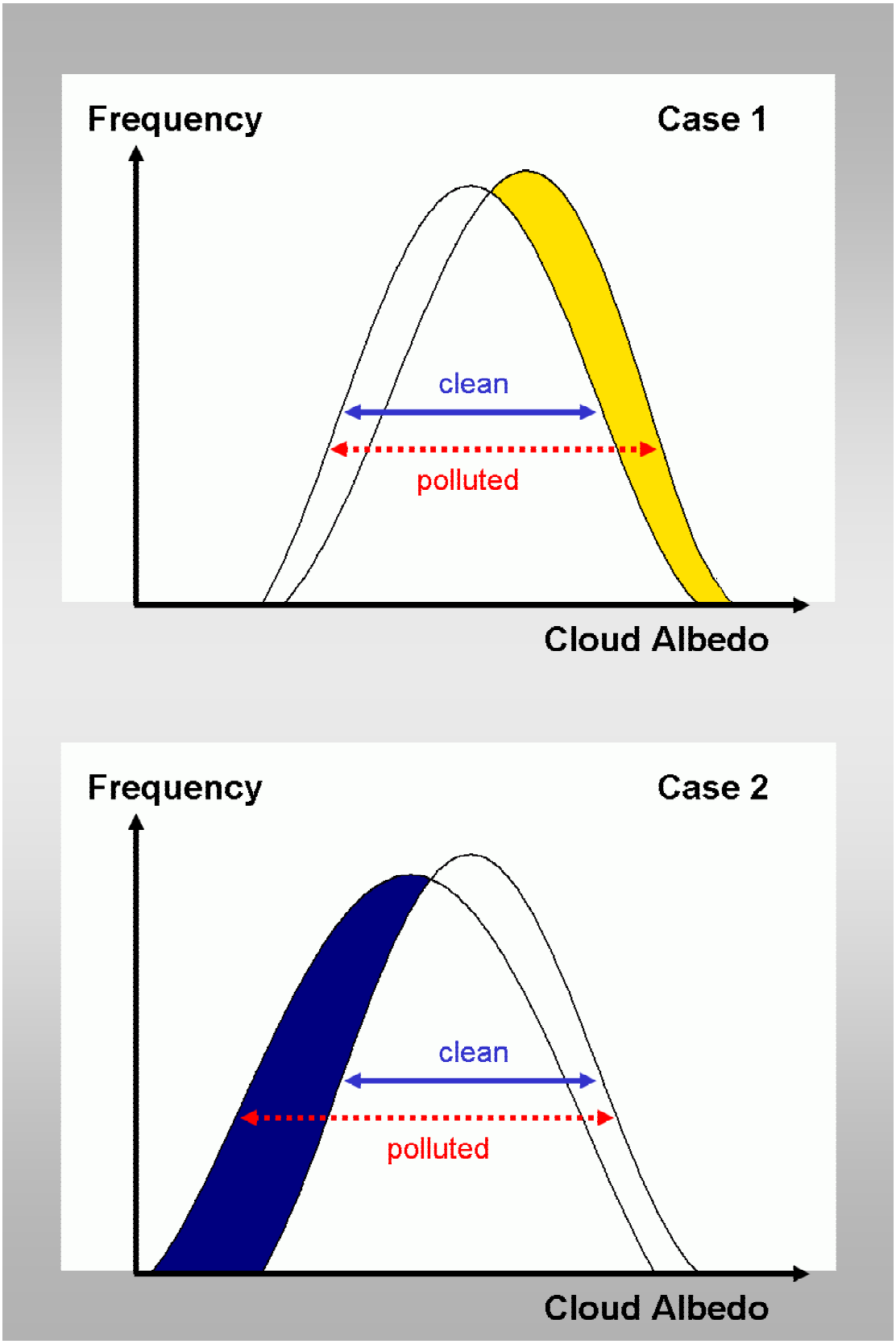

Figure 5. The influence of pollution on the frequency distribution of cloud albedo. Three frequency distributions are considered: The distribution without an anthropogenic influence (clean), with a strong influence by non-absorbing aerosols (see case 1) and oppositely for strong influence by absorbing aerosols (see case 2). If clean and polluted clouds occur, then the variability is enhanced in each case. When both extreme cases, case 1 and 2, can occur in a polluted region the variability (standard deviation) is increased further.

The Reflectance Ratio Cloud Test for Haze **RRCTH**: The RRCTH is applied additionally here to detect absorbing haze. This test is not a CLAVR test but was suggested by the studies presented in **papers II** and **III**, that showed the high sensitivity for the detection of aerosol layers having a high optical thickness, so-called haze layers as cloudy. Basically the Reflectance Ratio Cloud Test (RRCT), comparing channels 2 and 1 of AVHRR, is used here in order to separate haze from clouds. As described above the test is set to $0.9<R<1.1$ which assumes nearly wavelength independent scattering by clouds versus strong wavelength dependence in scenes dominated by cloudless conditions both over oceans and land. Under heavy aerosol load, with a strong contribution of absorption by soot, the upper planetary boundary layer (PBL), which is close to cloud formation (r.h.>0.9), scatters less wavelength dependent than typical aerosol and approaches cloud values for the channel ratio. Therefore strong absorbing haze is misclassified as a dark cloud. Very often small fair weather cumuli embedded in the upper PBL will also not be detected, especially if a layer of absorbing haze exists in the free troposphere after a strong convection the day before. Also under these conditions the algorithm by Stowe et al. [1999] classifies a low dark water cloud, the often very small sub-pixel cumuli not being detected. Since haze shows a clear secondary peak for lower values in the frequency distribution of cloud reflectance, it can be separated using a threshold. The threshold is set here to 0.2 because the contribution of haze in polluted regions is dominant below.

Since the major intention here is to detect changes of cloud properties on the regional scale a subdivision into low plus medium clouds on one hand and high clouds on the other is appropriate. In order to best characterize the indirect aerosol effects in this study low and medium level clouds are investigated as they are more affected by pollution. These cloud categories, which are expected to deliver most pronounced indirect aerosol effects are well represented by data accepted as cloudy by the cloud tests RGCT, RUT and RRCT.

The idea for this type of analysis was that the influence of pollution on cloud albedo generally should become visible via changes in the cloud albedo frequency distribution. While the change in cloud albedo (represented by the mean) will give hints on individual indirect aerosol effects, the variability (represented by the standard deviation, coefficient of variation) will point to the degree of cloud pollution. In figure 5 three idealized frequency distributions including clean and polluted clouds, with two extremely different anthropogenic aerosol types, are depicted. The distributions for the polluted clouds include in the first case purely non-absorbing aerosols and in the second case strongly absorbing aerosol. Since it can be expected that pollution affect clouds under very different atmospheric conditions, e.g. depending on cloud height and stability of the atmosphere, the cloud albedo frequency distributions in regions of strong air pollution will be much broader. Such variable atmospheric conditions are typically for Central Europe.

In addition the sequence of cloud tests also can be used to judge the changes in the local planetary albedo (LPA). If these LPA changes are separated into contributions from the clear, mixed, cloudy or hazy atmospheres, important signatures can become visible, giving an additional insight into the distinct influences of aerosols and clouds on LPA.

3. INDIRECT AEROSOL EFFECTS

In this chapter an introduction of the three basic studies dealing with the albedo changes in Europe, described in **papers I**, **III** [Krüger and Graßl, 2002, Krüger et al., 2004], and in China, **paper II** [Krüger and Graßl, 2004] is given. Europe and China are discussed separately, because of the very different trends in the emission of air pollutants. In both sections new results supporting the conclusions of the earlier papers and pointing to future research directions are presented. This section also includes the observation of indirect aerosol effects in the thermal spectral range, which are described in **paper IV** [Krüger et al., 2005].

3.1 Detection over Europe

The decision firstly to investigate indirect aerosol effects over Europe bases on the rather comprehensive knowledge about the emissions and concentrations of air pollutants, and in particular the availability of information about aerosols and their precursor gases since the start of satellite observations. The strong regional dispersion and mixing of air pollutants in the atmospheric boundary layer over large parts of Europe stimulated the investigation of satellite measurements. Measurements and model calculations in addition indicate a strong variability of this pollution plume due to changing emissions, chemical transformations, deposition and long-range transport of the manifold species all depending on season and weather type [see e.g. Eliassen and Saltbones, 1983**,** Krüger and Tuovinen, 1997, Petersen et al., 2001, EMEP, 2004, Schaap et al., 2004, van Dingenen et al., 2004, Putaud et al., 2004].

A strong contribution to the aerosol load over Europe originated from the enormous amounts of particulate matter and aerosol precursor gases emissions (figure 6a,b), such as sulphur dioxide, nitrogen oxides and ammonia. The exemplarily high sulphur dioxide emissions in the former German Democratic Republic (GDR), which amounted to even more than 5 Tg per year during the late 1980s, were of major importance for the secondary aerosol particle formation. The strong contribution of elevated point sources around Halle, Leipzig and Cottbus resulted in pronounced spatial differences of sulphur dioxide (SO_2) and particulate matter (PM) concentrations in air. In Cottbus, enormous amounts of PM were emitted from the industrial complex ‘Gaskombinat Schwarze Pumpe’. The particle emission of individual point sources reached there at least 10 000 tons per year. In the region Halle/Leipzig quite a number of point sources were located at the chemical plants ‘Chemie AG Bitterfeld-Wolfen’, but also in Schkopau (Halle) at ‘Chemische Werke Buna’ existed a major emission area (more details in **paper III)**.

The collapse of the East Bloc in 1989 resulted in significant reductions of industrial activities and thus atmospheric pollution. A pronounced declining trend was observed in the area of the so-called ‘Black Triangle’, whose name originates from the enormous damages to human health and ecosystems also caused by soot. This area, covering the southern part of Saxony (Germany), Northern Bohemia (Czech Republic) and southwestern Lower Silesia (Poland), is a prominent example for the extensive use of the lignite deposits in the region. Therefore, the Black Triangle should lie in the centre of the study area. The total study area includes parts of UK, Denmark, Sweden, France, Benelux, Germany, Poland, Czech Republic and Ukraine.

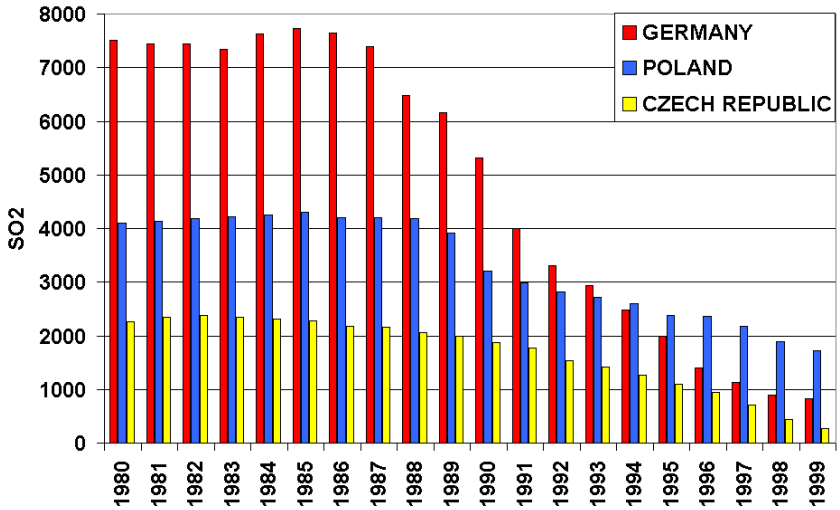

a

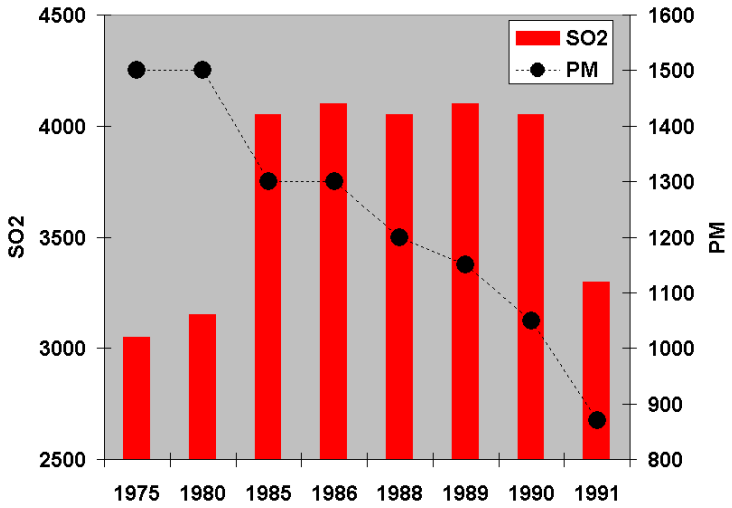

b

Figure 6. (a) Annual sulphur dioxide (SO_2) emissions from Germany (including the former GDR), Poland and the Czech Republic, in ktons for the period 1980-1999 according to the EMEP data [EMEP, 1999]. (b) Annual emissions of particulate matter (PM) and sulphur dioxide (SO_2) for power plants in the area of the former GDR, in ktons. Data are taken from the German Environmental Agency [Umweltbundesamt, 1994].

The objective of the study in Europe was to relate cloud albedo and distinct anthropogenic emissions of air pollutants for four-year episodes in order to reduce the influence of natural variability. Due to the emission trends of SO_2 and PM from 1980 to 1999 (see figure 6a,b) different periods both for winter (January, February, November, December, denoted as JFND, JF, ND) and summer (May, June, July, August, denoted as MJJA) are compared:

- The early 1980s from 1981 to 1984 (denoted as JFND8184, JF8184 and ND8184) , which are accompanied by high SO_2 and PM emissions in Central Europe (see figure 6a).

- The late 1980s from 1985 to 1989 (denoted as JFND8589, JF8589 and ND8589; the year 1987 is excluded because of partly missing satellite data), which are accompanied by lower PM emissions than during the early 1980s, but with highest SO_2 emissions in the former GDR (see figure 6b).

- The late 1990s from 1996 to 1999 (denoted as JFND9699, JF9699 and ND9699, which are accompanied by much lower SO_2 and PM emissions.

The first intention of the study over Europe was to answer the question:

Is there a change in cloud albedo as a consequence of declining emissions of particulate matter and sulphur dioxide since the late 80s?

The answer is presented in **paper I**. The pronounced decrease of cloud albedo higher than 2% in summer and in winter as well, observed from the late 80s to the late 90s, can be explained only by a weakening radius effect, caused by the strong decrease of aerosol precursor gas and particulate matter emissions.

The conclusion is supported by an additional aspect seen during winter: In source regions of anthropogenic particulate matter emissions the cloud reflectance is more than 5% lower than the average pointing to an absorption effect by black carbon (see figure 7a). The magnitude of the absorption effect in clouds is enhanced by the lower boundary layer heights during winter. The comparison with emission data, as well as results of long range transport modelling over Europe, leads to the general conclusion that indirect aerosol effects are responsible for significantly changed cloud optical properties (for references see **papers I and III**).

Another argument supporting the conclusion is the variability of cloud reflectance during winter, which was stronger for the early 1980s as compared to the other episodes (figure 8). It is extensively discussed in **paper III**. Aerosol particle number density, black carbon content, as well as secondary aerosol particle formation, all influencing the variability of cloud reflectance. The studies confirm that towards the late 1990s, both the radius effect and the absorption effect, as the two components of the so-called first indirect aerosol effect, have declined due to reduced particulate matter and sulphur dioxide emissions. The results also indicate a remarkable influence of thermodynamic stability on the indirect aerosol effect(s) over Central Europe.

The resulting frequency distributions of cloud reflectance (figure 7b) for areas with different degrees of pollution, as represented in figure 7a by the areas of mean cloud reflectance, clearly show characteristics, which are in line with radiative transfer calculations of the indirect aerosol effects, including the radius effect, the absorption effect and the saturation effect [for more details see: Grassl, 1978, Krüger et al. 2004].

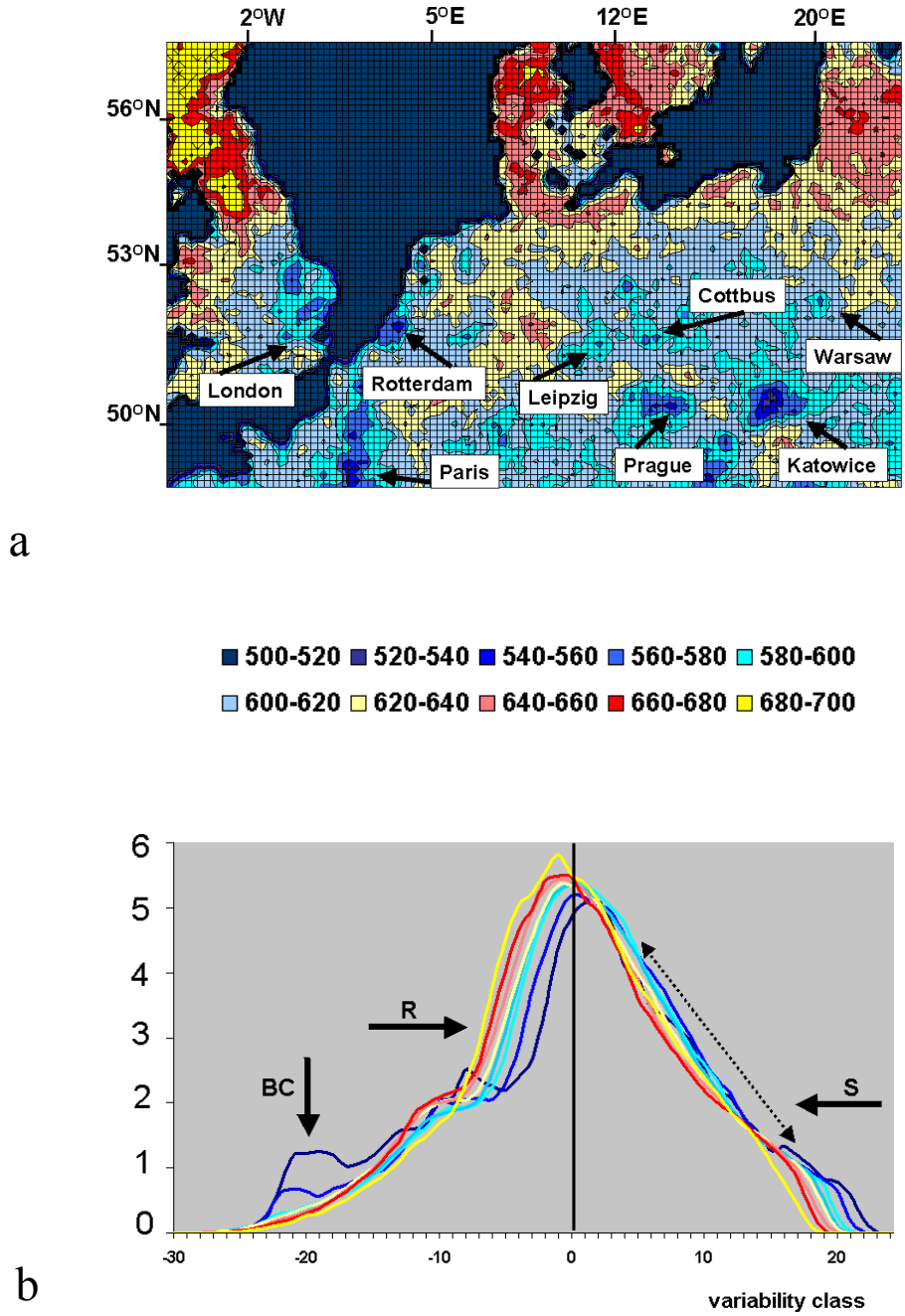

Figure 7. (a) Mean cloud reflectance of low and medium level clouds derived from AVHRR channel 2 data over parts of Europe, given in thousandth. Data are shown from 5.0^0W to 24.0^0E longitude and 48.5^0 to 57.5^0N latitude for the winter period JFND (January, February, November, December) from 1985 to 1989 (excluding data from 1987). The grid size is 0.25^0 longitude and 0.125^0 latitude. The area covers parts of UK, Denmark, Sweden, France, Benelux, Germany, Poland, Czech Republic, the Baltic countries and Ukraine. The North Sea and the Baltic Sea are in black. Strongly polluted areas are indicated.

(b) Frequency distribution of the deviation from the class mean cloud reflectance for JF8589 (January and February from 1985 to 1989 in percent per variability class interval of 2% width). Colours refer to different cloud reflectance classes in the upper figure (pollution source regions blue, more remote ones red). The main characteristics of the first indirect aerosol effect are indicated (R=radius effect, S=saturation effect through aerosol absorption). The curve in dark blue shown for data with a mean reflectance below 56% includes a black carbon peak (BC), which occurs only for frequency distributions in source regions of air pollution. This peak enables the haze detection.

In polluted urban regions the frequency distribution of cloud reflectance during winter includes a haze peak, here also called the black carbon peak, which enables the separation of haze. The occurrence of the haze peak again supports the conclusion of an anthropogenic aerosol influence. The changes in the cloud albedo frequency distribution are statistically significant.

The summertime cloud reflectance over Europe during MJJA8589 (figure 7c) delivers a clear indication for the classical Twomey effect accompanied with higher reflectance, which is initiated by increased sulphate concentration. Eastern and Central Europe show higher cloud reflectivity in comparison to the British Isles and Western Europe. Individual metropolitan and industrial regions are no longer directly visible in cloud reflectance, pointing to lower carbon emissions during summer and to a more rapid transformation of precursor gases into aerosol particles from gaseous emissions. The gradient of cloud reflectance from remote to polluted regions changes sign if compared to winter. Highest cloud reflectance occurs in regions of well-known maximum sulphur dioxide concentrations in the southern-easterly part of the study area. The average cloud reflectance decreases from MJJA8589 to MJJA9699 by about 2.1 percent (see **papers I and III**).

c

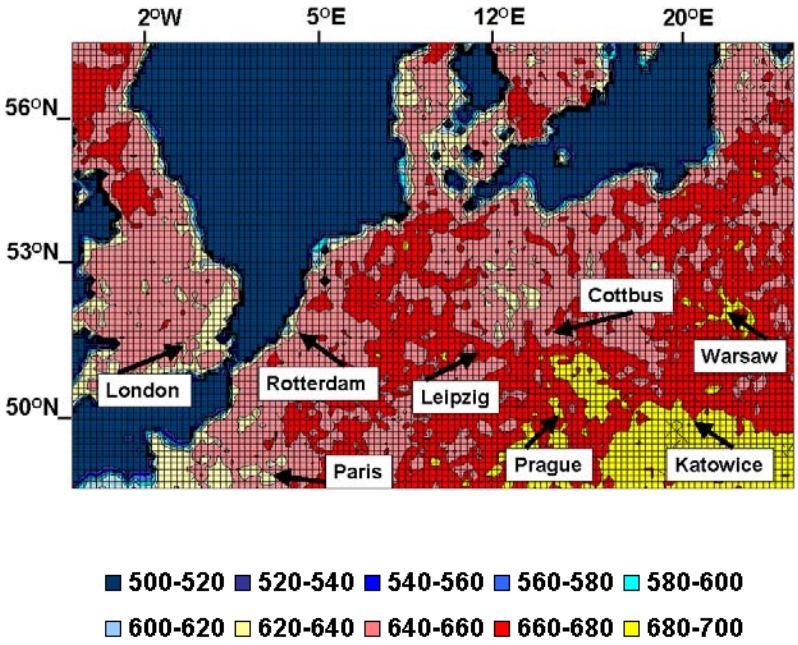

Figure 7. (c) Mean cloud reflectance of low and medium level clouds derived from AVHRR channel 2 data over parts of Europe, given in thousandth (same as 7a). Data are shown from 5.0^0W to 24.0^0E longitude and 48.5^0 to 57.5^0N latitude for the winter period MJJA (May, June, July, August) from 1985 to 1989 (excluding data from 1987). The grid size is 0.25^0 in longitude and 0.125^0 in latitude. The area covers parts of UK, Denmark, Sweden, France, Benelux, Germany, Poland, Czech Republic, the Baltic countries and Ukraine. The North Sea and the Baltic Sea are in black. Strongly polluted areas are indicated.

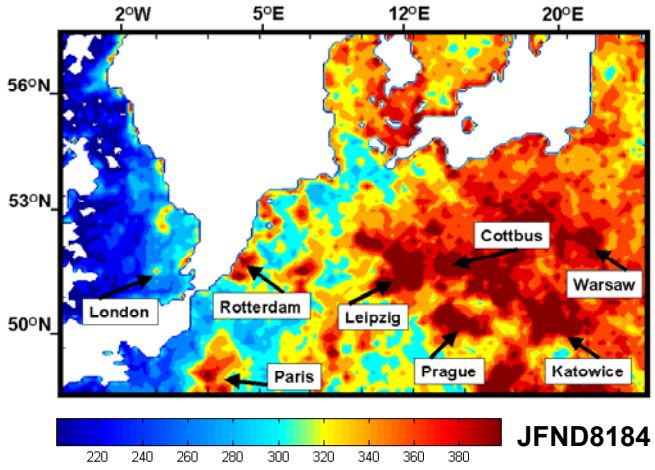

a

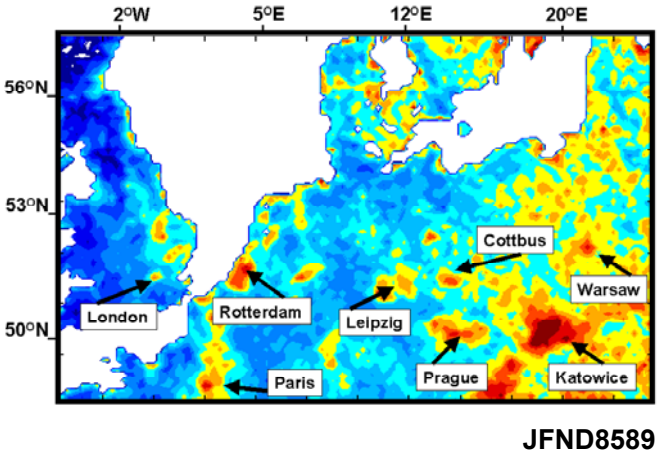

b

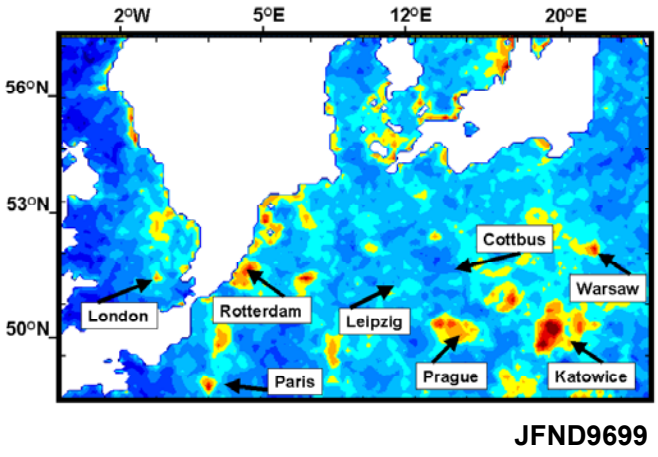

c

Figure 8. Mean coefficient of variation of cloud reflectance derived from AVHRR channel 2 data over parts of Europe, given in thousands; same area as in Figure 7, for the four winter months January, February, November, and December from (a) 1981 to 1984, (b) 1985 to 1989 and (c) 1996 to 1999.

Since the above results clearly point to indirect aerosol effect(s) in a polluted mid-latitude region a related question is:

Is the tendency of cloud albedo over Europe really independent of atmospheric circulation changes ?

In order to receive more details the satellite data are evaluated separately for different circulation conditions. The appropriate way to further subdivide satellite data is to consider European Atmospheric Circulation Patterns (Großwetterlagen). Here, the "catalogue on Großwetterlagen" containing the daily European atmospheric circulation patterns [see Gerstengarbe and Werner, 1993] from 1881 until today, provided by the Potsdam Institute for Climate Impact Research, together with the German Weather Service, is used.

Atmospheric circulation patterns, defined as a mean air pressure distribution over an area at least as large as Europe, are well suitably for further subdividing the satellite data over Central Europe (the data presented in **papers I and III**). The original classification scheme considers three circulation groups comprising 10 major types and 29 subtypes plus undetermined cases. Here, the two major groups, zonal and meridional circulation are taken into account to assess the aerosol influence on cloud albedo.

The zonal circulation group: High sea level pressure covers subtropical and lower middle latitudes and low sea level pressure exists in the sub arctic and higher middle latitudes. The upper airflow is west to east. Cyclone tracks run from the eastern North Atlantic into the European continent. The zonal circulations include all circulation types "West". The zonal circulation group during winter exists for 40% of the data for JFND8589 and 30% for JFND9699; but only 25% for MJJA8589 and 27% for MJJA9699 respectively.

The meridional circulation group: Stationary, blocking high-pressure centres at sea level, are characteristic for the meridional circulation. Depending on the location of the sea level pressure centres and the resulting main flow directions to Central Europe the types "North", "South", and "East" can be distinguished. In addition all troughs with a north to south axis are classified as meridional circulations. The major types "Northeast" and "Southeast" are also included in the meridional circulation group because they normally coincide with blocking highs over Northern and Eastern Europe. The meridional circulation group during winter is due to 25% of the data for JFND8589 and 35% for JFND9699; during summer 38% for MJJA8589 and 39% for MJJA9699 respectively.

The general cloud albedo trend for the subdivisions into individual circulation groups, is in line with the findings presented in **papers I and III** (see table 2 in **paper III**). The cloud albedo for the zonal and meridional circulation groups during winter (JF and ND) is shown in figure 9. Both the zonal as well as the meridional circulation group show the same tendencies (see figure 10a). The tendencies, which are obviously connected to PM emission changes on one hand (seen during ND) and SO_2 emission changes on the other (seen during JF) include:

Firstly, a decrease of reflectance from the early 1980s to the late 1990s occurs during early winter (ND). This albedo decrease primarily follows the emission reduction of PM in Germany. It is pronounced for meridional circulation.

The highest cloud albedo in ND during the early 1980s pollution episode is due to the radius effect. It is also a clear hint to the role of turbulence for effectively lifting primary

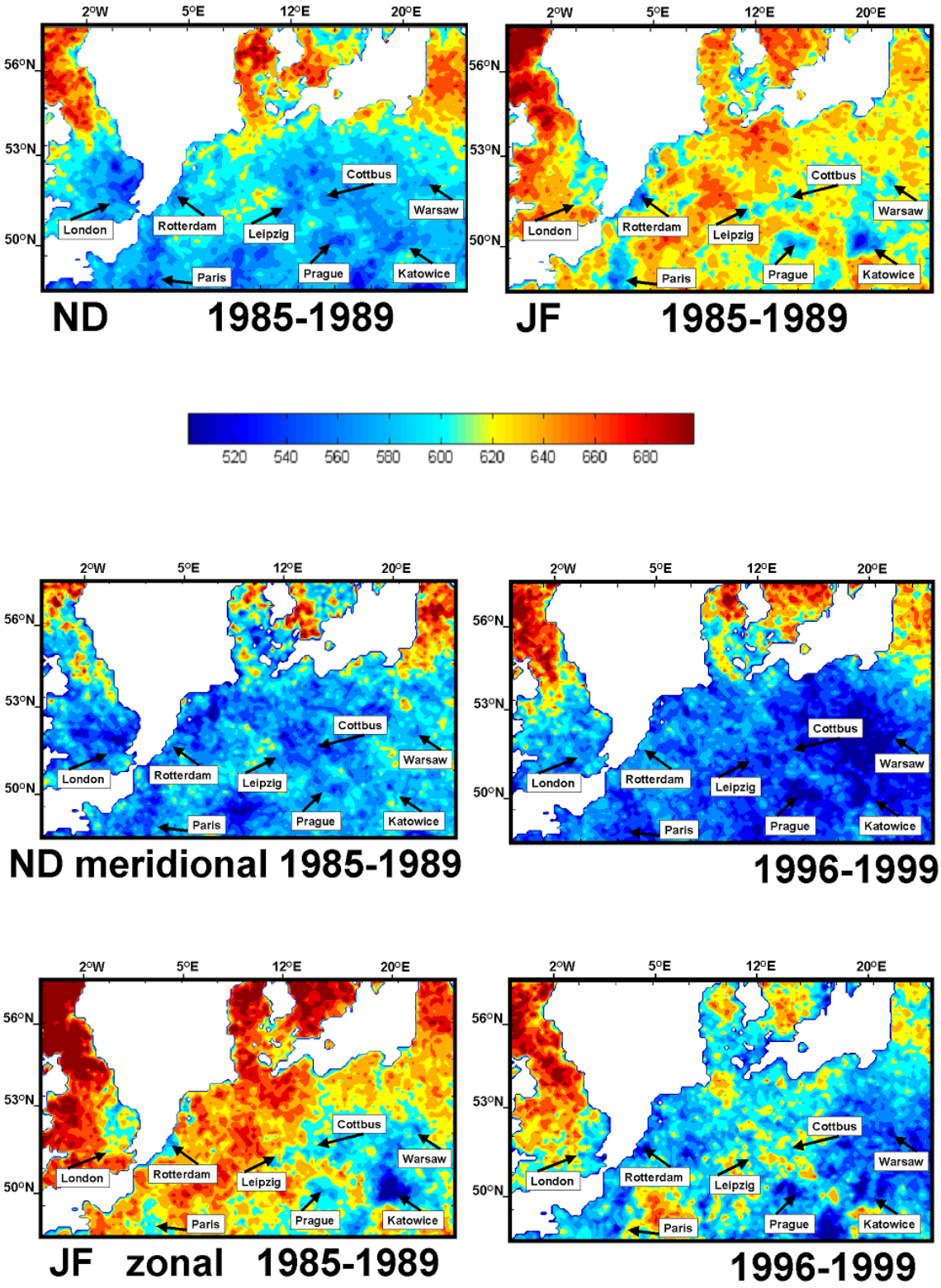

Figure 9. Mean cloud reflectance of low and medium level clouds derived from AVHRR channel 2 data over parts of Europe, given in thousandth. Same as figure 7, but for ND, JF and meridional and zonal circulation.

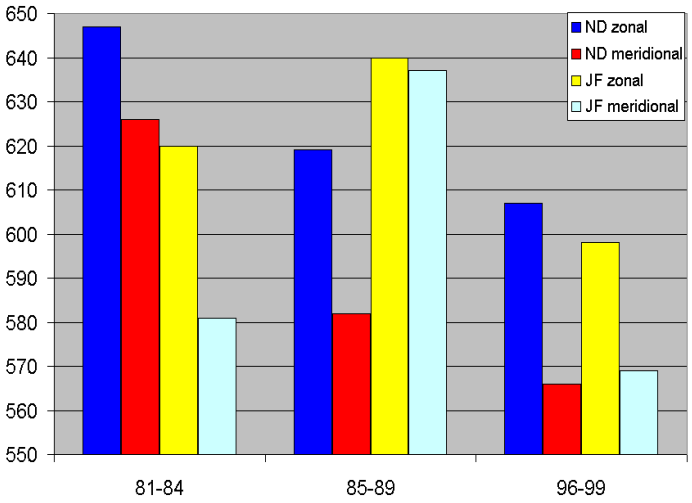

a

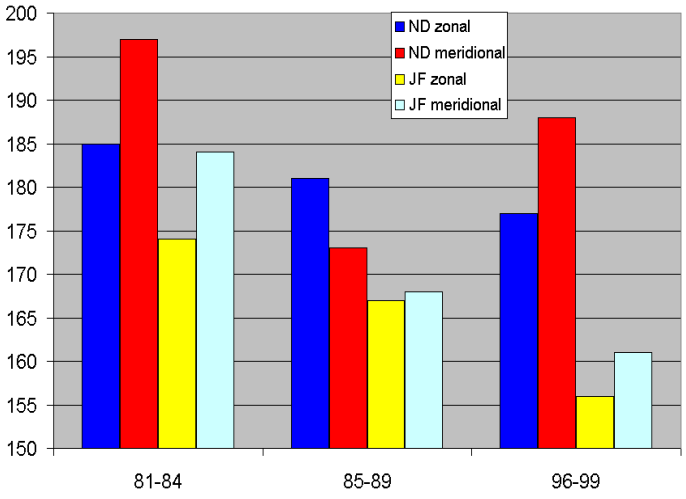

b

Figure 10. (a) Mean cloud reflectance of low and medium level clouds for three time periods derived from AVHRR channel 2 data over parts of Europe, given in thousandth (upper diagram). The values include the data from 5.0^0W to 24.0^0E longitude and 48.5^0 to 57.5^0N latitude for the two-month periods ND (November, December) and JF (January, February). A subdivision is made for zonal and meridional weather types. (b) The lower diagram shows the corresponding mean coefficient of variation.

aerosols to the cloud level. The cloud albedo during ND8184 as compared to ND9699 was 4% higher for zonal circulation and even 6% higher for meridional circulation (see figure 10a).

Secondly, in JF the magnitude of cloud albedo for both circulation groups (see figure 9a) has the tendency to follow the amount of SO_2 emission from power plants in the former GDR (see figure 6b). The albedo shows the highest value for JF8589, pointing to the major influence of secondary aerosols. As before the changes for the meridional circulation group are stronger. Also this is in accordance with **paper III**. The explanation is that the episodes in late winter with more often stably stratified atmospheres favour the formation of sulphate layers, i.e. haze, which in turn enhance the cloud albedo through the radius effect. The observation of haze over Central Europe is described in **paper III**.

Thirdly, the trend in variability (see figure 8) is highly influenced by the PM emissions, because of the higher BC content, which can lead to higher absorption and a lower cloud albedo. However, also secondary particles are contributing to the overall variability through an albedo increase.

Another interesting result becomes visible when comparing the change in variability for both circulation groups: Only for zonal circulation the variability in ND and JF is jointly decreasing; for meridional circulation the variability of cloud reflectance decreases from JF8589 to JF9699 but increases from ND8589 to ND9699. This principally could be explained with two processes: An increase of BC emissions within the study area as well as the advection of pollution from southern or eastern Europe outside the considered study area.

The major tendencies described above for three four-year episodes (figure 10a,b) for zonal and meridional circulation classes are well reproduced even when analyzing only two-year episodes. This points again to a dominant pollution influence and not to circulation changes.

So far, the changes of mean cloud albedo for the total study area show that the cloud reflectance is strongly influenced by indirect aerosol effects. Therefore, the final point which needs to be discussed are the changes in sub-regions within the study area in Central Europe. The question is related to the influence of spatially varying aerosol composition, which should lead to quite different balances of the absorption effect and the radius effect in Central Europe:

Are the changes in cloud albedo dependent on aerosol type ?

Such details are analyzed by comparing the albedo changes for the strongest emission change, i.e. from the late 80s to the late 90s, dependent on mean cloud albedo. This dependency is investigated because the lowering of cloud albedo, caused by absorbing aerosols during winter, indicates a high soot concentration characteristic for urban aerosol in Central Europeans metropolitan and industrial areas. The subdivision of the satellite data into different ranges of mean cloud albedo (as observed JFND8589) therefore should show whether the cloud albedo changes are dependent on the proportion of soot to sulphate concentration.

The results for the wintertime four-month means reveal that the indirect aerosol effect is dependent on distance to the emission centres (see **paper I**). The maximum decrease of cloud albedo, caused by the declining radius effect from JFND8589 to JFND9699, occurs in distances of a few hundred kilometres away from the sources of pollution.

In the following a further subdivision into different Großwetterlagen and two-month means is made. The major characteristics can be seen in figure 11. The most pronounced radius effect occurred during JF for both the zonal and meridional circulation. It is explained by the influence of sulphate layers in more often stable atmospheres. The maximum albedo decrease of 7.8% is due to the meridional circulation type in regions of mean JFND8589 reflectance (as shown in figure 7a) of about 60-62%. A detailed analysis for the area around Leipzig reveals that the radius effect is stronger for stratus clouds than for cumulus clouds (see **paper III** for further details).

Generally, in source regions of pollution the albedo decrease caused by decreasing radii is smaller. This smaller albedo decrease is caused by the absorption effect, which has opposite sign. It is most pronounced when a larger part of absorbing aerosol particles enters the clouds in ND during zonal flow condition. However, such a lowering is not seen for the meridional circulation during ND. Since this result could be caused by locally increasing soot particle numbers a geographical subdivision of the study area was performed in addition: A western of 12.0^0E longitude (figure 12a) and the remaining eastern part of the study area (figure 12b), the latter including Poland and a part of the Czech Republic.

The analysis confirms: While there is a slight albedo increase in source regions in the western part and even in remote regions (as seen for meridional circulation over parts of UK), there is a much stronger albedo decrease in source regions of the eastern part. Since a strong additional albedo decrease is only seen in the eastern part for meridional circulation, it is likely to caused by absorption of diesel soot originating from road traffic. Since soot particles at the time of the emission are assumed to be hydrophobic an aging during the meridional circulation could favour that these particles enter the clouds. An additional explanation could be the enhanced dry deposition of fine absorbing particles for the more often turbulent zonal circulation. Since the strongest albedo decrease occurs over the cities in Poland it is assumed that the soot particle number may have increased there from the late 80s to the late 90s. Especially the region around Warsaw shows conspicuously low cloud albedo values, which is a clear indication for the influence of soot emissions due to the rapid increase of road traffic in eastern Central Europe. The result is confirmed by analysis of the frequency distributions, which still show a radius effect during the winters of the late 1990s.

The results for summer (figure 13) also support the conclusion of an anthropogenic influence over the most polluted part of Central Europe including Germany, Poland and the Czech Republic. During summer, same as in winter, the most pronounced radius effect occurs over the regions of strongest pollution. The highest decrease in reflectance, by more than 4%, occurred in areas of highest SO_2 concentrations during the late 80s. The remote regions show, as for winter, a much weaker decrease of only 1% reflectance.

The stronger changes for the meridional circulation could be explained by less air mass exchange and a subsequent accumulation of pollutants in the atmospheric boundary layer. A very interesting result emerges for coastal areas: cloud albedo is increasing towards the 90s while it is decreasing for the areas of maximum sulphate concentration during the 80s. This phenomenon is just seen for more often turbulent weather situations during MJ, when advection of aerosol particles from source regions to the coastal lines is enabled by meridional circulation. The result again suggests that the number concentration of fine particles in parts of Central Europe may have increased from the late 80s to the late 90s.

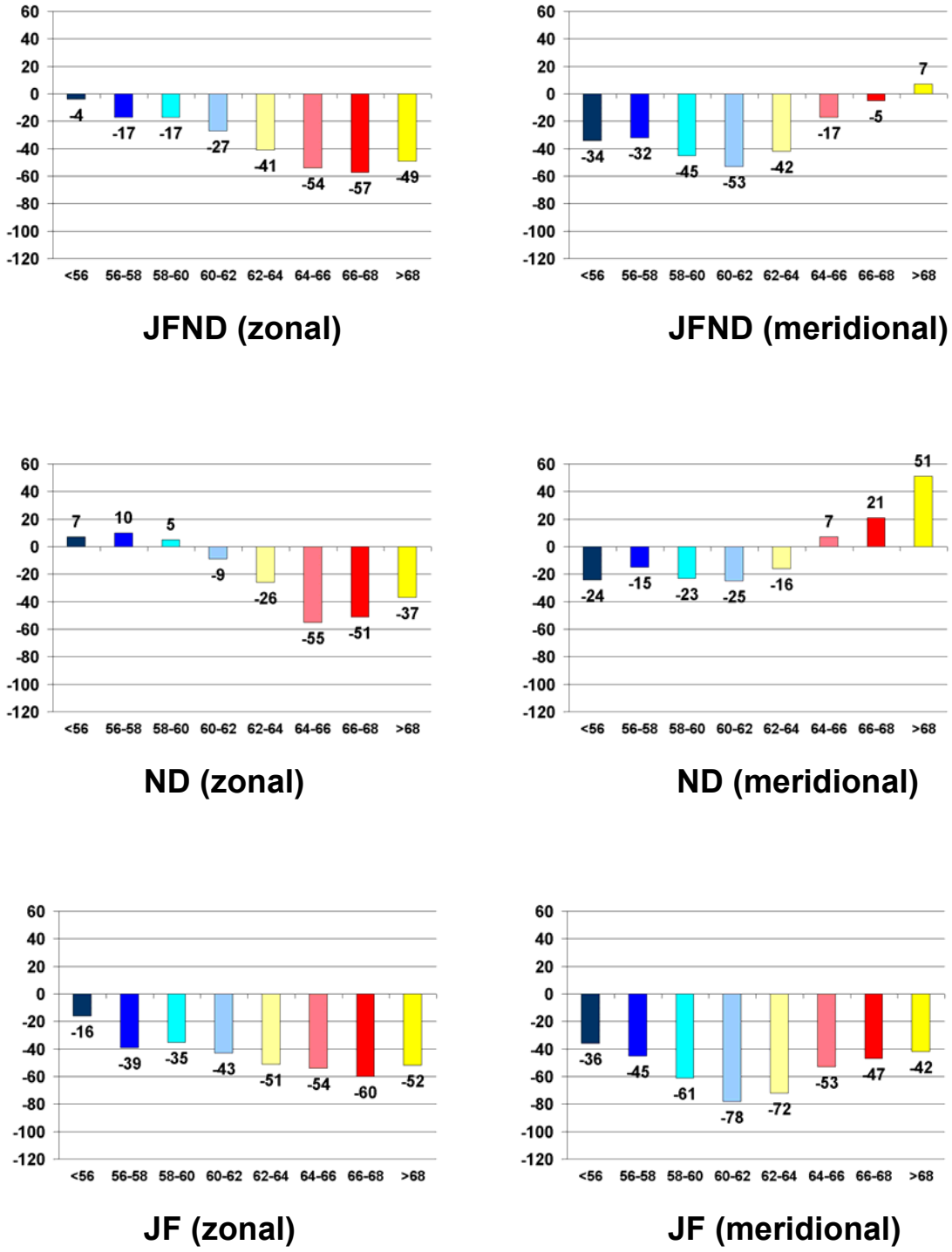

Figure 11. Change of cloud reflectance during winter in thousandth (axis of ordinate) from 85-89 to 96-99 (decrease is negative) for JFND (upper), ND (middle) and JF (lower) for different reflectance classes (unit: %) as depicted in figure 7a,b for JFND8589 (same colors). Changes are shown for zonal circulation (left column) and meridional circulation (right column).

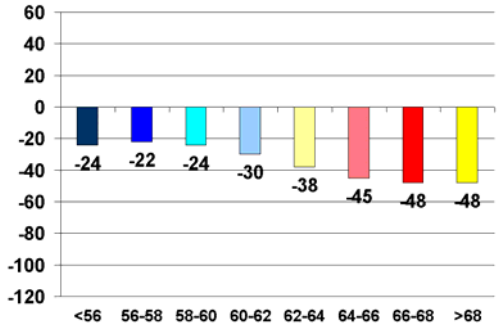

JFND (zonal) 5.0^{0}W - 12.0^{0}E

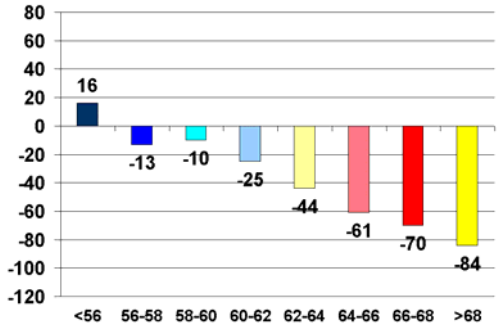

JFND (zonal) 12.0^{0}E - 24.0^{0}E

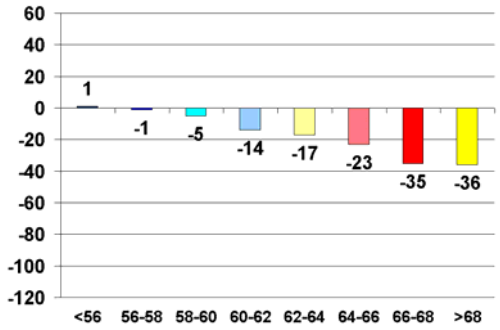

ND (zonal) 5.0^{0}W - 12.0^{0}E

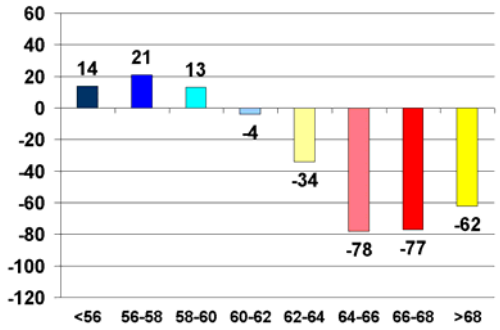

ND (zonal) 12.0^{0}E - 24.0^{0}E

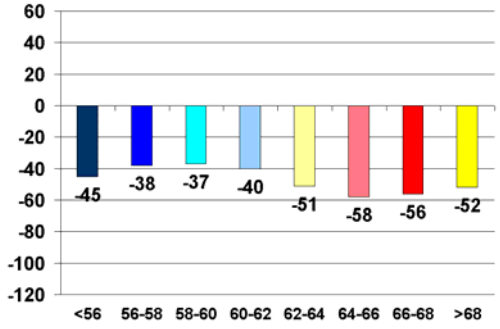

JF (zonal) 5.0^{0}W - 12.0^{0}E

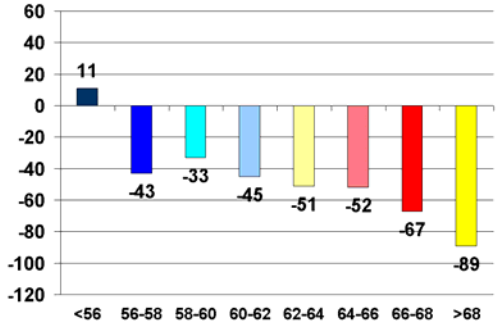

JF (zonal) 12.0^{0}E - 24.0^{0}E

Figure 12. (a) Change of cloud reflectance during winter in thousandth (axis of ordinate) from 85-89 to 96-99 (decrease is negative) for JFND (upper), ND (middle) and JF (lower) for different classes of mean reflectance (unit: %) as depicted in figure 7a,b for JFND8589 (same colors). Changes are shown for zonal circulation from 5.0^{0}W to 12.0^{0}E longitude (left column) and from 12.0^{0}E to 24.0^{0}E longitude (right column).

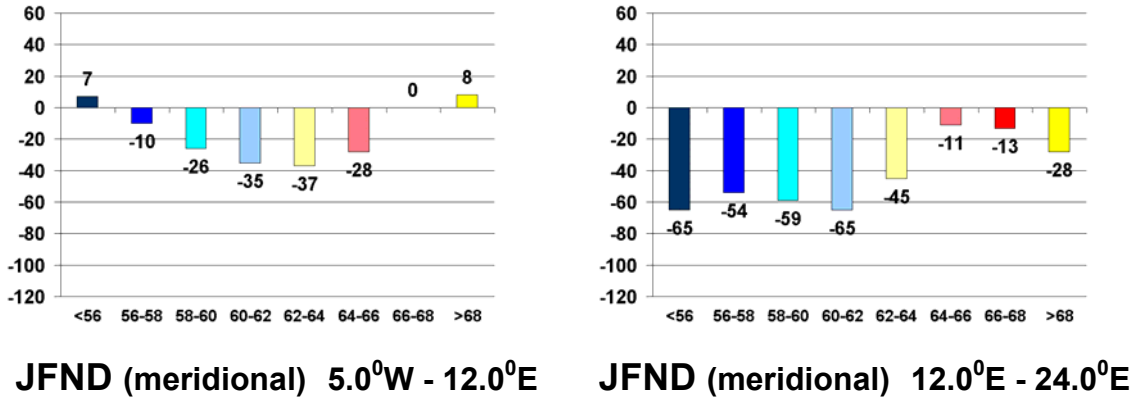

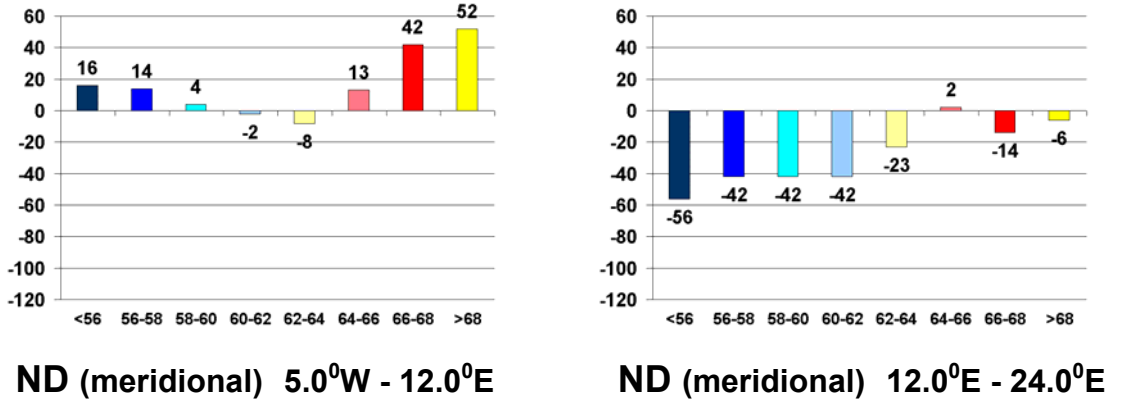

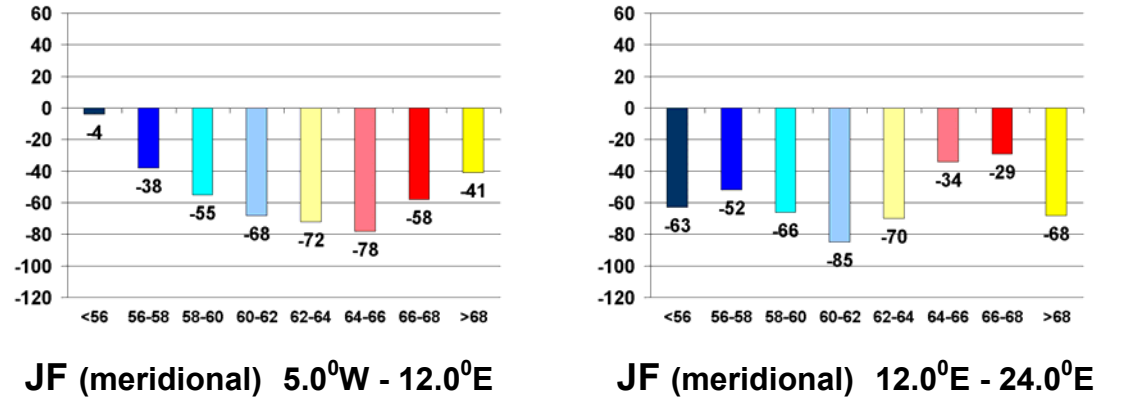

Figure 12. (b) Change of cloud reflectance during winter in thousandth (axis of ordinate) from 85-89 to 96-99 (decrease is negative) for JFND (upper), ND (middle) and JF (lower) for different classes of mean reflectance (unit: %) as depicted in figure 7a,b for JFND8589 (same colors). Changes are shown for meridional circulation from 5.0^{0}W to 12.0^{0}E longitude (left column) and from 12.0^{0}E to 24.0^{0}E longitude (right column).

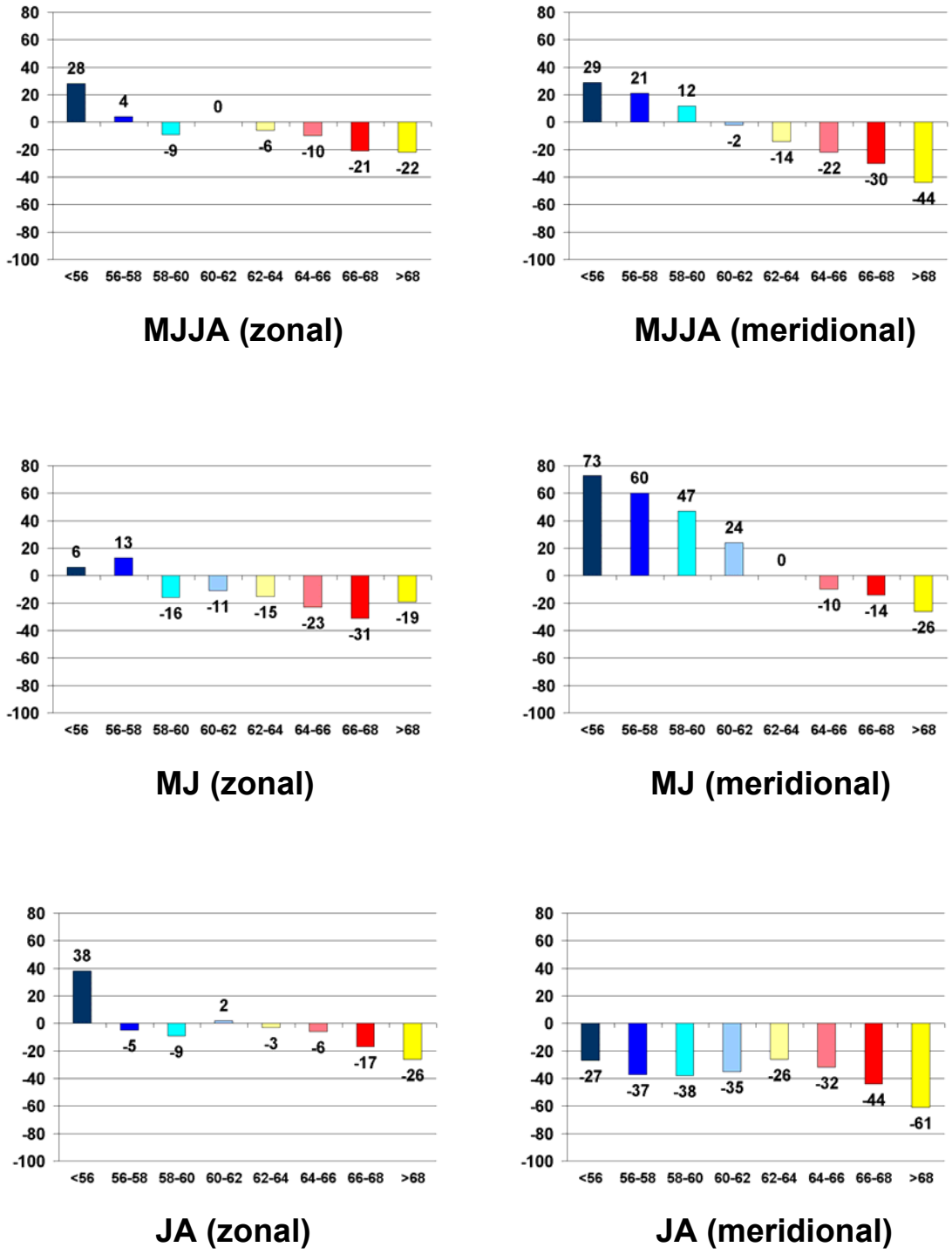

Figure 13. Change of cloud reflectance during summer in thousandth (axis of ordinate) from 85-89 to 96-99 (decrease is negative) for MJJA (upper), MJ (middle) and JA (lower) for different classes of mean reflectance (unit: %) as depicted in figure 7c for MJJA8589 (same colors). Changes are shown for zonal circulation (left column) and meridional circulation (right column).

3.2 Detection over South East Asia

The decision to study indirect aerosol effects over South East Asia was motivated by the conspicuous anomalies of temperature changes close to polluted regions worldwide. Schneider and Held [2001] identified significantly different temperature changes relative to the 1916-98 mean warming over parts of North America and Europe as well as in China: Temperature has decreased just in the most polluted regions of the continents while the global mean near surface air temperature was increasing.

The pollution in China mainly originates from burning of coal and biomass, traffic as well as secondary aerosol formation from precursor trace gases. In densely populated and industrialized regions of China high amounts of aerosols with a strong contribution by fine particles smaller than 2.5 micrometers in diameter (PM2.5) are directly emitted. The carbonaceous portion can account for about 40% of the total PM2.5 mass [Ye et al., 2003].

A plausible consequence for increasing air pollution would be an increased local planetary albedo (LPA). As discussed before this was observed over Europe, where cloud albedo decreased significantly, when air pollution levels decreased after the collapse of the former East Block and after clean air acts in OECD countries (**paper I**). Therefore changes with opposite sign for cloud optical properties could be expected because of increasing emissions over China.

Amazingly, the analysis of the same NOAA AVHRR data series over China shows another result: The LPA increases from the late 1980s to the late 1990s only during summer southward of 30^0 N. Northward of 30^0 N even a decrease becomes visible. During winter the LPA is strongly decreased in nearly all regions (figure 14a,b). The highest decrease (comparison of 4 year averages, as for Europe) of LPA in winter by up to 11% from the late 1980s to the late 1990s occurred over strongly polluted regions. Such a pronounced change with maximum values during winter is unique if compared to North America and Europe. The heterogeneity of the change in China, i.e. higher values of change in densely populated and industrialized areas, generally suggests that air pollution is the main cause.

However, air pollution in China was much more pronounced during the late 1990s than during the late 1980s [Xu, 2001]. Therefore the negative LPA change cannot be explained by a strong decrease of sulphur dioxide (SO_2) emissions, as it took place enforced by Clean Air Acts in North America over recent decades and in Europe since the early 1990s. In Europe, as discussed above, an extreme emission reduction by about 23 Tg y^{-1} sulphur, which is not seen at all in China, was the reason for a lowering of low and medium level cloud albedo of about 2-3% within a decade (**paper I**). Only a much lower average cloud optical thickness over southern China in combination with regionally extreme strong SO_2 reductions could have led to such a pronounced decrease of LPA. Also it would be unrealistic to assume that a strong reduction of secondary particles (sulfates formed from SO_2) is only limited to source regions.

On the contrary, evidence for an increase of air pollution in China is seen from increasing aerosol influence in AVHRR satellite measurements for cloudless episodes in densely populated areas. The change of apparent reflectance for cloudless episodes indicates that the optical thickness in the areas around Beijing, Shanghai and the Red Basin has increased. In these areas of China satellite data and models show highest values of present day aerosol optical thickness worldwide [Ramanathan et al., 2001]. The values are even twice as high as in metropolitan areas of the United States of America and in Europe.

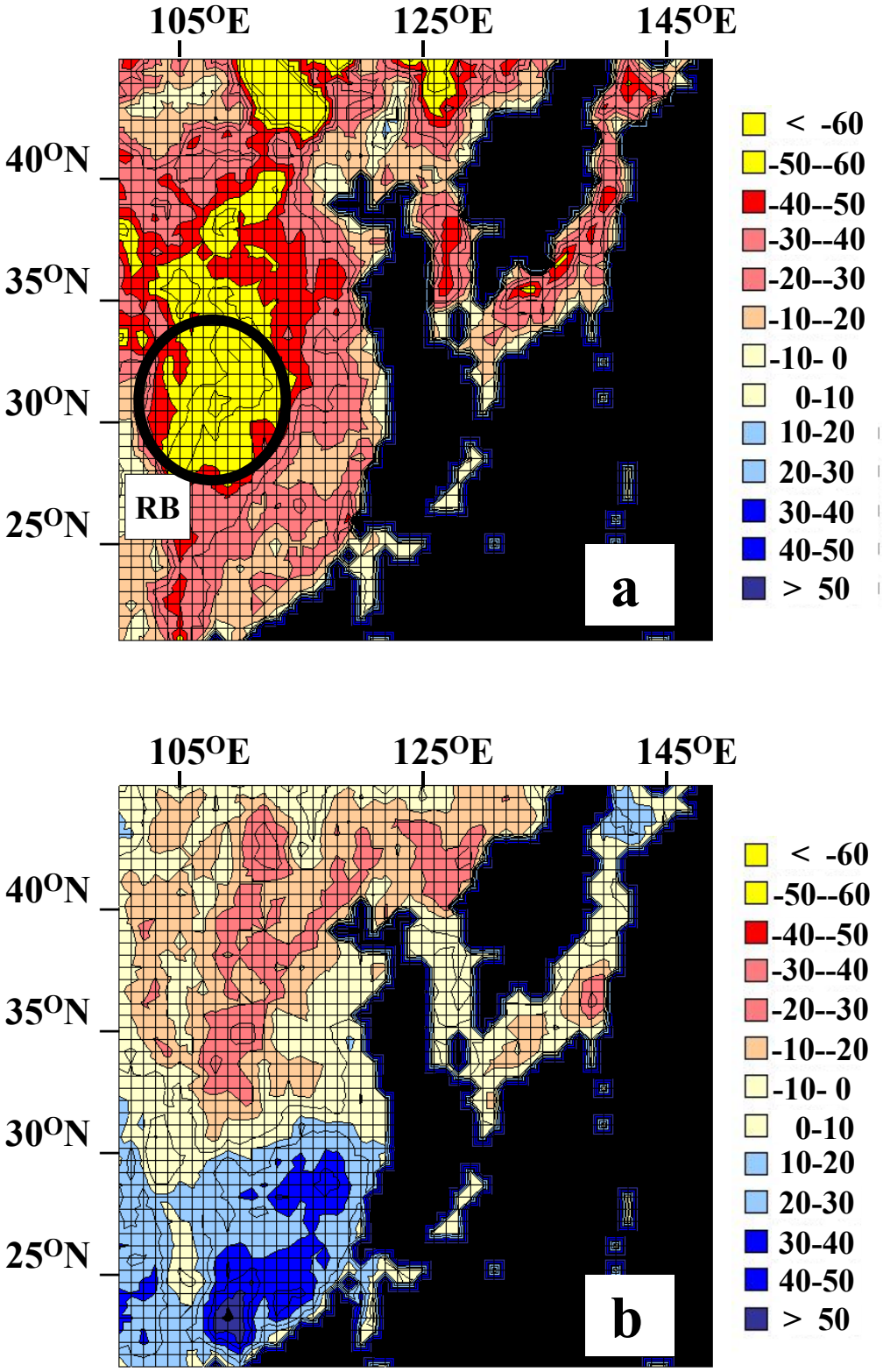

Figure 14. Changes of the local planetary albedo (LPA) in thousandth at ~0.8 μm wavelength (AVHRR, channel 2) from the late 1980s (1985, 1986, 1988, 1989) to the late 1990s (1996, 1997, 1998, 1999) over south-eastern Asia for winter, JFND **(a)** and summer, MJJA **(b)**. The grid size is 1^0 longitude and 0.5^0 latitude. The area covers China, Mongolia, North Korea, South Korea, Japan and parts of the Pacific (in black). The Red Basin (RB) is indicated.

In order to explain the strong decrease of LPA the investigations presented in **paper II** were focused on regions with enormously high aerosol optical depth. One of those areas is the Red Basin in southern China (see figure 15). The area is characterized by dense population and includes important industrial branches based on hard-coal, oil and natural gas use. The combination of high emission source strength and topography favour the accumulation of pollutants in the lower troposphere. Over the Red Basin the decrease of LPA from the late 1980s to the late 1990s is much stronger than in all other areas of China. The highest decrease is seen for winter.

Just over this part of China the LPA pattern for both the late 1980s and the late 1990s as well as during winter and summer points to another interesting feature: Highest LPA, when combining cloudless and cloudy areas, occurs within the Red Basin. The values decline with distance to the basin. Therefore it was investigated if pollutants originating from the Red Basin have such a dominant influence on the LPA of southern China. The positive correlation between the LPA values and its relative change in winter supports the hypothesis of indirect aerosol effects (see **paper II**).

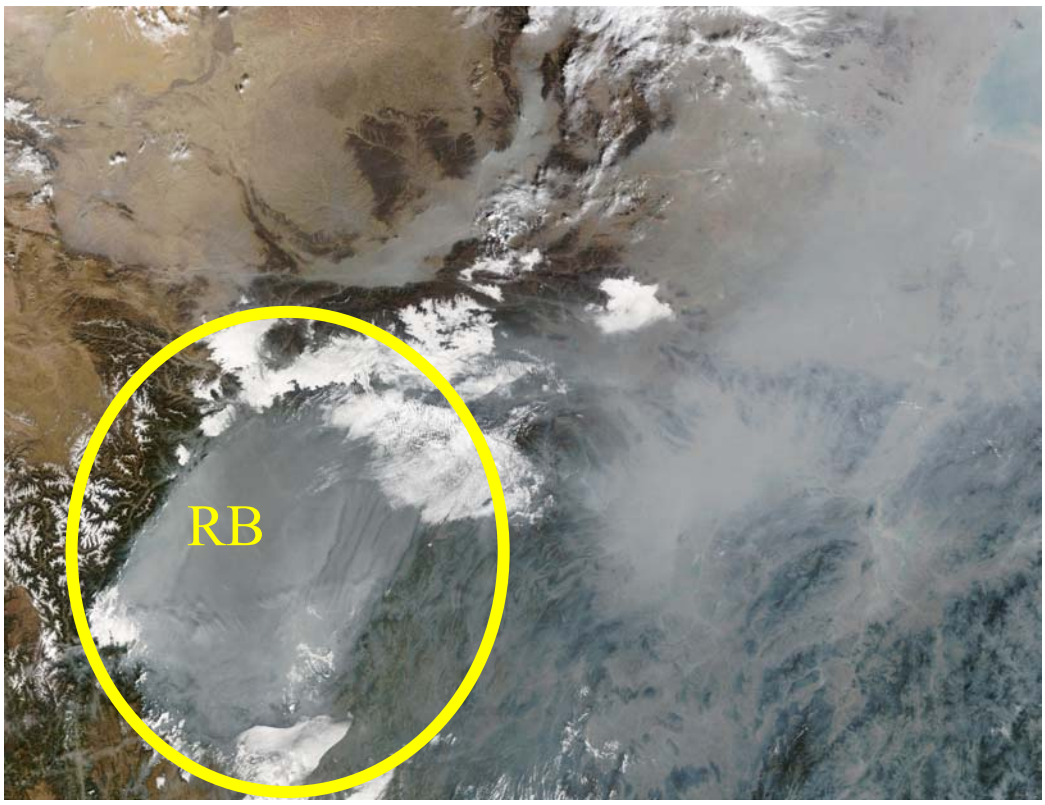

Figure 15. The Red Basin centered at 30^0 N latitude and 105^0 E longitude (RB) has a dimension of more than 300x300km^2 and is surrounded by high mountains in nearly all directions. The glacierized peaks of the Blue Tibetan Mountains in the west reach a height up to 7500m. The image observed by MODIS on TERRA on November 10, 2002 includes optically thick haze covering a large region of central China. In some areas (e.g. around Wuhan) the haze completely obscures the surface from the satellite's view. The polluted clouds within the Red Basin show a reduced albedo.

The finding above with respect to a LPA maximum over the most polluted area would agree with the assessment of Twomey et al. [1984] regarding the impact of pollution on global cloud albedo. However, the decrease of LPA for increasing pollution from the late 1980s to the late 1990s for all areas in winter and northward of 30^0 N in summer leads to the question: why is this reasoning not applicable on the regional scale over south-eastern Asia?

In order to find hints about the indirect aerosol effects contribution to LPA decrease firstly, the apparent albedo of low and medium level clouds was analysed. Generally the mean apparent albedo of these clouds over China shows a gradient from South to North. While south of 35^0 N the mean albedo amounts to more than 50% it decreases to lower values in North China. The low mean albedo can be explained by optically thinner clouds in the dry areas. During the summer monsoon period a low mean apparent cloud albedo is limited to areas approaching the Gobi desert.

Since the strongest radius effect can be expected for optically thin clouds the distinct cloud optical thickness in different areas of China enables to evaluate the influence of the pollution in more detail. The change of LPA due to low and medium level clouds from the late 1980 to the 1990 for the areas with a clear contribution of optically thin clouds illustrates this (see **paper II**). In the Gobi desert cloud albedo increases which indicates an effect of decreasing cloud droplet radius. However, the changes cannot be explained alone by enhanced natural emissions of mineral dust through sand storms. The seasonal dependency supports that particles of anthropogenic origin have the major influence. The radius effect is most pronounced during the summer monsoon when anthropogenic aerosols are advected to the north from emission areas in southern and eastern China. Several hundred kilometres farther southeast the indirect aerosol effect shows a different behaviour. Around Beijing the high black carbon content of aerosol causes a slight cloud albedo decrease from the late 1980s to the late 1990s, although the mean optical depth of low and medium level clouds is comparably low. An absorption effect as a consequence of high BC concentration in addition to a radius effect can explain it. The balance between the radius effect and the absorption effect is similar for winter and summer for the Beijing area.

In southern China where mean cloud optical thickness is much higher, and where major source regions of pollution exist, during summer only a slightly decreased albedo of low and medium level clouds is observed. However, here the strongest contribution of these clouds to the total decrease of LPA from the late 1980s to the late 1990s occurs, during winter, in densely populated and highly polluted areas. This is a clear reference to the dominance of absorption, i.e. the high black carbon content, in cloud air. It is remarkable that maximum values of LPA occur just around these areas for summer as well as for winter. Two key questions formulated in **paper II** arise from this conspicuous regional climate change:

Has cloud cover changed as a consequence of increased air pollution ?

Is brown haze responsible for the change of the local planetary albedo ?

In order to answer the first question cloud coverage of low and medium level clouds was analysed (see **paper II**). It shows another interesting result: A maximum exists just over the Red Basin. It is related to the additional indirect aerosol effect, the so-called lifetime effect. As a consequence of the radius effect it describes an increase in cloud lifetime and thus in cloud coverage. Over the Red Basin continuously high aerosol number concentrations can lead to a nearly permanent radius effect with a considerably

decreased effective radius of cloud droplets. Under these conditions coalescence is largely suppressed. Consequently the lifetime of clouds grows. But also the cloud water path increases thereby, which in turn increases cloud optical thickness, leading to increased cloud albedo in addition. Model studies of the indirect aerosol effect caused by sulphate and black carbon aerosols using the NCAR CCM3 climate model confirm this interpretation [Kristjansson, 2002]. Kristjansson estimated the worldwide largest decrease in cloud droplet radius and cloud water path increase due to anthropogenic aerosols over SE Asia. Since cloud cover by low and medium level clouds over the Red Basin increased from the late 1980s to the late 1990s it is concluded that an increasing lifetime effect is also involved. Therefore the first question can be answered preliminarily as follows: Cloud cover has changed as a consequence of increased pollution; however, the increase of cloud cover so far discussed is not consistent with the reduction of low and medium level cloud reflectance and it does not explain the decreased LPA from the late 1980s to the late 1990s.

From the discussion about the increased or decreased apparent cloud albedo as well as the increased cloud cover it becomes clear that air pollution in southern China strongly influences LPA. It is also evident that under such conditions enormous haze layers must occur in cloudless areas or above clouds. In principle these haze layers could also be the reason for the increased cloudiness if haze is interpreted as a cloud. On the other hand, a decrease of LPA by haze is less likely because an increase of haze generally leads to an increased LPA and cloud albedo, except for brown haze. Indeed, as seen from the frequency distribution of reflectance for all cases classified as cloudy there is strong brown haze over China. In order to study the influence of haze on LPA brown haze layers are separated from low and medium level clouds. These haze layers are already removed from the low and medium level clouds discussed above. Strong brown haze layers effects, which become in parts visible in the so-called, residual LPA change (see **paper II**), where clear atmospheres, high level clouds and optically thin sub-pixel cloudiness are combined, show the following characteristics:

The regional distribution of haze frequency in southern China is homogeneous in the northern and heterogeneous in the southern part. There is a much more homogeneous distribution of brown haze north of 30^0 N and east of 105^0 E. Peak values exceeding 10% of all measurements occur over the densely populated regions around Wuhan and Nanjing north of the mid-to-lower Jangtze Basin. The cities in the South show lower values. In many areas of the South mostly haze layers are detected in less than 6% of all cases.

In winter, there is a clear increase of brown haze from the late 1980s to the late 1990s. The decrease of the residual LPA shows that brown haze is dominant around 110^0 E starting from the mid to lower Jangtze Basin at 30^0 N northwards. It is concluded in **paper II** that the occurrence of brown haze alone cannot explain the strong LPA decrease.

Since neither the lifetime effect nor the occurrence of haze, nor both combined can explain the change of LPA it is concluded in **paper II** that the reason is a reduced mean single scattering albedo of cloud droplets or cloud droplets plus interstitial aerosol caused by a much higher BC content.

The argument above, which can well explain the strong LPA decrease from the 1980s to the 1990s in winter, however, fails to explain the strong LPA increase southward of 30^0 N during summer. Therefore another question arises:

Why is LPA increasing during summer ?

A closer look to the cloud coverage during summer confirms that there is a strong increase from the late 1980s to the late 1990s. Since during summer the vertical transfer of heat, efficiently established by the process of convection, is accompanied by cloud formation the brightness temperature is analyzed. A changing cloud top temperature indicates a changing cloud top height and consequently gives important hints to changes in convection during summer monsoon. Indeed the analysis reveals: The mean brightness temperatures for all atmospheres show in the south-eastern most part of China a conspicuous decrease from the late 1980s to the late 1990s with peak values higher than 10K (see **paper IV**). However, despite the strong decrease in the South, i.e. in the regions around Nanning, Hong Kong and the Pearl River Delta, there is also a remarkable increase by even more than 2 K in brightness temperature in the Red Basin (figure 16a).

When comparing these results with the conclusions in **paper II** it becomes clear: The mean brightness temperature decreases stronger in areas, where absorbing aerosols are less dominant. Such pronounced spatial heterogeneity of the change is an indication for the influence of air pollution (see also **papers I,II,III)**.

Since the areas of strongest cloud brightness temperature decrease coincide with areas of strongest LPA increase and vice versa (see figures 14b and 16a) only the cloudy atmospheres are now investigated. In order to explain the result further insight into the processes, which are involved, can be received with a separate discussion for the fully cloudy pixels and those classified as mixed, such as sub-pixel cloudiness (see **paper IV**). The more detailed subdivision is enabled through the spatial signature tests, which demand a uniform 2 x 2 pixel array (see cloud classification described in section 2). The so-called mixed pixels represent a heterogeneous part of the satellite scene, usually containing partially cloudy areas, e.g. scattered cumulus. The major results for the cloudy data are (see figure 16b):

- The mean cloud brightness temperature decreases generally from the 1980s to the 1990s reaching a maximum value of 12K.

- The strongest decrease in cloud brightness temperature occurs near to major cities Nanning, Guangzhou, Guilin, Xiamen, Fuzhou, Changsha, Nanchang, Wuhan, Chongquing, Chengdu and Nanchong.

The mixed data (partly cloudy pixels) amazingly show the opposite: In regions where fully cloud covered pixels show a maximum decrease in brightness temperature, the mixed data show a very small decrease or even an increase (figure 16c). The latter is seen just near to and within the Red Basin, where black carbon in clouds strongly reduced the cloud albedo (**paper II**). Obviously strong absorbing aerosol leads to a reduction of mixed pixels. The results point to the argument, that brown haze enhances solar heating and lowers relative humidity. Consequently the lifetime of clouds is shortened leading to lower mean cloud top height. The interpretation is in agreement with two other studies during INDOEX (Ackermann et al., 2000) and in the Amazon

region dealing with observation of scattered cumulus during biomass burning episodes (Koren et al., 2004).

In the southern part of the study area the negative brightness temperature trend (see figure 17a,b and **paper IV**) for mixed data is only observed in urban areas, e.g. close to Nanning, Guangzhou, Guilin and Fuzhou. Near to these cities, where air pollution locally shows strong haze, cloud top brightness temperature frequently is below 185K.

The overall conclusion that pollution changes cloud top temperature is supported by another study for Europe (Devasthale et al., 2005). Over Europe during the late 1980s, cloud top temperatures were colder by more than 2K for low and medium level clouds and even 4K lower for convective clouds, as compared to the 1990s (same study area as in **papers I, III**). Further, cloud top temperature in polluted regions was accompanied by a higher variability (as for channel 2 in **papers I, III**), suggesting an indirect aerosol effect in the thermal spectral range. In **paper IV** the indirect aerosol effect in the thermal spectral range is estimated to be in the same order of magnitude than in the solar one.

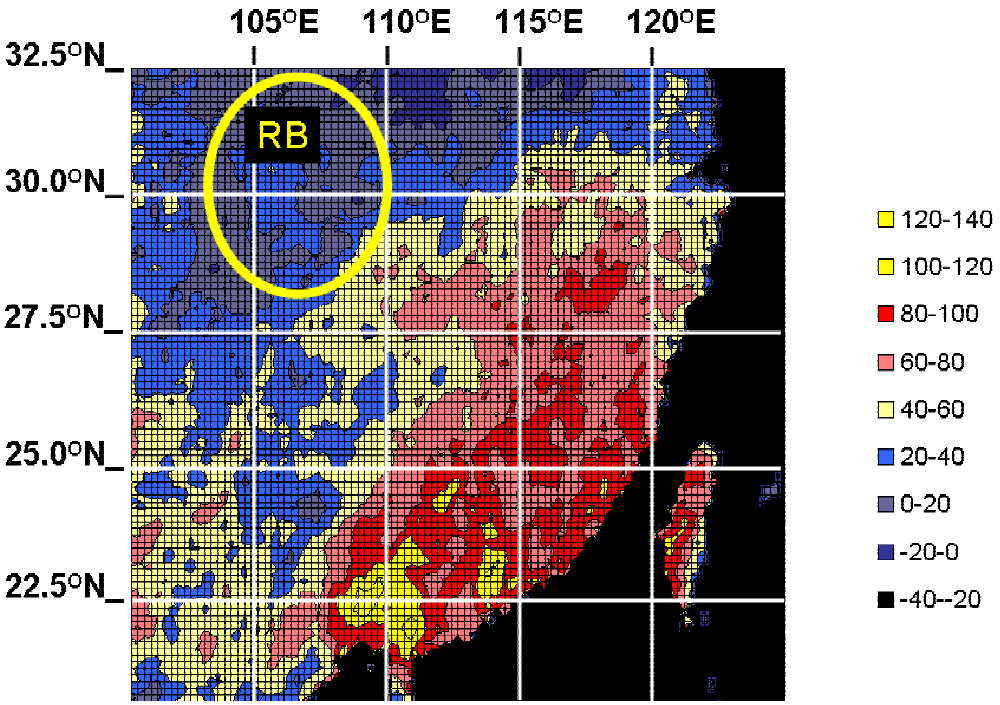

a

Figure 16. (a) Brightness temperature changes for southern China (AVHRR channel 5) in summer from MJJA8589 to MJJA9699 [unit: 0.1 K]. The grid size is 0.250^0 longitude and 0.125^0 latitude. The Red Basin (RB) is indicated.

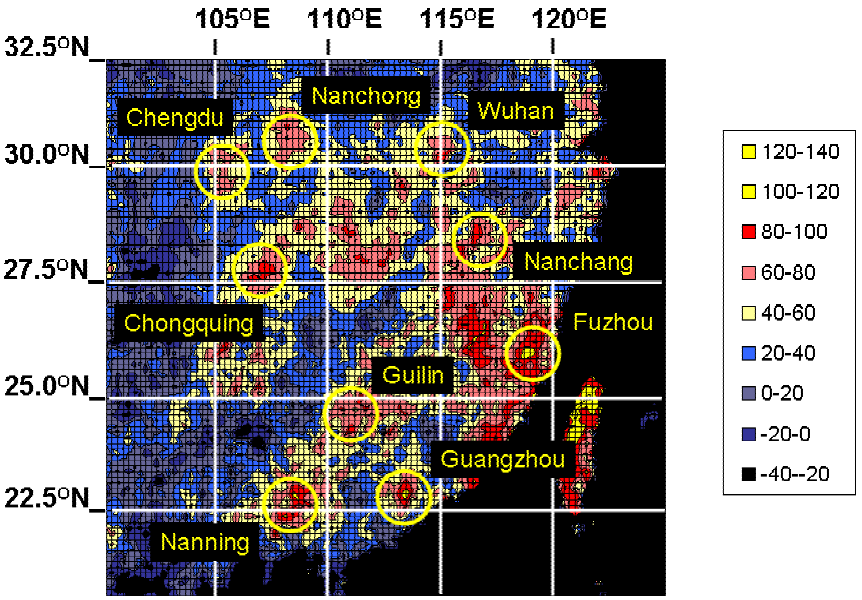

b

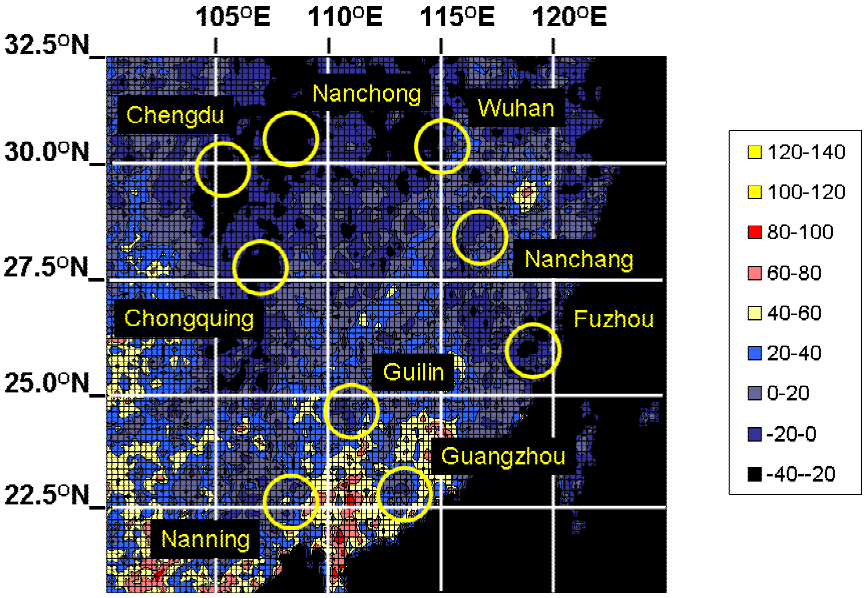

c

Figure 16. Same as **(a)**, but for **(b)** overcast areas and **(c)** partly cloudy pixels (see cloud classification in section 2).

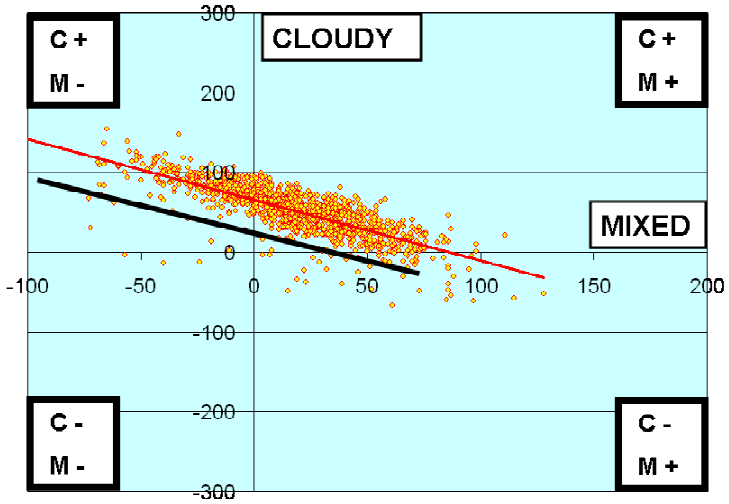

a

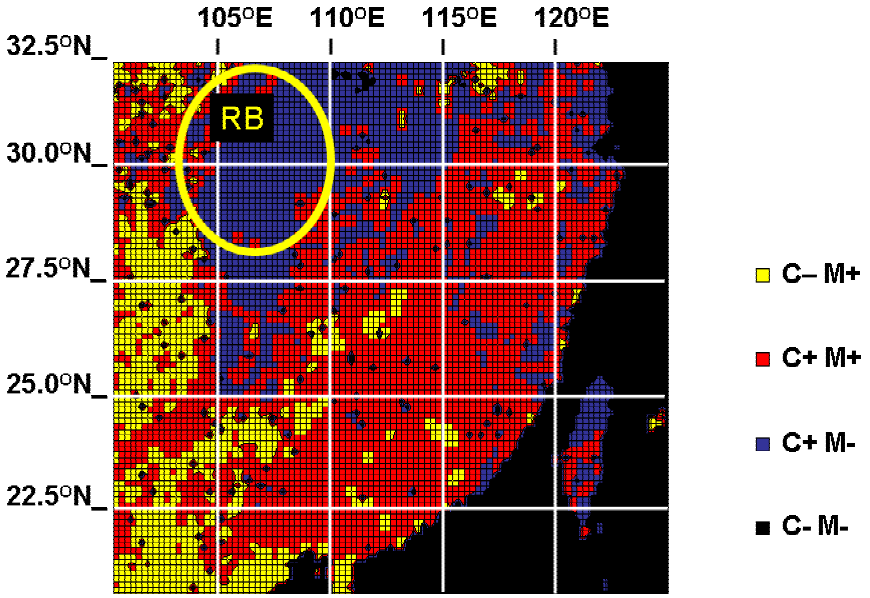

b

Figure 17. Trend in brightness temperature [unit: 0.1 K] for summer from MJJA8589 to MJJA9699 (AVHRR channel 5) for cloudy atmospheres (fully cloud covered pixels denoted as C) and mixed atmospheres (partly cloudy pixels denoted as M) in southern China (see cloud classification in section 2). The grid size is 0.25^0 in longitude and 0.125^0 in latitude. The scatter diagram (a) relates the trends for C and M (C+ means a decrease in brightness temperature or an increase in cloud top height for cloudy pixels, M- means an increase in brightness temperature or a decrease in cloud top height for partially cloud covered areas) for data in the South (from 20.0^0N to 26.0^0N and 100.0^0E to 125.0^0E), including a regression line (in red). The regression line for the Red Basin (from 27.5^0N to 32.5^0N and 100.0^0E to 115.0^0E) is also shown (in black). The tendencies for the total area are depicted in (b). The Red Basin (RB) is indicated.

4. FUTURE RESEARCH DIRECTIONS

The identification of indirect aerosol effects in satellite data, presented in section 3 and in the **papers I**, **II**, **III, IV** [Krüger and Graßl, 2002, Krüger and Graßl, 2004, Krüger et al., 2004, Krüger et al., 2005], stimulates further studies dealing with anthropogenic aerosol particle concentrations. Since the detection was successful on the regional scale a new focus now should be given to the magnitude of indirect aerosol effects during aerosol transport far away from anthropogenic sources. On the other hand the source regions itself deserve further attention. Also details about aerosol cloud interactions should be investigated. The first study type can be well investigated in remote oceanic regions by adding satellite observations in the microwave range to augment water cycle information. Further, a special focus should be haze cloud interaction with emphasis on the urban environment, especially those regions where the concentrations of air pollutants are dramatically enhanced, e.g. in China or India.

4.1 Studies over the Ocean

Studies in oceanic areas should be conducted to investigate indirect aerosol effects during the inter-continental transport of aerosols and their precursor gases. Here the overall effects of aerosols need to include studying the influence of air pollution on the dynamics, which even might change pressure patterns. Well suited for such studies are the oceanic areas on the northern hemisphere, where both the Pacific and the Atlantic would be perfect natural laboratories because of major pollution sources in China and the eastern United States of America.

Measurements from satellites over the ocean confirm a hazy picture [Chung, 1986], whereby large amounts of aerosol particles enter the marine atmosphere from the continents, (figures 18a,b,c). Additionally, differently than over the continents, where an enhanced number of anthropogenic aerosol particles increases or decreases the local planetary albedo (**papers I, II, III**), natural sources may have a strong contribution over the oceans. Besides the natural oceanic emissions, i.e. sea salt and dimethylsulfide (DMS), mineral dust and biomass burning aerosols from the continents are important contributions to the aerosol load over the ocean.

The radiative effects in cloudless atmospheres will be an increased apparent reflectance and a cooling at the ocean surface. During pollution events the cloud droplet number will be increased through an enhanced number of condensation nuclei, which results in more cloud droplets with smaller radii also contributing to an enhanced planetary albedo. In addition, because of the limited number of condensation nuclei over the ocean more aerosol particles could as well increase cloudiness and cloud liquid water content. Consequently anthropogenic influence favours a decrease in sea surface temperature by these effects.

The polluted parts of the Atlantic and the Pacific are under influence by a variety of emission sources. In South East and East Asia namely motor vehicles, industrial combustion, soil dust, forest and agricultural fires as well as biomass burning are contributing to pollution events in the North Pacific region, whereby primary soil particles of natural origin, particles from biomass and bio-fuel burning, secondary particles from non-sulphurous gas phase pollution and secondary sulfuric acid particles are leading to a broad spectrum.

Figure 18a: This image from TERRA MODIS on May 4, 2001, reveals a large, optically thick plume of aerosols blown eastward over the North Atlantic Ocean. The aerosol plume is the regional haze produced by the industrialized northeastern United States.

The relevant sources for the North Atlantic region are spread over North America, Africa and Europe. There an effective long-range transport of aerosols and their precursor gases over the North Atlantic is enabled by two mechanisms. First of all, cyclones transport aerosol particles effectively to higher latitudes. Secondly, trade winds transport desert dust and also aerosols of biomass burning from different sources of North Africa to lower latitudes over the North Atlantic. However, the Atlantic region in mid-latitudes is not only polluted by emissions from the industrial regions of the eastern USA and Canada. Also Europe can contribute considerably to the pollution over the North Atlantic. Areas where this might often occur are located around the British Isles.

The different transport characteristics in the North Atlantic region are well confirmed by observed aerosol optical thickness. In lower latitudes for example the Atlantic shows the highest values worldwide [Higurashi et al., 2000; Nakajima et al., 2001]. The large aerosol concentrations result from mineral dust from the Sahara and additionally in the boreal winter from emissions of biomass burning. Because of the relatively short lifetime of aerosols in the atmosphere of days or a few weeks, the longitudinal long distance transport depends on location of the aerosol sources, while the meridional mixing is less important. The zonal transport over the Atlantic can be indeed very efficient. Stohl and Trickl [1999], like Forster et al. [2001], detected such an effective transport of pollution from the North American continent over the North Atlantic.

Figure 18b: Intense African dust storm that sent a massive dust plume westward over the Atlantic Ocean on March 2, 2003, observed by MODIS on the TERRA satellite. The plume extends more than 1600 km, covering a vast swath of ocean extending from the Cape Verde Islands in the South, to the Canary Islands off the coast of Morocco.

Also, Wandinger et al. [2002] identified the long distance transport of aerosols over the North Atlantic by lidar measurements and analysis of air mass trajectories. While these studies above generally confirm that an enhanced concentration of aerosols over the North Atlantic originates from anthropogenic activities in North America, they also give a hint that strong temporary and spatial variability should be expected.

The impacts of anthropogenic aerosol emission on the marine atmosphere are far from being understood. In principle it seems possible that enhanced aerosol concentrations in the northern hemisphere leading to a cooling and a southward shift of the inter-tropical convergence zone will influence the general atmospheric circulation over the North Atlantic. This can well have an influence on the drought in the Sahel. How this in turn would affect the natural emissions is another question which also needs be investigated in the future. In addition a changed kinetic energy of cyclones due to aerosol abundance must be expected. The possible changes in the storm track and the positions of high-pressure systems need to be investigated by numerical modeling scenarios.

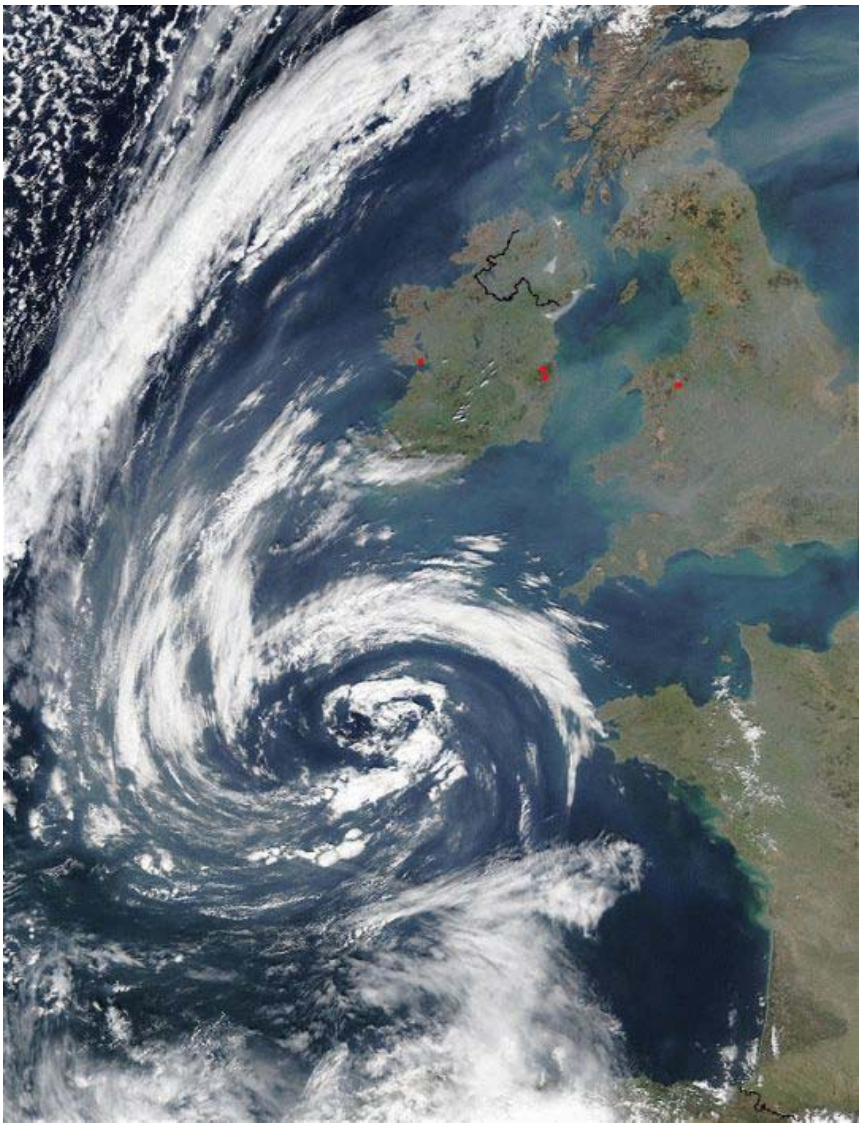

Figure 18c: Pollution and smoke get caught up in a swirl of clouds off the coasts of Spain, France, Ireland and the United Kingdom in this image acquired by MODIS on TERRA on March 23, 2003. The smoke and pollution appear as a grayish haze concentrated mostly over England and Ireland, blurring the landscape underneath.

Since these topics are at present close to the limits of model capability simulations must be evaluated by measurements, preferably from satellites. Therefore, an important task is the quantification of the aerosol cloud interaction by analysis of satellite measurements.

The aim of the new studies should be to detect the feedback between the water cycle and the aerosol cycle as well as the influence of natural and anthropogenic aerosols on atmospheric pressure systems over the oceans. Over the North Atlantic anthropogenic emissions originating from North America and Europe as well as desert dust from the Sahara have, after preliminary investigations, a significant influence on the radiation balance. The consequential influence on the dynamics of the atmosphere and on the water cycle is currently under investigation by analysing both satellite measurements since the 1980s and model simulations [SFB 512, 2005]. The main interest concentrates on the influence of aerosol particles on cloud formation and cyclone properties, especially concerning development and lifetime of cyclones, their tracks and their water

exchanges. The hypothesis is that cyclones, which are under strong influence of air pollution, show clearly modified properties.

The emphasis in analysing remote sensing data from AVHRR and MODIS is first of all the identification of the aerosol load and the detection of its influence on physical and optical properties of water and ice clouds. Besides the variability of the cloud albedo the change in cloudiness and particularly, the feedback between cloudiness and SST is considered. Further, cloudiness and the cloud water needs to be investigated with regard to the North Atlantic Oscillation (NAO). Since air temperature and wind are most important factors affecting emission, aerosol formation and transport, the aerosol load over the North Atlantic is also connected to the NAO index. An analysis using Integrated Atmospheric Deposition Network-Great Lakes Monitoring data underlines it. It could be shown that for the positive NAO mode during winter a warmer-than-normal spring in the north-western North America occurs which favours the volatilization of persistent organic pollutants (POP) from contaminated terrestrial surfaces [Ma et al., 2004]. On the other hand a stronger zonally eastward flow from major source regions of pollution is just associated with the positive mode of the NAO during winter and spring.

Different simulations with an atmospheric general circulation model including an interactice aerosol modul [SFB 512, 2005] are already under way. The calculated fields of aerosols and clouds as well as water cycle parameters will be evaluated and compared to the results of the analysis of satellite measurements. These investigations will also focus on a possible movement of the inter-tropical convergence zone as well as a possible influence of aerosols on the intensity of the Hadley cell.

Since individual strong pollution events are characteristic for the transport over the ocean [Brock et al., 2004] the detection of haze layers plays a key role. In order to identify the air pollution events the new haze detection developed in this study, as described in section 2, needs to be applied.

In many cases the haze layers will not occur in layers just near to the ocean surface. Aircraft measurements confirm that aerosol layers can exist in the whole troposphere above the marine boundary layer [Mari et al., 2004]. It was shown that these pollution layers, whose dimensions can be of 0.3 to 1.5km in the vertical and 950km in the horizontal, are connected to the frontal movement of cyclones. Two mechanisms for lifting the pollutants into the upper troposphere layers are under discussion: Localized deep convection and rising warm humid air masses ahead of cold fronts. The latter are known as so-called warm conveyor belts which favour the incorporation of aerosol particles as well as highly soluble gas phase species, such as nitric acid, sulphuric acid and ammonia into clouds. These warm conveyor belts accompanied by comparably slow air mass movement, which takes place within a time scale of days, favour also the transformation of gaseous pollutants into aerosol particles. In contrast to this slow synoptic or regional scale exchange the lifting on the cloud scale by deep convection is much faster. It should be mentioned that once the haze is lifted into the upper layers the further movement of cyclones is not necessarily needed for the inter-continental transport of aerosol particles. Since the strength of the inter-continental air mass transport grows with altitude in the troposphere the lifting through convection will be more efficient than the slow ascent in the warm sector of the cyclones. However, when the air mass in the warm sector is embedded in the strong westerly flow at higher altitudes then inter-continental transport will be rather efficient as well.

This discussion suggests that an aerosol influence on climate over the ocean could be detected by investigating atmospheric key properties. It points again to changes in the

- behaviour of strong convective clouds.

- occurrence of haze layers.

The experimental studies, which considerably contributed to our knowledge, give a clear preference to satellite remote sensing and aircraft measurements.

4.2 Studies over land

The location of increasing cloud top heights over China corresponds well to areas of above average precipitation amount, noted during summer monsoons in recent years. Many of these areas with precipitation amounts higher than 300mm per month are located south of the Jangtze River. Among them are the provinces Guangxi, Zhuangzu, Zizhiqu, Yunman, Guangdong, Fujian, Jiangxi, as well as Chonqing and Hubei. The cities showing high monthly anomalies above 150%, compared to the period prior to high air pollution, are Nanning, Guilin, Guangzhou, Nanchang and Wuhan. It is remarkable that days with more than 100mm rain have contributed strongly to the monthly total precipitation amount [Fuchs and Rapp, 2004].

These observed characteristics imply that future studies should show emphasis on highly polluted regions, i.e. close to emission sources of aerosol particles and their precursor gases, thus focussing on the role of enhanced cloud condensation nuclei numbers. Especially haze layers over large polluted cities or within basins and numerous valleys in China, e.g. the Red Basin, the Jangtze River Basin or the Pearl River Delta Region, must be further investigated with regard to their influence on the cloud formation process. In these studies emphasis should be given to the constraints, which favour the occurrence of extreme precipitation events.

Trying to explain these precipitation events in China, which caused heavy flooding in recent years, two hypotheses have been published. The first, by Xu [2001] discusses a reduced move of the summer monsoon rain belt northward connected to a slight southward shift of the mid-summer west Pacific high. The investigation was performed using radiation and precipitation measurements. Xu [2001] explains the abnormal climate pattern of “north drought and south flooding” by an enhanced negative radiative forcing of sulphate aerosols in central east China, which by far exceeds the radiative forcing by greenhouse gases in summer. The consequence is a cooling over land and a less strong northward shift of the summer monsoon rain belt. This argument neglects the role of black carbon. But there is also no clear shift of precipitation anomalies, which rather show a heterogeneous pattern including pronounced minima and maxima.

The second hypothesis by Menon et al. [2002], regarding the climate effects of air pollution in China, gives the preference to black carbon. They stated that absorbing aerosols have a strong influence on radiative transfer in clouds. Menon et al. argue that absorbing aerosols heat the air, alter regional atmospheric stability and thus vertical motions, which affect the hydrological cycle. This explanation, which includes the surface cooling caused by aerosol extinction has been derived from climate model experiments.

It is not possible to evaluate the pronounced differences in precipitation in small areas by using climate model results with the present day coarse resolution. On the other hand the findings presented in **paper II** about the strong influence of BC on cloud albedo principally would support the hypothesis of Menon et al. However, the results of Menon et al. cannot explain the heterogeneity of the changes in precipitation found by Xu.

The satellite data evaluation, as presented in **paper II**, instead shows strong similarities with the results of Xu. If one compares the cloud cover and the LPA with the average anomalies of mid-summer precipitation, an amazing result becomes visible: In areas where the lifetime effect is dominant (Red Basin, Beijing, Shanghai, Hong Kong) total precipitation amount declines during the recent 20 years. On the other hand the new results presented in section 3.2 reveal that convection is strengthened near highly polluted regions of China. Both findings combined give a hint on the redistribution of precipitation through aerosol abundance. An obvious question then is:

Can large cities induce extreme precipitation intensities?

In the few studies dealing with rainfall modification near to urban areas so far three factors of major influence are discussed: A higher surface roughness, the urban heat island and the enhanced number of condensation nuclei through urban air pollution.

Generally the roughness of a city, strongly varying with type and density of the built-up areas, has a strong influence on turbulence and consequently vertical motion. An increased surface roughness in many cases intensifies the vertical transports of heat, moisture and aerosols. During horizontal advection of a stable air mass an internal boundary layer, so-called urban boundary layer will form, dependent on temperature gradient and vertical mixing. In such cases despite a cloud-free situation in non-urban area, clouds can form within the urban boundary layer through cooling in the upper part. On the other hand the heating of the urban canopy layer can lead to thermal winds, which intensify vertical motion. An influence of surface conditions on cloud development and convective rainfall, particularly most significant the sensible heat flux, could be demonstrated by meso-scale modelling [Thielen et al., 2000].

Indeed, radar measurements during the prominent Metropolitan Meteorological experiment (METROMEX) have shown that there is an enhanced frequency of strong convective clouds near to cities [Changnon et al., 1976]. The factors leading to these events near the urban area were identified as follows: Increased cloudiness, higher cloud base and convergence. It was stated that a more vigorous coalescence process due to urban aerosols in turn could easily intensify precipitation. Observations from space-borne rain radar on the TRMM Satellite confirm the early findings while they show that rainfall rates are increased on average by 28% within 30-60 km downwind in direction of the urban plume [Shepherd et al., 2002].

Not only the daytime precipitation is affected. At night a city with strong air pollution easily is embedded into a haze dome, e.g. most pronounced during calm weather situations accompanied by a weak horizontal flow. The main characteristic of the haze dome at night is an additional warming caused by aerosols, because it increases the down-welling long-wave radiation. Under those conditions the nocturnal air temperature decrease of the urban canopy layer will be much slower then the more rapid cooling of the surface layer in the non-urban surrounding. The latter process is called the heat island effect [Oke, 1973]. Since the resulting vertical density and temperature profiles are quite different for the urban area and its surrounding the atmosphere is baroclinic. Finally under these conditions a thermal circulation can develop including

an urban breeze at the surface directed to the city centre besides the updraft over the city.

It is concluded that cities with a strong heat island effect induce thunderstorms [Bornstein and Lin, 2000; Dixon and Mote, 2003]. However, the events, which were more frequent for the most humid air masses, were found mostly during night. A pronounced influence of stability was also observed depending on the strength of the synoptic flow. Very often unstable conditions favour an influence of the anomalous urban heat on the initialization of precipitation. It is remarkable that already a slightly unstable stratification combined with a weak synoptic flow could be sufficient for development of the urban updraft.

With regard to an influence of cities on precipitation the discussion above refers firstly to heating of the urban area as a major reason. Since satellite measurements show an increase of the cloud top height during daytime, i.e. early afternoon, another question arises:

Can enhanced aerosol concentrations enable the development of an urban heat island during daytime in southern China ?

In order to answer this question important hints are received again from field campaigns. The results of INDOEX show that the direct aerosol forcing at the surface of the polluted Tropical Indian Ocean amounts to $-14 W/m^2$ [Ramanathan et al., 2001]. A continental field campaign at the urban location Bangalore in India confirms the cooling due to absorbing aerosols aloft with a typical value of $-23 W/m^2$ [Babu et al., 2002]. Further hints for a decreasing intensity of heat islands underneath haze layers are given by Krishnan and Ramanathan [2002]. The authors investigated long-term temperature records over India and found also evidence of surface cooling of 0.3K caused by absorbing aerosols since the 1970s, which is statistically significant.

An analysis of temperature trends in eastern China clearly indicates a cooling at the surface during summer [Yu et al., 2001]. It can be seen by the negative trend of the daily maximum temperatures for 81% of the analyzed stations. The results, which also confirm the presence of large amounts of absorbing aerosols during winter (see **paper II**), are in general agreement with the findings of Easterling et al. [1997]. Therefore it can be concluded that an increase of either frequency, or intensity of heat islands during daytime in southern China is rather unlikely. The increased frequency of extreme precipitation events needs another explanation.

A possible explanation for the extreme rainfall near to urban areas stimulated by the results presented in section 3.2, is given here. The argumentation is based on the occurrence of optically rather thick haze over strongly polluted cities. The explanation (schematically depicted in figure 19) separated into two parts, is called the “Haze Dome Hypothesis”:

Step 1: Lifting of aerosols and aerosol precursor gases into the cloud (condensation) level. Since cities are strong sources of air pollution the concentration of aerosols and precursor gases is strongly enhanced. A haze dome develops over the urban area due to accumulation of pollution. Within the haze dome the formation of secondary aerosols is favoured. Since an effective below and in-cloud scavenging of particles in summer monsoon conditions likely lowers the concentration of pollutants

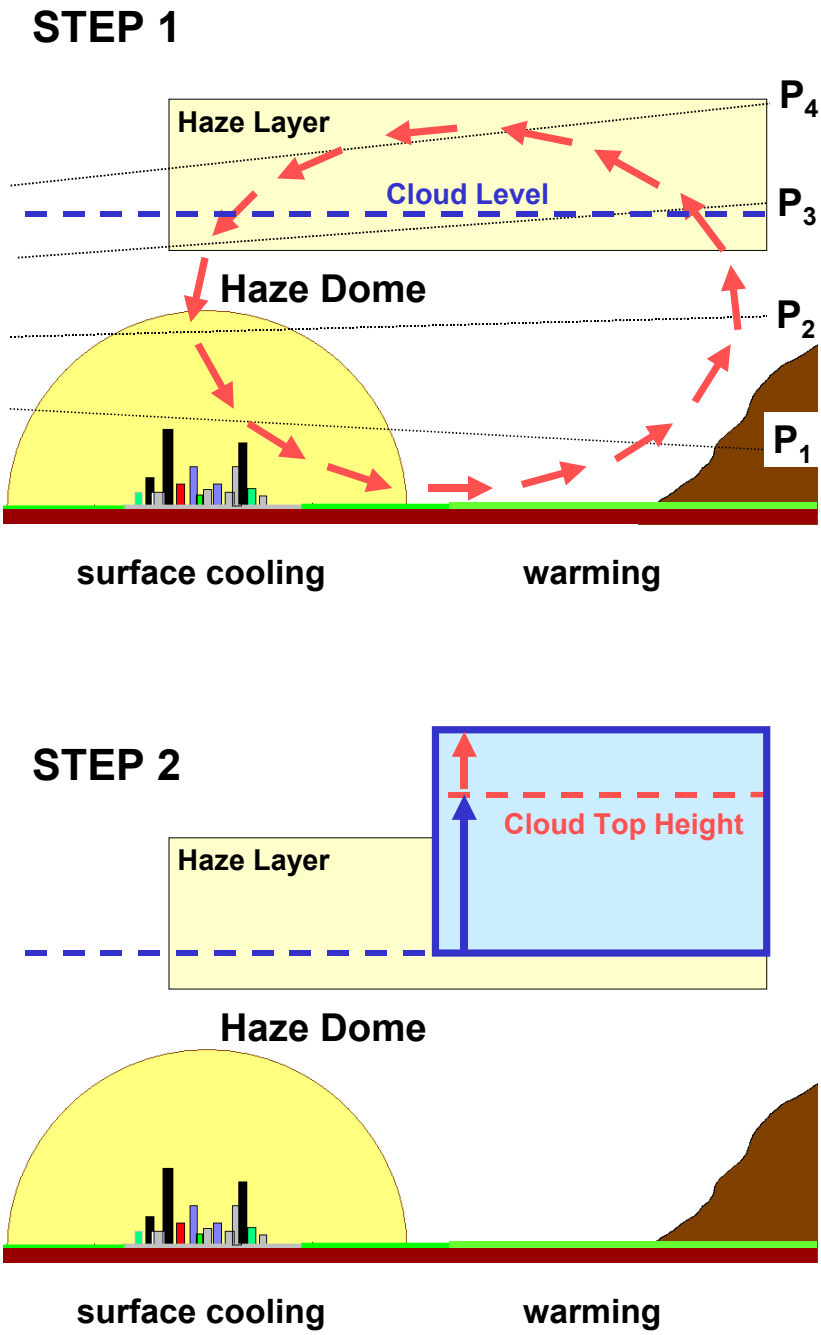

Figure 19. Schematic illustrating the 'Haze Dome Hypothesis'. **Step 1:** During daytime the atmosphere in mountain areas in southern China is baroclinic, which enables development of thermal circulation (in red). Since within haze domes (in yellow) enhanced backscattering takes place the surface cooling can intensify a thermal circulation over polluted cities. **Step 2:** An increased aerosol number density at the cloud condensation level intensifies convection and hence enhances cloud top height. Once the number of condensation nuclei is strongly enhanced more small droplets form inhibiting drizzle formation. The characteristics of such clouds are an increased cloud water concentration and a droplet spectrum shifted to smaller sizes. The suppression of the warm rain formation will prolong cloud lifetime and allow the development of more vigorous convection. Such clouds with a high number of super-cooled small droplets at temperatures well below 250K, will - when freezing sets in - enhance the vertical movement again by the additional release of heat during freezing. Under such conditions extreme events of precipitation might occur. The powerful deep convective clouds might also penetrate the tropopause and inject polluted air (only less soluble compounds) into the stratosphere over China.

the haze domes over the sources might be the major reservoirs of anthropogenic aerosols.

A sufficient vertical movement of these haze domes could lift pollutants into cloud level. The study for Europe, as presented in **paper III,** shows that primary particles are efficiently mixed into the cloud level if the atmosphere is unstable. In China the vertical transport of condensation nuclei could likely be established through thermal circulations induced by the numerous and often very high mountains. In addition a heat island effect during night could as well lead to a vertical transport of aerosols or precursor gases into upper layers. Haze layers near to the source regions, as it was seen in Europe (see **paper III**), could also be the result of secondary aerosol formation.

Step 2: Aerosol abundance in the cloud (condensation) level intensifies convection and enhances cloud top height. During the summer monsoon when large amounts of water vapour are advected from the Pacific the clouds in regions of aerosol abundance, i.e. near to the haze domes, will contain more water droplets. The characteristics of these clouds are a shifted droplet spectrum to smaller cloud droplets suppressing coalescence. The consequent suppression of precipitation formation will not only prolong the cloud lifetime but lead to higher liquid water content that allows the development of more vigorous convective clouds. It can be expected that in such clouds a high number of super-cooled small liquid droplets will exist. In case of an enormous layer of super-cooled droplets the freezing, which would occur at temperatures below 250K and above 7000m height, will enhance the vertical movement again by the additional release of heat. Under such conditions extremely high amounts of precipitation can occur. The powerful deep convective clouds could also break through the tropopause and enter the lowest stratosphere over China.

The second step is well supported by the findings of the LBA-SMOCC campaign [Andreae et al., 2004]. The smoking rain clouds over the Amazon showed a reduced droplet size and a delayed onset of precipitation. Just this invigorates the updrafts, intensifies precipitation and possibly allows for overshooting cloud tops into the stratosphere.

The regional pattern of cloud top height increase in southern China and the conspicuous relation to the growing cities suggests that extreme events of precipitation can be induced by air pollution. Therefore it needs to be investigated how in detail air pollution affects the precipitation over southern China. The complexity of the question would demand for a combination of regional modelling, experiments including high flying aircraft, as well as satellite data.

5. CONCLUSIONS

Indirect aerosol effects on regional scale have been observed from space. It is shown that there can be either a dominance of the scattering or absorption effect for a certain area. The results reveal that both an emission reduction of air pollutants and an increase can lead to the same effect: Decreasing cloud albedo.

With respect to present nomenclature on indirect aerosol effects, as e.g. outlined in the latest IPCC report, the radius effect (first indirect aerosol effect), the absorption effect (first indirect aerosol effect), the cloud lifetime effect (second indirect aerosol effect) and a strong indication for the cloud burning (semi-direct aerosol effect), have been detected on regional scale. The major findings, which have been achieved by the comparison of three four-year periods (from 1981 to 1984, 1985 to 1989 and 1996 to 1999) for winter and summer, are:

Emissions of aerosol precursor gases, such as sulphur dioxide, nitrogen oxides and ammonia as well as particulate matter, including black carbon, have a pronounced influence on cloud reflectance and its variability. In Europe the reduction of the sulphur dioxide emissions by about 50% (23 Tg y^{-1}), after the collapse of the East Block in 1989, is accompanied by a reduction of cloud albedo by about 2.8% in winter and 2.1% in summer. In addition, black carbon emissions in the order of magnitude of 1 Tg y^{-1} lower the cloud reflectance in source regions by more than 5%. The trend in reflectance over Europe occurs both for zonal and meridional circulation types.

Also atmospheric turbulence can have an influence on the indirect aerosol effect(s). The so-called first indirect aerosol effect, i.e. the effect of smaller cloud droplet radii and stronger absorption in clouds, can be caused differently: Under less stable conditions primary particle emissions dominate and in more stable boundary layers secondary aerosol formation.

The growing amount of absorbing aerosols has reduced the local planetary albedo (LPA) over China. The LPA decrease, with maxima higher than 5%, is due to the very strong cloud albedo reduction, up to 10%, caused by black carbon in clouds. Cloud albedo is reduced in all regions in winter in southern and central China. The maximum cloud albedo decrease in the northern part of the Red Basin can be explained by the high degree of air pollution around the cities Chengdu and Nanchong.

Clouds over China experience, most pronounced within the Red Basin, the cloud lifetime effect. As a consequence of the radius effect, an increase in cloud lifetime and thus enhanced cloud cover occurs. Over the Red Basin continuously high aerosol number concentrations can lead to a nearly permanent radius effect with a considerably decreased effective radius of cloud droplets. Under such conditions coalescence that starts drizzle formation is largely suppressed.

> Partially cloudy atmospheres show an increase in brightness temperature for regions with strong LPA decrease. The finding is a strong indication for the semi-direct aerosol effect, also called cloud burning. The decrease in cloud top height is much more pronounced in regions around the Red Basin where extended haze layers are detected more frequently and where the concentration of black carbon particles is high.

Besides the indirect aerosol effect(s) related to cloud-radiation interaction in the solar radiation range, discussed in the latest IPCC report, also an influence of air pollution on cloud dynamics has been detected. Since cloud top temperatures decrease strongest in areas of high pollution increase, i.e. near to growing cities, it is concluded that strong air pollution intensifies convection:

> The mean cloud top temperatures over southern China for summer show a remarkable decrease from the late 1980s to the late 1990s by more than 10K in areas of strongest LPA increase. The increase in the frequency of very low cloud top temperatures below 185K and a mean cloud top temperature decrease up to 12K clearly indicate a hitherto unknown effect of air pollution. The lowest cloud top temperatures are found near to the cities Nanning, Guangzhou, Guilin and Fuzhou in Southern China.

Some final remarks are:

The results above imply that a third indirect aerosol effect needs to be considered: The influence of pollution on cloud dynamics, detected here via reduced cloud top temperatures.

The regions with increasing cloud top heights over China coincide with areas of extreme precipitation amounts during summer monsoons in recent years. Therefore further investigations how air pollution affects the cloud dynamics and precipitation in detail are suggested. In general there would be a need for high flying aircraft measurements to detect the cloud top heights and elevated haze layers over strongly polluted regions in China.

With regard to the third indirect aerosol effect, an influence of air pollution on the intensity and consequently on the tracks of low-pressure systems should be expected as well. Therefore the inter-continental pollution transport needs to receive a special focus.

The complexity of indirect aerosol effects suggests that future investigations with respect to aerosol cloud interactions should involve a combination of measurements and numerical modelling.

The real answer for many of the open questions would come from a regional climate model embedded in a global coupled one initialised by satellite data on aerosol load, cloud albedo and liquid water path as well as a validation by an airborne regional survey.

6. ACKNOWLEDGEMENTS

First of all I would like to thank Hartmut Graßl for his continuous interest in my research and for all advices within the past 15 years. I enjoyed the scientific discussions with him.

The work was initiated at the GKSS Research Center Geesthacht and mainly performed during my 5 year period as an assistant professor in meteorology at the University of Hamburg. I would like to express my gratitude to Stephan Bakan, Michael Schatzmann, Klaus Fraedrich, Burghard Brümmer, Heinke Schlünzen, Christian Klepp, Gerhard Peters, Gerhard Lammel, Andreas Chlond, Jens Bösenberg, Johann Feichter, Irene Fischer-Bruns, Hendrik Hobe, Abhay Devasthale and Ehrhard Raschke, as well as colleagues and students at the University of Hamburg and the Max-Planck Institute for pleasant working conditions and co-operation within the ‘Sonderforschungsbereich 512’.

Finally, I would like to thank Barbara Zinecker for her excellent support during all the years.

7. REFERENCES

Ackerman, A.S., Toon, O. B., Stevens, D. E., Heymsfield, A. J., Ramanathan, V., Welton, E. J. (2004)
Reduction of Tropical Cloudiness by Soot.
Science **288**, 1042-1047.

Andreae, M.O., Rosenfeld, D., Artaxo, P., Costa A. A., Frank, G.P., Longo, K.M., Silva-Dias, M.A.F. (2004)
Smoking Rain Clouds over the Amazon.
Science **303**, 1337-1342.

Armalis, S. (1999)
Wet deposition of elemental carbon in Lituania.
The Science of the Total Environment **239**, 89-93.

Babu, S.S., Satheesh, S.K. and Moorthy, K.K. (2002)
Aerosol radiative forcing due to enhanced black carbon at an urban site in India.
Geophysical Research Letters **29**, doi:10.1029/2002GL015826.

Bates, T.S. et al. (1998)
International global atmospheric chemistry (IGAC) project's first aerosol characterization experiment (ACE-1): Overview.
Journal of Geophysical Research **103**, 16297-16318.

Bornstein, R. and Lin, Q. (2000)
Urban heat islands and summertime convective thunderstorms in Atlanta: Three case studies.
Atmospheric Environment **34**, 507-516.

Brock, C.A. et al. (2004)
Particle characteristics following cloud-modified transport from Asia to North America.
Journal of Geophysical Research **109**, doi:10.1029/2003JD004198.

Budyko, M.I. (1969)
The effect of solar radiation variations on the climate of the Earth.
Tellus **21**, 611.

Cao, C., Weinreb, M., Sullivan, J. (2001)
Solar contamination effects on the infrared channels of the advanced very high resolution radiometer (AVHRR).
Journal of Geophysical Research **106**, 33463-33469.

Carrier, L.W., Cato, G.A. and von Essen, K.J. (1967)
The Backscattering and Extinction of Visible and Infrared Radiation by Selected Major Cloud Models.
Applied Optics **6**, 1209-1216.

Changnon, S.A., Jr., Semonin, R.G., Huff, F.A. (1976)
A Hypothesis for Urban Rainfall Anomalies.
Journal of Applied Meteorology **15**, 544-560.

Clarke, A.D. and Noone, K.J. (1985)
Soot in the Arctic snowpack: a cause for perturbations in radiative transfer.
Atmospheric Environment **19**, 2045-2053.

Charlson, T.N. (1979)
Atmospheric Turbidity in Saharan Dust Outbreaks as Determined by Analysis of Satellite Brightness Data.
Monthly Weather Review **107**, 322-325.

Charney, J.G. (1975a)
Dynamics of deserts and drought in the Sahel.
Quaterly Journal of the Royal Meteorological Society **101**, 193-202.

Charney, J.G., Stone, P.H., Quirk, W.J. (1975b)
Drought in the Sahara: A Biogeophysical Feedback Mechanism.
Science **187**, 434-435.

Charney, J.G., Stone, P.H., Quirk, W.J. (1976)
Drought in the Sahara: Insufficient Biogeophysical Feedback?
Science **191**, 100-102.

Chung, Y.S. (1986)
Air pollution detection by satellites: The transport and deposition of air pollutants over the oceans.
Atmospheric Environment **20**, 617-630.

Coakley, J.A. et al., (1987)
Effect of ship stack effluents on cloud reflectivity.
Science **237**, 1020-1022.

Conover, J.H. (1966)
Anomalous Cloud Lines.
Journal of the Atmospheric Sciences **23**, 778-785.

Deirmendjian, D. (1969)
Electromagnetic scattering on polydispersions.
Journal of Atmospheric and Oceanic Technology **16**, 656-681.

Devasthale, A., Krüger, O., Graßl, H. (2005)
Change in Cloud Top Temperatures over Europe.
IEEE Geoscience and Remote Sensing Letters, accepted for publication.

Dixon, P.G. and Mote, T.L. (2003)
Patterns and causes of Atlanta's Urban Heat Island-Initiated Precipitation.
Journal of Applied Meteorology **42**, 1273-1284.

Döscher, A.H., Gäggeler, W., Schotterer, U. and Schwikowski, M. (1995)
A 130 years deposition record of sulphate, nitrate, and chloride from a high-alpine glacier.
Water, Air and Soil Pollution **85**, 603-609.

Easterling, D.R., Horton, B., Jones, P.D., Peterson, T.C., Karl, T.R., Parker, D.E., Salinger, M.J., Razuvayev, V., Plummer, N., Jamason, P., Folland, C.K. (1997)
Maximum and Minimum Temperature Trends for the Globe.
Science **277**, 364-367.

EMEP, Co-operative Programme for Monitoring and Evaluation of the Long-Range Transmission of Air Pollutants in Europe (1999)
EMEP emission data, Status report 1999.
EMEP Note 1/1999, Meteorological Synthesizing Centre - West, Norwegian Meteorological Institute, Oslo, Norway.

EMEP, Co-operative Programme for Monitoring and Evaluation of the Long-Range Transmission of Air Pollutants in Europe (2004)
Transboundary particulate matter in Europe, Status report 2004: Joint CCC & MSC-W & CIAM Report 2004.
EMEP Report 4/2004, Chemical Coordination Centre, Norwegian Institute for Air Research (NILU), Kjeller, Norway.

Eliassen, A., C. and Saltbones, J. (1983)
Modelling of long-range transport of sulphur over Europe: A two year model run and some model experiments.
Atmospheric Environment **9**, 425-429.

Ferek, R.J., Garrett, T., Hobbs, P.V., Strader, S, Johnson, D., Taylor, J.P., Nielden, K., Ackerman, A.S., Kogan, Y., Liu, Q., Albrecht, B.A., Babb, D. (1966)
Drizzle Suppression in Ship Tracks.
Journal of the Atmospheric Sciences **57**, 2707-2728.

Feichter, J., Lohmann, U., Liepert, B. and Roeckner, E. **(**2003)
Nonlinear aspects of the climate response to greenhouse gas and aerosol forcing.
Journal of Climate, (accepted).

Fischer, H., Wagenbach, D. and Kipfstuhl, J. (1998)
Sulphate and nitrate firn concentrations on the Greenland ice sheet. 2. Temporal anthropogenic deposition changes.
Journal of Geophysical Research **103**, 21935-21942.

Forster, C., Wandinger, U., Wotawa, G., James, P., Mattis, I., Althausen, D., Simmonds, P., O'Doherty, S., Jennings, S.G., Kleefeld, C., Schneider, J., Trickl, T., Kreipl, S., Jager, H. and Stohl, A. (2001)
Transport of boreal forest fire emissions from Canada to Europe.
Journal of Geophysical Research **106**, 22887-22906.

Fuchs, T. and Rapp, J. (2004)
Anomalous precipitation in the catchment area of the Yangtze river in China during summer 1998.
http://www.dwd.de/en/FundE/Klima/KLIS/int/GPCC/Reports_Publications/QR/FuchsRapp-Yangtse-flood-1998.pdf

Gerstengarbe, F.-W. and Werner, P.C. (1993)
Katalog der Großwetterlagen Europas nach Paul Hess und Helmut Brezowski: 1881 – 1992.
Berichte des Deutschen Wetterdienstes **113**, 249pp.

Gras, J.L. (1995)
CN, CCN and particle size in Southern Ocean air at Cape Grim.
Atmospheric Research **35**, 233-251.

Grassl, H. (1974a)
Influence of different absorbers in the window region on radiative cooling (and on temperature determination).
Contributions to Atmospheric Physics **47**, 1-13.

Grassl, H. (1974b)
Erwärmung und Abkühlung durch atmosphärisches Aerosol.
Annalen der Meteorologie **9**, 55-59.

Grassl, H. (1975)
Albedo Reduction and Radiative Heating of Clouds by
Absorbing Aerosol Particles.
Contributions to Atmospheric Physics **48**, 199–210.

Grassl, H. (1978)
Strahlung in getrübten Atmosphären und in Wolken.
Hamburger Geophysikalische Einzelschriften **37**, Universität Hamburg.

Gray, W.M., Frank, W.M., Corrin, M.L. and Stokes, C.A. (1976)
Weather Modification by Carbon Dust Absorption of Solar Energy.
Journal of Applied Meteorology **15**, 355-386.

Gutman, G. (1988)
A Simple Method for Estimating Monthly Mean Albedo of Land Surfaces From AVHRR Data.
Journal of Applied Meteorology **27**, 973-988.

Hauglustaine, D.A., Brasseur, G.P., Walters, S., Rasch, P.J., Müller, J.F., Emmons, L.K. and Carroll, M.A. (1998)
MOZART, a global chemical transport model for ozone and related chemical tracers: 2. Model results and evaluation.
Journal of Geophysical Research **103**, 28291-28335.

Hansen, J., Sato, M. and Ruedy, R. (1997)
Radiative forcing and climate response.
Journal of Geophysical Research **102**, 6831-6864.

Higurashi, A., Nakajima, T., Smirnov, A., Holben, B.N., Frouin, R. and Chatenet B. (2000)
A study of global aerosol optical climatology with Two-channel AVHRR remote sensing.
Journal of Climate **13**, 2011-2027.

Husar, R.B., Prospero, J.M. and Stowe, L.L. (1997)
Characterization of tropospheric aerosols over oceans with NOAA advanced very high resolution radiometer optical thickness operational product.
Journal of Geophysical Research **102**, 16889-16909.

IPCC (2001)
The scientific basis, *Contribution of Working Group I to the third assessment report of the Intergovernmental Panel on Climate Change*, J.T. Houghton et al. (eds.), Intergovernmental Panel on Climate Change, Working Group I.
Cambridge University Press, pp. 881, 2001.

James, M.E. and Kalluri, S.N.V. (1994)
The Pathfinder AVHRR land data set: An improved coarse resolution data set for terrestrial monitoring.
International Journal of Remote Sensing **15**, 3347-3363.

Jones, A. and Slingo, A. (1996)
Predicting cloud-droplet effective radius and indirect sulphate aerosol forcing using a general circulation model.
Quaterly Journal Royal Meteorological Society **122**, 1573-1595.

Kaufman, J. et al. (1998)
Smoke Clouds and Radiation-Brazil (SCAR-B).
Journal of Geophysical Research **113**, 31783-31808.

Kidwell, K.B. (1995)
NOAA Polar Orbiter Data Users Guide (TIROS-N, NOAA-6, NOAA-7, NOAA-8, NOAA-9, NOAA-10, NOAA-11, NOAA-12, NOAA-13 and NOAA-14).
National Environmental Satellite, Data and Information Service, Washington, DC, 394 pages.

Krishnan, R. and Ramanathan, V. (2002)
Evidence of surface cooling from absorbing aerosols.
Geophysical Research Letters **29**, doi:10.1029/2002GL014687.

Koren, I., I., Kaufman,Y.J. ,Remer, L.A., Martins, J.V. (2002)
Measurement of the Effect of Amazon Smoke on Inhibition Cloud Formation.
Science **303**, 1342-1345.

Korff, H.C. and Flohn, H. (1969)
Zusammenhang zwischen dem Temperaturgefälle Äquator-Pol und den planetarischen Luftdruckgürteln.
Annalen der Meteorologie **NF4**, 163-164.

Kriebel, K.T. (1976)
On the variability of the reflected radiation field due to differing distributions of the irradiation.
Remote Sensing of Environment **4**, 257.

Kriebel, K.T. (1977)
Reflection Properties of Vegetated Surfaces: Tables of Measured Spectral Biconical Reflectance Factors.
Münchener Universitätsschriften **29**, Universität München.

Kristjansson, J.E. (2002)
Studies of the aerosol indirect effect from sulphate and black carbon aerosols.
Journal of Geophysical Research **107**, 10.1029/201JD000887.

Krüger, O. and Fischer, J. (1994)
Correction of Aerosol Influence in Landsat 5 Thematic Mapper Data.
GeoJournal **32**, 61-70.

Krüger, O. and Tuovinen, J.-P. (1997)
The effect of variable sub-grid deposition factors on the results of the lagrangian long-range transport model of EMEP.
Atmospheric Environment **31**, 4199-4209.

Krüger, O. and Graßl, H. (2002)
The indirect aerosol effect over Europe.
Geophysical Research Letters **29**, doi:10.1029/2001GL014081.

Krüger, O. and Graßl, H. (2004)
Albedo reduction by absorbing aerosols over China.
Geophysical Research Letters **31**, doi:10.1029/2003GL019111.

Krüger, O., Marks, R., Graßl, H. (2004)
Influence of Pollution on Cloud Reflectance.
Journal of Geophysical Research **109**, doi:10.1029/2004JD004625.

Landsea, C.W. and Gray, W.M. (1992)
The Strong Association between Western Sabelian Monsoon Rainfall and Intense Atlantic Hurricanes.
Journal of Climate **5**, 453-453.

Langner, J. and Rodhe, H. (1966)
A three-dimensional model of the tropospheric sulphur cycle.
Journal Atmospheric Chemistry **13**, 225-263.

Lawanchy, V.M.H. et al. (1999)
A historical record of carbonaceous particle concentrations from a European high-alpine glacier.
Journal of Geophysical Research **104**, 21227-21236.

Le Treut, H. and McAvaney, B. (2000)
Equilibrium climate change in response to a CO2 doubling : an intercomparison of AGCM simulations coupled to slab oceans.
Technical Report **18**, Institut Pierre Simon Laplace.

Linke, F. and Bauer, F. (1962)
Meteorologisches Taschenbuch.
Akademische Verlagsgesellschaft Geest & Portig K.-G., Leipzig.

Lopez, R.E. (1973)
A parametric model of cumulus convection.
Journal Atmospheric Sciences **30**, 1354-1373.

Lohmann, U., Feichter, J., Chuang, C.C., Penner, J.E. (1999)
Predicting the number of cloud droplets in the ECHAM GCM.
Journal of Geophysical Research **104**, 9196-9198.

Ma, J., Cao, Z., Hung, H. (2004)
North Atlantic Oscillation signatures in the atmospheric concentrations of persistent organic pollutants: An analysis using Integrated Atmospheric Deposition Network-Great Lakes monitoring data.
Journal of Geophysical Research **109**, doi:10.1029/2003JD004435.

Mari, C., Evans, M.J., Palmer, P.I., Jacob, D.J., Sachse, G.W. (2004)
Export of Asian pollution during two cold front episodes of the TRACE-P experiment.
Journal of Geophysical Research **109**, doi:10.1029/2003JD004307.

McClain, E.P., Pichel, W.G., Walton, C.C. (1985)
Comparative performance of AVHRR-based multi-channel sea surface temperatures.
Journal of Geophysical Research **90**, 11587-11601.

Menon, S., Hansen, J., Nazarenko, L., Luo, Y. (2002)
Climate Effects of Black Carbon Aerosols in China and India.
Science **297**, 2250-2253.

Nakajima, T., Higurashi, A., Kawamoto, K. and Penner, J.E. (2001)
A possible correlation between satellite-derived cloud and aerosol microphysical parameters.
Geophysical Research Letters **28**, 1171-1174.

Nober, F.N., Graf, H.F., Rosenfeld, D. (2003)
Sensitivity of the global circulation to the suppression of precipitation by anthropogenic aerosols.
Global and Planetary Change **37**, 57-80.

Noone, K.J. and Clarke, A.D. (1988)
Soot scavenging measurements in Arctic snowfall.
Atmospheric Environment **22**, 2773-2778.

Oke, T.R. (1973)
City size and urban heat island.
Atmospheric Environment **7**, 769-779.

Orville, H.D. (1965)
A numerical study of the initiation of cumulus clouds over a mountainous terrain.
Journal Atmospheric Sciences **22**, 684-699.

Petersen, G., Bloxam, R., Wong, S., Krüger, O., Schmolke, S.R., Kumar, A.V. (2001)
A comprehensive Eulerian modeling framework for airborne mercury species: Model development and applications in Europe.
Atmospheric Environment **35**, pp. 3063-3074.

Prabhakara, C., Fraser, R.S., Dalu, G., Wu, M.C. and Curran, R.J. (1988)
Thin cirrus clouds: seasonal distributions over the oceans deduced from NIMBUS-4 IRIS.
Journal of Applied Meteorology **27**, 379-399.

Prospero, J.M. and Lamb, P.J. (2003)
African Droughts and Dust Transport to the Caribean: Climate Change Implications.
Science **302**, 1024-1027.

Pruppacher, H.R. and Klett, J.D. (1978)
Microphysics of Clouds and Precipitation.
Reidel, Dordrecht, 1978.

Putaud, J.P., Raes, F., Van Dingenen, R., Brüggemann, E., Facchini, M.C., Decesari, S., Fuzzi, S., Gehrig, R., Hüglin, C., Laj, P., Lorbeer, G., Meanhaut, W., Mihalopoulus, N., Müller, K., Querol, X., Rodriguez, S., Schneider, J., Spindler, G., ten Brink, H., Torseth, K., Wiedensohler, A. (2004)
A European aerosol phenomenology - 2: chemical characteristics of particulate matter at kerbside, urban, rural and background sites in Europe.
Atmospheric Environment **38**, 2579-2595, doi:10.1016/j.atmosenv.2004.01.041.

Radke, L.F., Coakley Jr., J.A. and King, M.D. (1989)
Direct remote sensing observations of the effects of ships on clouds.
Science **246**, 1146-1149.

Ramanathan, V., Crutzen, P. J., Kiehl, J. T., Rosenfeld, D. (2001)
Aerosols, Climate and the Hydrological Cycle.
Science **294**, 2119-2124.

Randel, W.J. and Wu, F. (1999)
A stratospheric ozone trend data set for global modelling studies.
Geophysical Research Letters **26**, 3089-3092.

Rao, C.R.N. (1987)
Prelaunch calibration of channels 1 and 2 of the advanced Very High Resolution Radiometer.
NOAA Technical Report NESDIS **36**, U.S. Department of Commerce.

Rao, C.R.N. (2000)
Private Communication.

Raschke, E., Vonder Haar, T.H., Bandeen, W.R., Pasternak, M. (1973)
The annual radiation balance of the earth-atmosphere system during 1969-70 from NIMBUS 3 measurements.
Journal of the Atmospheric Sciences **30**, 341-364.

Rosenfeld, D. (2000)
Suppression by Rain and Snow by Urban and Industrial Air Pollution.
Science **287**, 1793-1796.

Rosenthal, S.L. (1971)
A circularly symmetric primitive equation model of tropical cyclones and its response to artificial to artificial enhancement of the convective heating functions.
Monthly Weather Review **99**, 414-426.

Rotstayn, L.D. (2000)
Indirect forcing by anthropogenic aerosols: A global climate model calculation of the effective radius and cloud lifetime effects.
Journal of Geophysical Research **104**, 9369-9380.

Raes, F., Bates, T., McGovern, F., Van Liedekerke, M. (2000)
The 2nd Aerosol Characterization Experiment (ACE-2): General overview and main results.
Tellus **52B**, 111-125.

Saunders, R.W. and Kriebel, K.T. (1988)
An improved method detecting clear sky and cloudy radiances from AVHRR data.
International Journal of Remote Sensing **9**, 123-150.

Saxena, V.K., Anderson, J., Lin, N.-H. (1995)
Changes in Antartic stratospheric aerosol characteristics due to volcanic eruptions as monitored by SAGE II satellite.
Journal of Geophysical Research **100**, 16735-16751.

Saxena, V.K. (1996)
Bursts of cloud condensation nuclei (CCN) by dissipating clouds at Palmer Station, Antarctica.
Geophysical Research Letters **23**, 60-72.

Schaap, M., Van Der Gon, H.A.C.D., Dentener, F.J., Visschedijk, A.J.H., Van Loon, M., ten Brink, H.M., Putaud, J.-P., Guillaume, B., Liousse and Builtjes, P.J.H. (2004)
Anthropogenic black carbon and fine aerosol distribution over Europe.
Journal of Geophysical Research **109**, D18207, doi:10.1029/2003JD004330.

SFB 512 (2005)
http://www.sfb.uni-hamburg.de/sfb512/tpd3.html

Shepherd, J.M., Pierce, H., Negri, A. (2002)
Rainfall Modification by Major Urban Areas: Observations from Spaceborne Rain Radar on the TRMM Satellite.
Journal of Applied Meteorology **41**, 689-701.

Schneider, S.H. (1972)
Cloudiness as a Global Climatic Feedback Mechanism: The Effects on the Radiation Balance and Surface Temperature of Variations in Cloudiness.
Journal of the Atmospheric Sciences **29**, 1413-1422.

Schneider, T. and Held, I.M. (2001)
Discriminants of Twentieth-Century Changes in Earth Surface Temperatures.
Journal of Climate **14**, 249-254.

Stohl, A. and Trickl, T. (1999)
A textbook example of long-range transport: Simultaneous observation of ozone maxima of stratospheric and North American origin in the free troposphere over Europe.
Journal of Geophysical Research **104**, 30445-30462.

Stowe, L.L., Davis, P.A., McClain, E.P. (1999)
Scientific Basis and Initial Evaluation of the CLAVR-1 Global Clear/Cloud Classification Algorithm for the Advanced Very High Resolution Radiometer.
Journal of Atmospheric and Oceanic Technology **16**, 656-681.

Thielen, J., Wobrock, W., Gadian, A., Mestayer, P.G., Creutin, J.-D. (2000)
The possible influence of urban surfaces on rainfall development: a sensitivity study in 2D in the meso-γ-scale.
Atmospheric Research **54**, 15-39.

Twomey, S. (1974)
Pollution and the Planetary Albedo.
Atmospheric Environment **8**, 1251-1256.

Twomey, S. (1977)
The Influence of Pollution on the Shortwave Albedo of Clouds.
Journal of the Atmospheric Sciences, **34**, 1149-1152.

Twomey, S., Piepgrass, M. and T.L. Wolfe, T.L. (1984)
An assessment of the impact of pollution on global cloud albedo.
Tellus **36b**, 356-366.

Twomey, S. (1991)
Aerosols, Clouds and Radiation.
Atmospheric Environment **25A**, 2435-2442.

Umweltbundesamt (1994)
Daten zur Umwelt, 1992/3, Berlin, Germany.

Van Dingenen, R., C., Raes, F., Putaud, J.-P., Baltensperger, U., Charron, A., Facchini, M.C., Decesari, S., Fuzzi, S., Gehrig, R., Hansson, H.-C., Harrison, R.M., Hüglin, C., Jones, M., Laj, P., Lorbeer, G., Meanhaut, W., Palmgren, F., Querol, X., Rodriguez, S., Schneider, J., ten Brink, H., Tunved, P., Torseth, K., Wehner, B., Weingartner, E., Wiedensohler, A., Wahlin, P. (2004)
A European aerosol phenomenology - 1: physical characteristics of particulate matter at kerbside, urban, rural and background sites in Europe.
Atmospheric Environment **38**, 2561-2577, doi:10.1016/j.atmosenv.2004.01.040.

Wandinger, U., Müller, D., Böckmann, Althausen, D., Matthias, V., Bösenberg, J., Weiß, V., Fiebig, M., Wendisch, M., Stohl, A. and Ansmann, A. (2002)
Optical and microphysical characterization of biomass-burning and industrial-pollution aerosols from multiwavelength lidar and aircraft measurements.
Journal of Geophysical Research **107**, doi:10.1029/2000JD000202.

Warner, J. and Twomey, S. (1967)
Comparison of measurements of cloud droplets and cloud nuclei.
Journal of the Atmospheric Sciences **24**, 702-703.

WCP-55 (1983)
Experts Meeting on Aerosols and their Climate Effects.
Deepak, A., Gerber, H.E.: *WMO – CAS and Radiation Comission of IAMAP*, Williamsburg, Virginia, March 1983.

Xu, Q. (2001)
Abrupt change of the mid-summer climate in central east China by the influence of atmospheric pollution.
Atmospheric Environment **35**, 5029-5040.

Ye, B., Ji, X., Yang, H., Yao, X., Chan, C. K., Cadle, S. H., Chan, T., Mulawa, P. A. (2003)
Concentration and chemical composition of PM2.5 in Shanghai for a 1-year period.
Atmospheric Environment **37**, 499-510.

Yu, S., Saxena, V.K., Zhao, Z. (2001)
A comparison of signals of regional aerosol-induced forcing in eastern China and the southeastern United States.
Geophysical Research Letters **28**, 713-716.

8. LIST OF SYMBOLS, UNITS AND ACRONYMS

IPCC	Intergovernmental Panel on Climate Change
SAGE	Stratospheric Aerosol and Gas Experiment
TOMS	Total Ozone Mapping Spectrometer
BRDF	Bidirectional Reflectance Distribution Function
BC	Black Carbon
AGCM	Atmospheric General Circulation Model
TAR	Third Full Assessment Report
TOA	Top of the Atmosphere
CFR	Cloud Radiative Forcing
MIR	Meteorological Research Institute (Japan)
LMD	Laboratoire de Meteorologie Dynamique (France)
CCSR	Centre for Climate System Research (Japan)
GFDL	Geophysical Fluid Dynamics Laboratory (USA)
HC	Hadley Centre (UK)
MPI-M	Max Planck Institute for Meteorology (Germany)
CSIRO	Commonwealth Scientific and Industrial Research Organization (Australia)
NCAR	National Centre for Atmospheric Research (USA)
BMRC	Bureau of Meteorology Research Centre (Australia)
ITCZ	Inter-Tropical Convergence Zone
CCN	Number of Condensation Nuclei
TIROS	Television Infrared Observation Satellite Program
TRMM	Tropical Rainfall Measuring Mission
LBA-SMOCC	Large-scale Biosphere-Atmosphere Experiment in Amazonia subproject on Smoke, Aerosols, Clouds, Rainfall, and Climate
SCAR-B	Smoke, Clouds, Radiation-Brazil
TARFOX	Tropospheric Aerosol Radiative Forcing Experiment
INDOEX	Indian Ocean Experiment
ACE	Aerosol Characterization Experiment
AVHRR	Advanced Very High Resolution Radiometer
NOAA	National Oceanic and Atmospheric Administration (USA)
NASA	National Aeronautics and Space Administration (USA)
GAC	Global Area Coverage Data
ICT	Internal Calibration Target
NESDIS	National Environmental Satellite, Data and Information Service of NOAA (USA)
CLVAR	Clouds from AVHRR
RGCT	Reflective Gross Cloud Test
RUT	Reflectance Uniformity Test
MCSST	Multi Channel Sea Surface Temperature Algorithm
C3AT	Channel 3 Albedo Test
C3AR	Channel 3 Albedo Restoral Test
TUR	Thermal Uniformity Restoral Test
RRCT	Reflectance Ratio Cloud Test
TUT	Thermal Uniformity Test
FMFT	Four Minus Five Test
TGCT	Thermal Gross Cloud Test

RRCTH	Reflectance Ratio Cloud Test for Haze
PBL	Planetary Boundary Layer
LPA	Local Planetary Albedo
GDR	German Democratic Republic
PM	Particulate Matter
JFND	January, February, November, December
JF	January, February
ND	November, December
MJJA	May, June, July, August
MJ	May, June
JA	July, August
OECD	Organisation for Economic Cooperation Development
MODIS	Moderate Resolution Imaging Spectroradiometer
CCM	Community Climate Model
DMS	Dimethylsulfide
SFB 512	Sonderforschungsbereich 512
SST	Sea Surface Temperature
NAO	North Atlantic Oscillation
POP	Persistent Organic Pollutant
METROMEX	Metropolitan Meteorological experiment

9. LIST OF FIGURES AND TABLES

APPENDIX

REPRINTS OF PAPERS

Paper I

The indirect aerosol effect over Europe

Olaf Krüger
Meteorologisches Institut, Universität Hamburg, Germany

Hartmut Graßl
Meteorologisches Institut, Universität Hamburg and Max-Planck-Institut für Meteorologie, Germany

Received 17 September 2001; revised 28 March 2002; accepted 5 April 2002; published 10 October 2002.

[1] In order to assess the influence of anthropogenic emissions on cloud albedo over Europe a reprocessed set of satellite measurements from 1985 to 1999 was investigated. Special emphasis was given to the Central European main emission area, including the so-called 'Black Triangle' which covered parts of Germany, the Czech Republic and Poland. Due to the decrease of aerosol precursor gases the analysis reveals a pronounced decrease of cloud albedo of about 2% from the late 80s to the late 90s. During winter in source regions of anthropogenic particulate matter emissions the cloud reflectance is more than 5% lower referring in addition to an absorption effect caused by black carbon in clouds. The comparison with emission data as well as model results of long range transport over Europe strongly supports the conclusion that the changed indirect aerosol effect is responsible for significantly changed cloud optical properties. Radiative transfer calculations indicate for the classical Twomey effect a change in radiative forcing of about 1.5 W/m^2 from the late 80s to the late 90s. In addition during winter a radiative forcing of about 3 W/m^2 due to the absorption effect for both the late 80s and the late 90s is estimated. *INDEX TERMS:* 3359 Meteorology and Atmospheric Dynamics: Radiative processes; 3339 Meteorology and Atmospheric Dynamics: Ocean/atmosphere interactions (0312, 4504); 3374 Meteorology and Atmospheric Dynamics: Tropical meteorology; 3319 Meteorology and Atmospheric Dynamics: General circulation; 1821 Hydrology: Floods. **Citation:** Krüger, O., and H. Graßl, The indirect aerosol effect over Europe, *Geophys. Res. Lett.*, *29*(19), 1925, doi:10.1029/2001GL014081, 2002.

1. Introduction

[2] Radiative forcing of climate due to the influence of tropospheric aerosols on cloud albedo is highly uncertain. One reason is that this indirect aerosol effect is always a combination of two competing processes. Firstly, aerosols act in part as cloud condensation nuclei. For constant cloud liquid water content an increasing number of condensation nuclei would shift the mean droplet size to smaller radii. In theoretical studies [*Twomey*, 1974] it has been shown, that this process may increase cloud albedo strongly, especially for thin stratus decks. Besides this influence of aerosols on droplet number and size there is a second process acting on cloud albedo: absorption by aerosol particles (e.g. black carbon or soot, fly ash). The interaction of both processes determines the radiative characteristics of clouds and consequently the cloud albedo [*Graßl*, 1975; *Twomey*, 1977].

0094-8276/02/2001GL014081$05.00

[3] Mainly based on model results, the Intergovernmental Panel on Climate Change (IPCC) estimated the indirect aerosol forcing to be negative, reaching in the global mean up to 2 W/m^2 [*Climate Change*, 2001]. But this estimate is marked as highly uncertain and even a negligible indirect effect seems possible. The objective of the present study was to determine cloud albedo changes with time as a function of emission characteristics for Central Europe, where major emission changes have occurred especially after the fall of the Berlin wall. We used official emission inventories and operational satellite data, i.e. the Pathfinder data set published by NASA containing measurements from AVHRR sensors on several NOAA satellites. In order to exclude the potential effect of volcanoes only satellite measurements within the periods 1985–1989 and 1996–1999 were investigated, largely free of volcanic aerosols in the stratosphere.

2. Observation of Cloud Reflectances

[4] Since the crucial point of the study is the evaluation of long term cloud reflectances over Europe the reprocessed global NOAA/NASA Pathfinder data set from the Advanced Very High Resolution Radiometers (AVHRR) on board the afternoon-viewing NOAA series satellites (NOAA-7, 9, 11, and 14) was used. The data set has been processed by NASA using best available methods for a consistent time series of unprecedented quality. Methods used in preprocessing include cross-satellite calibration, application of a precision navigation system and correction for Rayleigh scattering [*James and Kalluri*, 1994]. The AVHRR instrument measures both reflected solar and emitted terrestrial radiation in five spectral channels which take advantage of maximum transmittance in the atmospheric windows. The instrument enables a detailed cloud detection. In this study, for delineating optical characteristics of clouds, the NOAA/NESDIS algorithm [*Stowe et al.*, 1991] was applied. The technique utilizes the five-channel AVHRR multi-spectral information, individual values as well as spatial differences, in series of sequential decision-tree type tests and includes established or empirically optimized thresholds. The procedure allows to identify cloud-free, mixed and cloudy atmospheres. The cloud detection is based on the magnitudes of emitted and reflected radiation, the wavelength dependence and spatial variability.

3. Evaluation of Satellite Measurements

[5] The indirect aerosol effect is difficult to assess from an instantaneous satellite image. It appears to be nearly impossible to interpret a cloud system in individual satellite

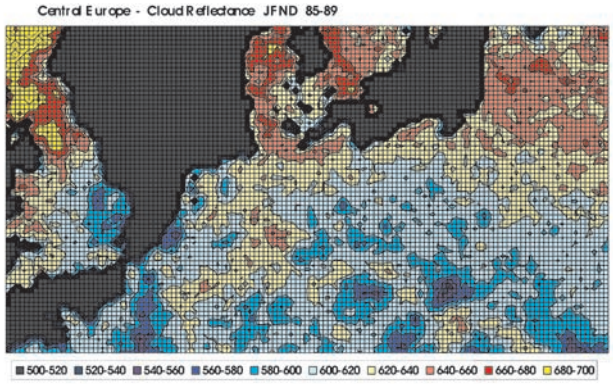

Figure 1. Mean cloud reflectance derived from AVHRR channel 2 satellite measurements over parts of Central Europe in thousandth. Data are shown from −5.0° to 28.5° longitude and 48.5° to 57.5°N for the winter period (January, February, November, December) from 1985 to 1989 (excluding data from 1987).The grid size is 0.25° longitude and 0.125° latitude. The area covers parts of UK, Denmark, Sweden, France, Benelux, Germany, Poland, Czech Republic and Ukraine. The North Sea and the Baltic Sea are in black.

pictures without information on cloud development. Also cloud water content should be known to derive the order of magnitude of the indirect effect. Further, because of the complex characteristics of the formation of secondary aerosols and the various processes being involved in cloud microphysics it is a comprehensive task to follow anthropogenic emissions from the source to the receptor cloud system. It is also easier to catch the indirect effect at or near the source regions of anthropogenic emissions. The interpretation of the indirect effect in more remote regions would demand mesoscale and regional modeling including radiative transfer. However, since indications for the indirect effect known from measurements are rare, we assume that modeling may not describe the cloud aerosol interactions adequately at present.

[6] In order to detect the indirect effect we decided to analyze long term changes of cloud reflectance in satellite measurements. Therefore we evaluated the AVHRR channel 2 frequency distributions of cloud reflectance for all cloudy pixels. Special emphasis was given to the mesoscale spatial variability over Central Europe. Channel 2 was chosen because of minor influence of Rayleigh scattering. As the aim also was to strongly reduce inter-annual variability, we considered frequency distributions over 4 years. We focused our evaluation on two main aspects:

The comparison of cloud reflectance for two episodes of distinct amount of SO_2 emission.

The analysis of spatial heterogeneity of cloud reflectance.

[7] Applying an algorithm for cirrus cloud detection the intension was to restrict the evaluation to water clouds. The parameters of interest were the arithmetic mean, the coefficient of variation, the standard deviation and the frequency of occurrence of water clouds. Since we expected the indirect aerosol effect mostly near the strong emission sources of PPM and SO_2 the area of interest was Central Europe including parts of Western and Eastern Europe (longitude −5°W to 31°E, latitude 48°N to 60°N). The former GDR is in the centre of this area, a region of extremely high emissions of precursor gases as well as primary particles during the period 1985 to 1989 with stronger contributions from elevated point sources as compared to other European countries.

[8] We investigated the influence of air pollution on the reflectance of clouds for the four-year periods from 1985 to 1989 (excluding 1987 because of problems with data for several months) and from 1996 to 1999. In our study we considered also seasonal differences. The winter episode covers the months January, February, November and December of four years (hereafter referred to as JFND8589 and JFND9699 respectively), the summer episode includes data from May, June, July and August of four years (MJJA8589, MJJA9699).

[9] The EMEP model results [*EMEP*, 2000] show that in our area of interest there exist strong gradients of annual mean concentrations of PM from more remote regions to the emission areas which we name source regions. The location of extreme values of the mean AVHRR reflectance is found in areas of above 20 $\mu g/m^3$ PM. These source regions contain significantly increased PM concentrations as compared to remote regions with 5 $\mu g/m^3$.

[10] The annual mean SO_2 concentrations vary from 1 $\mu g/m^3$ (sulphur) in remote regions to above 10 $\mu g/m^3$ over the former GDR, the Czech Republic and Poland. The areas of lowest mean reflectance during winter (see Figure 1) and the areas of highest mean reflectance during summer (see Figure 3) are nearly identical with the areas of highest PM concentrations, or highest SO_2 concentrations respectively. While we see several minima of reflectance over Central Europe the pattern is more homogeneous during summer with a dominant maximum located over the Czech Republic and Poland.

3.1. Indirect Aerosol Effects

[11] In detail the spatial heterogeneity of the wintertime cloud reflectance over Europe shows a clear gradient from Great Britain, Scandinavia and former Soviet Union to the densely populated industrial regions of Central Europe with up to 10% smaller reflectance over Central Europe.

[12] Main emission centers show lower cloud reflectance in all western, central and eastern European countries evaluated so far for both the JFND8589 (Figure 1) and the JFND9699 period. The areas of minimum cloud reflectance with values even lower than 58% are located around London, Paris, Rotterdam, Frankfurt/Main, Leipzig, Prague, Kattowice, Cracow and Vienna. We interpret the strong reflectance decrease from remote to source regions by the impact of BC emissions originating mainly from power plants, small combustion and mobile sources. During JFND8589 also fly ash emitted from power plants should be taken into consideration.

[13] The long term difference of cloud reflectance for the total area is lower by about 2.8 percent in the period JFND9699 than during JFND8589 (Table 1). This is a further clear indication that the Twomey effect worked. However, our results also show that the magnitude of the Twomey effect is not only due to the increase of droplet concentration and thereby optical thickness, but also due to changes of the absorption coefficient, that becomes domi-

Table 1. Mean Cloud Reflectances (in %) Derived From AVHRR Channel 2 Satellite Measurements Over Parts of Central Europe (−5.0° to 28.5° Longitude and 48.5° to 57.5°N) for the Winter Period JFND (January, February, November, December) and for the Summer Period MJJA (May, June, July, August) From 1985 to 1989 (Excluding Data From 1987) and 1996 to 1999 Respectively

	1985–1989	1996–1999	Difference
Winter JFND	61.5	58.7	−2.8
Summer MJJA	65.7	63.6	−2.1

nant for optically thick clouds. The lower boundary layer height and the slow formation of secondary aerosols from precursor gases during winter favours the dominance of the absorption effect in source regions of Central Europe.

[14] The summertime cloud reflectance over Europe during MJJA8589 delivers a clear indication for the classical Twomey effect accompanied with higher reflectances which are initiated by increased droplet concentration (Figure 2). Eastern and Central Europe show higher cloud reflectivity in comparison to the British Isles and Western Europe. Individual metropolitan and industrial regions are no longer directly visible in cloud reflectance, pointing to decreased carbon emissions during summer and to a more rapid transformation of precursor gases into aerosol particles from gaseous emissions. The gradient of cloud reflectance from remote to polluted regions changes sign if compared to winter. Highest reflectances occur in regions of well known maximum sulphur dioxide concentrations over the black triangle of Europe. The average cloud reflectance decreases between MJJA8589 and MJJA9699 by about 2.1 percent (Table 1).

3.2. Indirect Radiative Forcing of Tropospheric Aerosols

[15] The long term differences of the measured reflectances if expressed solely by the classical Twomey effect are eqivalent to a decrease from 6 μm to 3 μm for the effective radius of the cloud droplets. Calculations with a numerical radiative transfer model [*Key and Schweiger*, 1998] for a stratus cloud over vegetation (cloud base ∼500 m, cloud top ∼1000 m, cloud liquid water content 0.2 g/m^3, single scattering albedo 0.997 and optical thickness 30) in a mid-latitude atmosphere including an urban aerosol model (optical thickness 0.66) translate this shift into a cloud forcing of about 1.5 W/m^2.

[16] As seen from the spatial heterogeneity of cloud reflectance in addition an absorption effect caused by BC emissions has to be considered. This is clearly indicated by the decrease of the measured reflectances from remote to source regions for both winter periods. Figure 1 shows strong gradients that occur from Scandinavia to Germany, from the western to the polluted eastern part of England and from Lithuania to Poland. But there is an even stronger gradient from East Europe to Central Europe (not shown in Figure 1).

[17] In radiative transfer calculations we neglect a radius effect of BC at the time of the emission since BC particles are hydrophobic and chemically inert [*Crutzen et al.*, 1984]. We rather assume that the high amount of particles in source regions favour the physical transformation of black carbon into a hydrophilic form. Therefore the condensation close to source regions is based on internally mixed aerosol and consequently the albedo of cloud droplets is significantly reduced referring to a single scattering albedo of about 0.997. Due to wet deposition the black carbon content in aerosols decreases in remote areas with distance from sources. An additional explanation for the absorption effect might be that low clouds in source regions contain a higher portion of BC particles in the interstitial aerosol. For quantifying the absorption effect we take into account a 5% smaller reflectance over the densely populated industrial regions of Central Europe which is equivalent to a reduction of single scattering albedo from 0.999 to 0.997 for the stratus cloud above. The positive radiative forcing of this additional absorption is about 3 W/m^2 whose magnitude is higher than the 1.5 W/m^2 that originate from the Twomey effect for a 50% reduction of SO_2 emission.

[18] Combining the results for the radius effect and the absorption effect even a net positive radiative forcing for Central Europe might have been the case during the winters 85–89. Due to the strong decrease of SO_2 emissions from 1989 to date the net forcing might even have increased during the 1990s. The rapid increase of private traffic in Central Europe and the growing share of diesel engines are given here as arguments. However, no BC emission trends have been published for this part of Europe. Therefore, it is too early to fix the sign of the indirect aerosol radiative forcing for strongly polluted regions.

4. Discussion and Conclusions

[19] The geographical location of the changes in cloud reflectance for the winter episodes caused by the absorption effect as discussed above is generally in accordance with modelled particulate matter [*EMEP*, 2000] using the best available information on emission inventories. Also black carbon emission inventories and model simulations *Cooke and Wilson* [1996] and *Liousse et al.* [1996] are in agreement with our results. The strongest decrease in cloud reflectance is seen exclusively around emission areas. According *Twomey* [1977] the decrease in reflectance as shown in Figure 1 would be roughly translated in a reduction of cloud optical thickness by 30–50% for optical

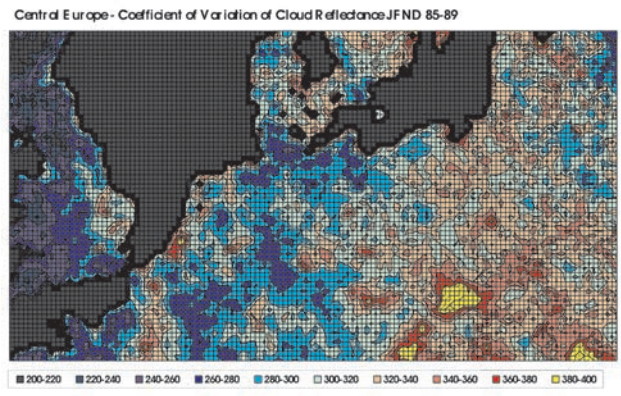

Figure 2. Mean coefficient of variation of cloud reflectance derived from AVHRR channel 2 satellite measurements over parts of Central Europe in hundredth. The area and the years are the same as for Figure 1. The numbers are due to the winter periods (January, February, November, December) from 1985 to 1989.

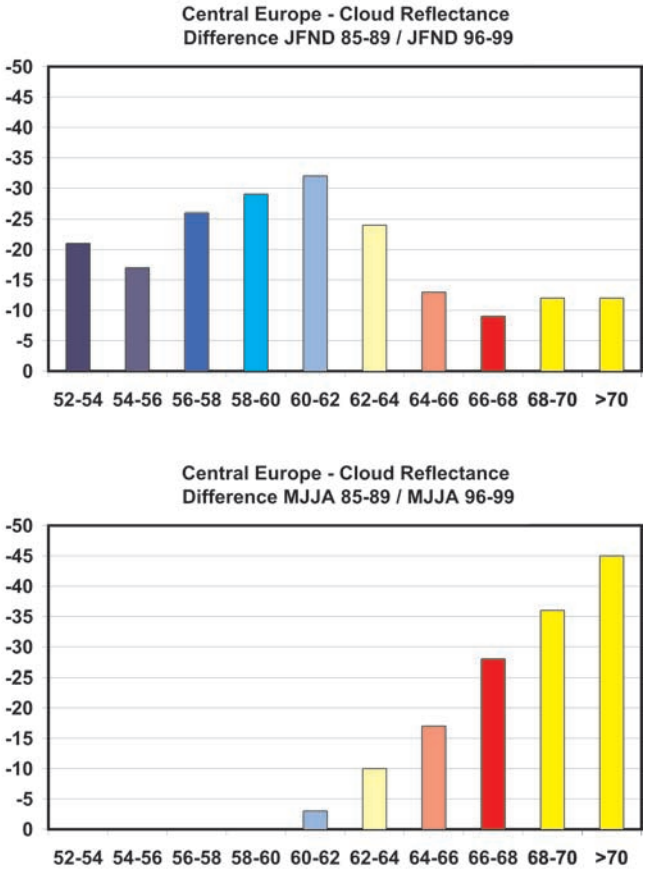

Figure 3. (a, b) Decrease of cloud reflectance in thousandth (axis of ordinate) from 85–89 to 96–99 for the different areas of mean reflectance (unit: %) as depicted in Figures 1 and 2 (same colors).

thick clouds (optical thickness 50) and more than 50% for optical thin clouds (optical thickness 10). This makes it clear that such mesoscale reflectance patterns over Europe can not be explained by the natural variation of the cloud optical thickness. Except for an anthropogenic influence there is no other reason why clouds should have such a decreased optical thickness just over the areas of highest PM concentration.

[20] Regarding the radius effect we again exclude that the differences in reflectance are mainly caused by natural variability of the cloud optical thickness. Firstly during winter we see for the comparison of the two winter episodes the strongest reductions from 85–89 to 96–99 of about 3% reflectance near the main emission centres (see Figure 3a). In remote regions we only have a decrease of 1% reflectance. It is not likely that based on climatological variations of the cloud optical thickness the reflectance in the vicinity of the emission sources of PPM and precursor gases has reduced by 3% while in remote regions the changes only amount to 1%.

[21] During summer again we see the most pronounced radius effect over the regions of strongest pollution (Figure 3b).

[22] These are the areas of highest SO_2 concentrations during the 80s were highest decrease in reflectance by more than 4% occurred. The remote regions show, as for winter, a decrease of only 1% reflectance. Again it is not likely that without an anthropogenic influence just in these regions over Poland and the Czech Republic the optical thickness of clouds has changed while the changes in remote areas are, as in winter, very small.

[23] We conclude that our study reveals evidence for the regional occurrence of an indirect aerosol effect over Europe. A pronounced seasonal variability of the indirect aerosol forcing is shown. The reduction of the sulphur dioxide emissions by about 50% (23 Tg y^{-1}) is accompanied by a change in radiative forcing of about 1.5 W/m^2. Further, black carbon emissions in the order of magnitude of 1 Tg y^{-1} reduce the cloud reflectance in source regions by more than 5%. However, since information about BC emission changes is lacking a precise relation between BC emission and cloud albedo can not be given.

References

Climate Change, The scientific basis, contribution of Working Group I to the third assessment report of the Intergovernmental Panel on Climate Change, Intergovernmental Panel on Climate Change, Working Group I, J. T. Houghton et al. (Eds.), Cambridge University Press, p. 881, 2001.

Cooke, W. F., and J. J. N. Wilson, A global black carbon aerosol model, *Journal of Geophysical Research*, *101*(D14), 19,395–19,409, 1996.

Crutzen, P., I. Galbally, and C. Bruhl, Atmospheric effects from post nuclear fires, *Climate Change*, *6*, 323–364, 1984.

EMEP, Status Report with respect to Measurements, Modelling and Emissions of Particulate Matter in EMEP: An integrated approach, Joint CCC and MSC-W Report 2000, EMEP MSC-W Note 5/00, August 2000 Meteorological Synthesizing Centre - West, Norwegian Meteorological Institute, P.O. Box 43 - Blindern, N-0313 Oslo, Norway, 2000.

Graßl, H., Albedo reduction and radiative heating of clouds by absorbing aerosol particles, *Contributions Atmospheric Physics*, *48*, 199–210, 1975.

James, M. E., and S. N. V. Kalluri, The Pathfinder AVHRR land data set: An improved coarse resolution data set for terrestrial monitoring, *International Journal of Remote Sensing*, *15*(17), 3347–3363, 1994.

Key, J. R., and A. J. Schweiger, Tools for Atmospheric Radiative Transfer: STREAMER and FLUXNET, *Computers and Geosciences*, Vol. 24, No.5, pp. 443–451, 1998.

Liousse, C., J. E. Penner, C. Chuang, J. J. Walton, H. Eddleman, and H. Cachier, A global three-dimensional model study of carbonaceous aerosols, *Journal of Geophysical Research*, *101*(D14), 19,411–19,432, 1996.

Stowe, L. L., E. P. McLain, R. Carey, P. Pellegrino, G. G. Gutman, P. Davis, C. Long, and S. Hart, Global distribution of cloud cover derived from NOAA/AVHRR operational satellite data, *Advances in Space Research*, *11*(3), (3)51–(3)54, 1991.

Twomey, S., Pollution and the planetary albedo, *Atmospheric Environment*, *8*, 1251–1256, 1974.

Twomey, S., The Influence of Pollution on the Shortwave Albedo of Clouds, *Journal of the Atmospheric Sciences*, *34*, 1149–1152, 1977.

O. Krüger, Meteorologisches Institut, Universität Hamburg, Bundesstraße 55, D-20146 Hamburg, Germany. (olaf.krueger@dkrz.de)

H. Graßl, Max-Planck-Institut für Meteorologie, Bundesstraße 55, D-20146 Hamburg, Germany. (grassl@dkrz.de)

Paper II

Albedo reduction by absorbing aerosols over China

Olaf Krüger[1] and Hartmut Graßl[1,2]

Received 19 November 2003; revised 12 December 2003; accepted 23 December 2003; published 21 January 2004.

[1] Long-term observations with satellites show that absorbing aerosols have reduced the local planetary albedo (LPA) over China during the recent decade. While the reduction of air pollution was leading to an LPA decrease in Europe, an increase of pollution in China also lowered the LPA. The strong absorption in clouds is accompanied by a cloud lifetime effect over the Red Basin and surrounding areas in southern China. *INDEX TERMS:* 0305 Atmospheric Composition and Structure: Aerosols and particles (0345, 4801); 0320 Atmospheric Composition and Structure: Cloud physics and chemistry; 0345 Atmospheric Composition and Structure: Pollution—urban and regional (0305). **Citation:** Krüger, O., and H. Graßl (2004), Albedo reduction by absorbing aerosols over China, *Geophys. Res. Lett.*, *31*, L02108, doi:10.1029/2003GL019111.

1. Introduction

[2] During the last two decades East Asia was the most rapidly developing area in the world. The population growth in East Asian countries and the rapid economic development are accompanied by an air pollution increase [*UNEP and C*^{4}, 2002]. The enormously increased concentration of aerosol particles leads to massively lowered visibility and also shortwave radiation reaching the surface [*Xu*, 2001].

[3] A plausible consequence would be an increased local planetary albedo (LPA) for cloudless and cloudy atmospheres. We investigated changes of LPA at $\sim$0.8 μm wavelength using AVHRR channel 2 data. The LPA here is represented by a reflectance which is calculated from the radiance at the satellite and the solar irradiance [*Rao*, 1987].

[4] Since the 1970s an effect on clouds induced by air pollution has been discussed [*Twomey*, 1974]. Theoretical studies on the basis of measurements suggested that near the source regions of pollution there are two competing processes [*Twomey et al.*, 1984]. Firstly, there is an increase of the concentration of cloud droplets via increased cloud condensation nuclei. This results – at unchanged cloud water – in a larger surface area of the droplets and therefore in an increased cloud albedo. Secondly, the absorption effect by black carbon (BC) often will be increased and thus lower the albedo of clouds [*Grassl*, 1975] and reduce the albedo increase of optically thin clouds that are more strongly influenced by the radius effect.

2. Evaluation of Satellite Measurements

[5] Our analysis of NOAA AVHRR data, i.e., the Pathfinder data set [*James and Kalluri*, 1994], from the late 1980s (4 years average) to the late 1990s (again 4 years average) over China shows an amazing result: The LPA increases only during summer southward of 30°N (Figure 1a). Northward of 30°N even a decrease becomes visible. During winter (Figure 1b) the LPA is decreased in nearly all regions. The highest decrease of LPA in winter from the late 1980s to the late 1990s occurred over polluted regions. This pronounced change with maxima higher than 5% is unique if compared to North America and Europe. The heterogeneity of the change in China, i.e., higher values of change in densely populated and industrialized areas, suggests that changing air pollution is the main cause.

[6] Since air pollution in China generally was much more pronounced during the late 1990s than during the late 1980s [*Xu*, 2001] the negative LPA change cannot be explained by a strong decrease of sulphur dioxide (SO_2) emissions, as took place enforced by Clean Air Acts in North America over recent decades and in Europe since the early 1990s. In Europe, for example, during this time an extreme emission reduction by about 23 Tg y^{-1} sulphur, which is not seen at all in China, was the reason for a lowering of low and medium level cloud albedo of about 2–3% [*Krüger and Graßl*, 2002]. Two key questions arise from this conspicuous regional climate change:

- Has cloud cover changed as a consequence of increased air pollution?

- Is brown haze responsible for the reduction of the local planetary albedo?

[7] First hints regarding the influence of indirect aerosol effects on LPA change can be derived by separating the total LPA change into the contribution by low and medium level clouds on one hand and the residual change of all other atmospheres on the other. The residual LPA change therefore contains cloudless atmospheres (including haze), partially cloud covered pixels and high level clouds. We expected, in case the aerosol is absorbing, that the absorption effect becomes visible for the often optically thick low and medium level clouds while the radius effect is dominant for the much lower mean optical thickness of the partly cloudy atmospheres. In case of a strong increase of absorbing aerosol concentration, which might be due to so-called brown haze or dust or both in a mixture, for clear or partially cloud covered pixels a decrease of LPA must become also visible for the residual atmospheres.

[8] The residual LPA changes in the Gobi desert and around Liuzhu north-west of Hong Kong confirm that aerosol effects have these pronounced influences on residual LPA. In the Gobi desert the LPA of low and medium level clouds increases by more than 3% which indicates an effect of decreasing cloud droplet radius (Figures 1c and 1d). However, these changes can not be explained alone by enhanced emissions of mineral dust through sand storms. The seasonal dependency supports that particles of anthropogenic origin may have also a strong influence. The radius

[1]Meteorologisches Institut, Universität Hamburg, Germany.
[2]Max-Planck-Institut für Meteorologie, Hamburg, Germany.

0094-8276/04/2003GL019111$05.00

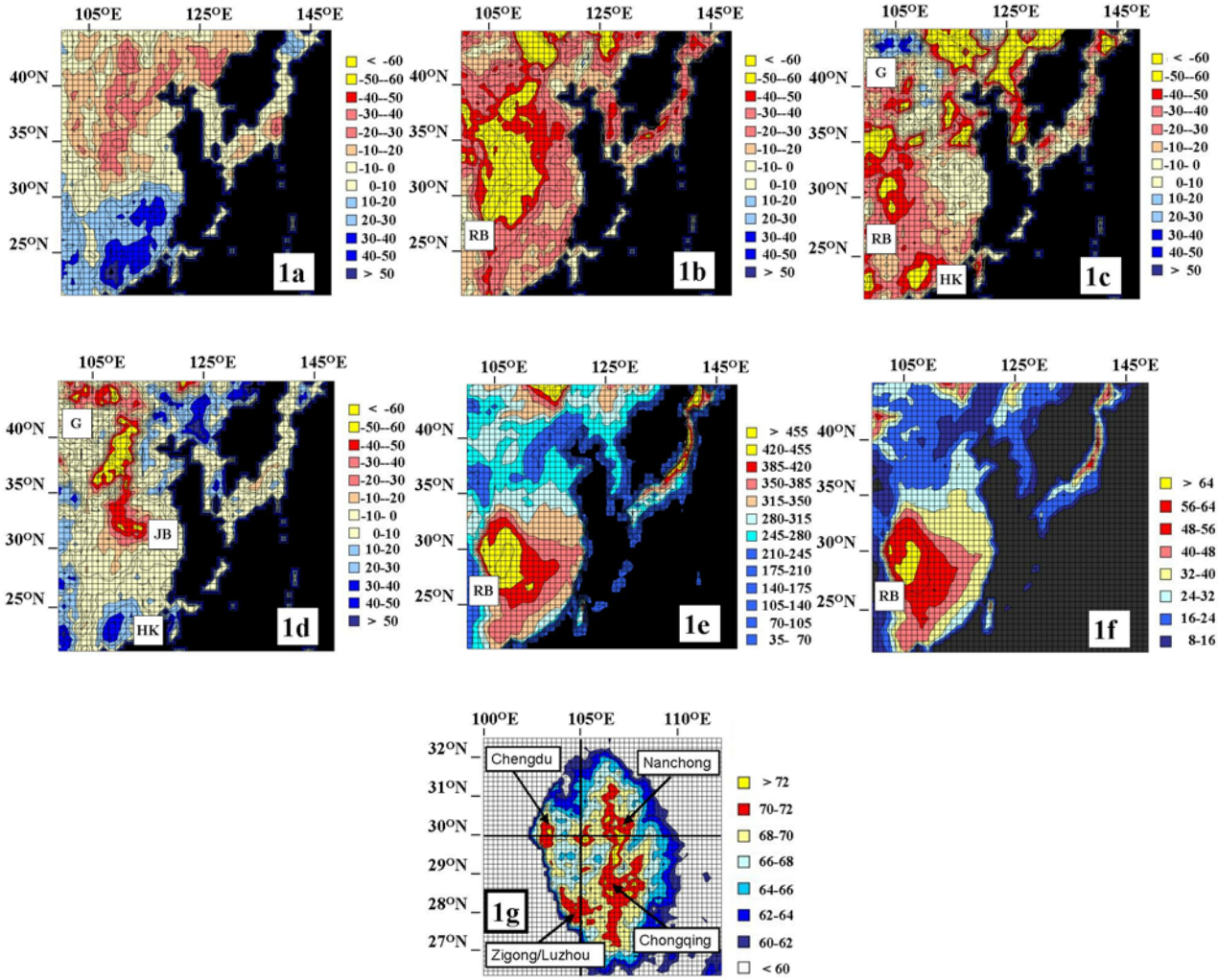

Figure 1. Changes of the local planetary albedo (LPA) in thousandth at ~0.8 μm wavelength (AVHRR, channel 2) from the late 1980s (1985, 1986, 1988, 1989) to the late 1990s (1996, 1997, 1998, 1999) over south-eastern Asia for summer, MJJA (a) and winter, JFND (b). The grid size is 1° longitude and 0.5° latitude. The area covers China, Mongolia, North Korea, South Korea, Japan and parts of the Pacific (in black). The Red Basin (RB), the Gobi desert (G), Hong Kong (HK) and the Jangtze Basin (JB) are indicated. The total mean LPA change is subdivided into the contributions of low and medium level clouds for winter (c) as well as into the residual change for cloudless atmospheres (including haze), plus partially cloud covered pixels and high level clouds (d). The maximum values of the mean local planetary albedo (e), in thousandth, and also of cover by low and medium level clouds (f, g), in percentage, occur in the Red Basin over densely populated regions (the winter for the late 1990s is shown).

effect is most pronounced during the summer monsoon when anthropogenic aerosols are advected to the north from emission areas in southern and eastern China. In addition the LPA decrease of the residual atmospheres for winter and summer in the Gobi desert indicates an increasing concentration of absorbing aerosols.

[9] During winter in southern China, where mean cloud optical thickness is much higher, and where major source regions of pollution exist, the strongest contribution of low and medium level clouds to the total decrease of LPA occurs. In Liuzhu north-west of Hong Kong for example the maximum decrease from the late 1980s to the late 1990s amounts to more than 5%. At the same time in the same area the LPA increased for the residual atmospheres (Figures 1c and 1d). This clearly confirms that indirect aerosol effects, i.e., the absorption effect for low and medium level clouds and the radius effect for residual atmospheres, change the LPA.

[10] In order to investigate the strong decrease of LPA in more detail we focused on southern China where present day world wide highest fine aerosol optical depth was detected [*Kaufman et al.*, 2002]. Here in the Red Basin an even larger LPA decrease occurs than in the region north of Hong Kong. The Red Basin at about 30°N latitude and 105°E longitude has a dimension of more than 300 × 300 km^2 and is surrounded by high mountains in nearly all directions reaching up to 7500 m height. The area is characterized by dense population and includes important industrial branches based on hard-coal, oil and natural gas. The combination of high emission source strength and topography favour the accumulation of pollutants in the lower troposphere. Over the Red Basin the strongest decrease

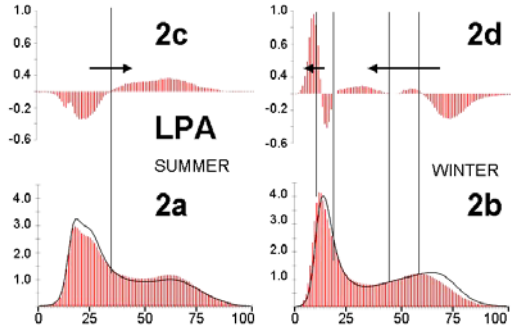

Figure 2. Frequency distribution of LPA (in percent per LPA interval of 1% width) south of 32.5° N over southern China (including the Red Basin and the lower Jangtze Basin) for summer (a) and winter (b) during the late 1980s (solid black line) and the late 1990s (red). In addition the differences between the late 1980s and the late 1990s are detailed in (c) and (d). During summer higher LPA is more frequent (see arrow indicating the shift). In winter there is a shift to lower LPA when the absorption effect in clouds and brown haze is dominating.

from the late 1980s to the late 1990s occurs for winter in areas of highest LPA (Figure 1e). The values decline with distance to the basin.

[11] The analysis of cloud cover by low and medium level clouds (Figures 1f and 1g) in this area shows: A maximum exists just over the Red Basin. As for LPA the values for cloud cover continuously decline over several hundred kilometres distance to the basin. The comparison of the late 1980s and the late 1990s for distinct LPA classes shows that there is only a rather small change of cloudiness in winter (Figure 3a). Therefore the strong LPA changes in winter can not be explained by a reduction of cloudiness.

[12] Generally also an influence of brown haze on LPA is possible. If the haze layers become more intense then the LPA changes of the residual atmospheres must show it. Indeed, northward of 30°N there is an increase of haze (Figure 1d). However, over the Red Basin where the strongest decrease of LPA takes place we see no indication for a strong increase of haze indicated by a lowering of LPA.

[13] Therefore we can answer the second question as follows: We detect an increase of brown haze in some regions, but brown haze has only a limited contribution on the total decrease of LPA during winter from the late 1980s to the late 1990s. The main decrease by brown haze occurs north of the Jangtze Basin.

[14] The main processes causing a change of LPA are indicated by the frequency distribution of LPA (Figures 2a and 2b). The change of the LPA frequency distribution for winter points to two major shifts: One for optically thick clouds at high LPA and one for the cloud-free part at the lower limit. At the latter the frequency distribution function shows a clear shift to low LPA. Since generally the LPA for the clear atmosphere tends to increase by pollution, a slight decrease can only be explained by dominance of the absorbing component, i.e., brown haze. South of 32.5°N this is mainly due to the emissions in the Jangtze Basin. However, the strongest change occurs for optically thick clouds that show LPA reduction. Again it becomes visible: Brown haze reduces the LPA in China, but haze in cloudless areas alone can not explain the strong decrease of LPA as seen for example in the Red Basin. In contrast to the winter albedo reduction LPA is clearly increased in summer south of 32.5°N. This might be due to an increasing radius effect because major changes are detected for the residual atmospheres.

3. Discussion and Conclusions

[15] Since we identified changing cloud optical properties as the major reason for the downward trend of LPA in southern China the characteristics of these changes are discussed now in more detail. For that a subdivision of the area south of 32.5° into areas of different mean LPA around the Red Basin (Figure 1e) is useful. Two major characteristics arise from the subdivision: Firstly, the LPA of medium and low level clouds for winter shows a much stronger decrease with total LPA (equivalent with distance to the Red Basin) than during summer (Figure 3a). This is due to the much lower mean cloud optical thickness, as seen from mean LPA for low and medium level clouds, in the areas north-east of the Red Basin. Secondly, the winter cloud cover from the late 1980s to the late 1990s for all areas is nearly identical (Figure 3a). Therefore no major climate change for clouds is seen which could explain the changing LPA. Since a much higher reduction of LPA (Figure 3b) occurs in areas of higher cloud amount and

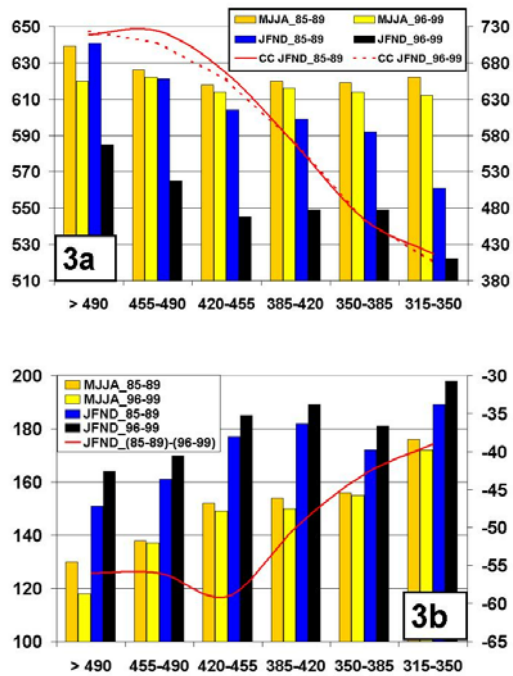

Figure 3. (a) LPA of low and medium level clouds (left axis, coloured columns) and cloud cover for winter (right axis, red lines) over southern China south of 32.5° N in thousandth as a function of mean reflectance in and around the Red Basin (late 1990s, Figure 1e). (b) Standard deviation (left axis, coloured columns) and LPA change of low and medium level clouds (right axis, solid red line) in thousandth (same areas as in (a)).

higher optical thickness, with maximum values just over the densely populated regions of the Red Basin (Figure 1g), the LPA changes are due the absorption effect. The analysis of temperature trends in China [*Yu et al.*, 2001] supports our conclusion that there must be enormously high concentrations of absorbing aerosols during winter. The maximum LPA decrease (Figures 3a and 3b) in the northern part of the Red Basin can be explained by a high degree of pollution around Chengdu and Nanchong and an advection of pollution from the Xian region.

[16] We get further evidence for this interpretation by the behaviour of the standard deviation which confirm an anthropogenic influence on cloud LPA (Figure 3b). In all areas in and around the Red Basin the variability is clearly higher in winter than in summer. This is due to the strong influence of black carbon which, if integrated into the cloud, reduces LPA so strongly that we can see a high difference between the cases of highly polluted and less polluted clouds. Therefore the high variability is an indication of the absorption effect as well. The same variance characteristics have been derived for Europe [*Krüger and Graßl*, 2002]. The increase of variability for all regions in winter shows evidence for increasing black carbon concentrations.

[17] In summer the absorption effect is much weaker, as in Europe, because of higher sulphate formation rates and higher boundary layers. Only in the source regions of pollution around densely populated regions in the Red Basin (Figure 3a and 1g) there is still a dominating influence of black carbon on summertime cloud LPA.

[18] Evidence for the radius effect is seen by the continuous decrease of standard deviation from remote regions to the source regions of pollution in the Red Basin. This is due for both summer and winter. It can be explained by the radius effect because it increases the LPA for optically thin clouds and therefore reduces the width of the frequency distribution for LPA of low and medium level clouds. The decrease of the standard deviation from the late 1980s to the late 1990s in summer also indicates an increase of pollution. The maximum change occurs in the Red Basin.

[19] We conclude that the increased cloud cover over the Red Basin is an indication for an additional indirect aerosol effect, the so-called lifetime effect. As a consequence of the radius effect it describes an increase in cloud lifetime and thus in cloud cover. Over the Red Basin continuously high aerosol number concentrations can lead to a nearly permanent radius effect with a considerably decreased effective radius of cloud droplets. Under those conditions coalescence is largely suppressed. Consequently the lifetime of clouds grows. Our study shows that mainly inside the Red Basin cloud cover is clearly higher in the regions around Chengdu, Nanchong, Chonquing and Zigong/Luzhu. These densely populated cities are strong sources of air pollution. The cloud lifetime effect over the Red Basin corresponds well to the precipitation decrease there in mid-summer during the last decades [*Xu*, 2001; *Rosenfeld*, 2000].

References

Grassl, H. (1975), Albedo Reduction and Radiative Heating of Clouds by Absorbing Aerosol Particles, *Contributions to Atmospheric Physics*, *48*, 199–210.

Kaufman, Y., D. Tanre, and O. Boucher (2002), A satellite view of aerosols in the climate system, *Nature*, *419*, 215–223.

Krüger, O., and H. Graßl (2002), The indirect aerosol effect over Europe, *Geophys. Res. Lett.*, *29*(19), 1925, doi:10.1029/2001GL014081.

James, M. E., and S. N. V. Kalluri (1994), The Pathfinder AVHRR land data set: An improved coarse resolution data set for terrestrial monitoring, *Int. J. Remote Sens.*, *15*(17), 3347–3363.

Rao, C. R. N. (1987), Prelaunch calibration of channels 1 and 2 of the advanced Very High Resolution Radiometer, NOAA Technical Report, *NESDIS 36*, U.S. Dept. of Commerce.

Rosenfeld, D. (2000), Suppression by Rain and Snow by Urban and Industrial Air Pollution, *Science*, *287*, 1793–1796.

Twomey, S. (1974), Pollution and the planetary albedo, *Atmos. Environ.*, *8*, 1251–1256.

Twomey, S., M. Piepgrass, and T. L. Wolfe (1984), An assessment of the impact of pollution on global cloud albedo, *Tellus*, *36b*, 356–366.

UNEP and C^4 (2002), The Asian Brown Cloud: Climate and Other Environmental Impacts, UNEP, Nairobi.

Xu, Q. (2001), Abrupt change of the mid-summer climate in central and east China by the influence of atmospheric pollution, *Atmos. Environ.*, *35*, 5029–5040.

Yu, S., V. K. Saxena, and Z. Zhao (2001), A comparison of signals of regional aerosol-induced forcing in eastern China and the southeastern United States, *Geophys. Res. Lett.*, *28*(4), 713–716.

O. Krüger, Meteorologisches Institut, Universität Hamburg, Bundesstraße 55, D-20146 Hamburg, Germany. (olaf.krueger@dkrz.de)

H. Graßl, Max-Planck-Institut für Meteorologie, Bundesstraße 55, D-20146 Hamburg, Germany. (grassl@dkrz.de)

Paper III

Influence of pollution on cloud reflectance

Olaf Krüger
Meteorological Institute, University of Hamburg, Hamburg, Germany

Roman Marks
Institute of Marine Sciences, University of Szczecin, Szczecin, Poland

Hartmut Graßl
Max Planck Institut for Meteorology, Meteorological Institute, University of Hamburg, Hamburg, Germany

Received 11 February 2004; revised 13 May 2004; accepted 28 June 2004; published 23 December 2004.

[1] After the collapse of the East Bloc in 1989, the political and economic changes resulted in significant reductions of industrial activities and thus atmospheric pollution that modified cloud reflectance over and in the lee of the main European emission sources. This impact during a two-decade transition (1981–1999) of atmospheric pollution in Europe, in particular in East Germany and Poland, was studied on the basis of emission data, measured aerosol concentrations, and satellite observations of cloud reflectance. In these main European emission areas the high degree of air pollution generally enhanced variability of cloud reflectance during the 1980s. The variability was strongest for the early 1980s. A distinct influence of increased particle number density and increased black carbon content as well as secondary aerosol formation is detected. Toward the late 1990s, both the radius effect and the absorption effect, as the two components of the so-called first indirect aerosol effect, have declined because of reduced particulate matter and sulphur dioxide emissions. The results indicate a pronounced influence of stability on the indirect aerosol effect over Central Europe. The analyzed frequency distributions of cloud reflectance show characteristics that are in line with the theory of radiative transfer. *INDEX TERMS:* 0305 Atmospheric Composition and Structure: Aerosols and particles (0345, 4801); 0320 Atmospheric Composition and Structure: Cloud physics and chemistry; 0345 Atmospheric Composition and Structure: Pollution—urban and regional (0305); 0360 Atmospheric Composition and Structure: Transmission and scattering of radiation; 0368 Atmospheric Composition and Structure: Troposphere—constituent transport and chemistry; *KEYWORDS:* indirect aerosol effect, air pollution, black carbon, sulphur dioxide, cloud albedo, Black Triangle

Citation: Krüger, O., R. Marks, and H. Graßl (2004), Influence of pollution on cloud reflectance, *J. Geophys. Res.*, *109*, D24210, doi:10.1029/2004JD004625.

1. Introduction

[2] *Twomey* [1977] discussed the influence of air pollution on the shortwave albedo of clouds. He postulated that air pollution acts to increase the reflectance (albedo) of clouds by an increase of cloud droplet concentration. On the other hand, an increase of the absorption coefficient of aerosols alone would lead to a decrease of the reflectance. In the past this so-called first indirect aerosol effect, sometimes called the Twomey effect, was of interest in many mostly theoretical investigations. The third full assessment report of the *Intergovernmental Panel on Climate Change* (*IPCC*) [2001] indicated that the mean global radiative forcing caused by the indirect aerosol effect is negative and could reach -2 W/m^2.

[3] Lately, we investigated this indirect aerosol effect on a regional scale over parts of Europe on the basis of long-term satellite measurements by advanced very high resolution radiometers (AVHRR) [*Krüger and Graßl*, 2002]. The main result was a reduction in mean cloud reflectance between the late 1980s and the late 1990s due to an air pollution decrease in both Western and Central Europe.

[4] In the present article we focus on the variability of cloud reflectance due to anthropogenic activity for the same area. Our hypothesis was as follows: In polluted areas, cloud reflectance should vary more strongly as reflectance is higher on average and varies depending on the direction of flow.

[5] The paper concentrates on the impact of atmospheric pollution on cloud reflectance variability during the episode of strongest emissions in parts of Europe. In order to investigate the reflectance transition patterns, we focus on the industrialized regions of Poland and Germany, which were part of the earlier so-called Black Triangle of Europe. The most important emission centers were located in the heavily industrialized Krakow-Katowice region, in southern Poland, and the other southern part of the former German

0148-0227/04/2004JD004625$09.00

Democratic Republic (East Germany) including the cities of Halle, Leipzig, Bitterfeld, and Cottbus. These areas, which strongly influenced the cloud reflectance over Europe as shown by *Krüger and Graßl* [2002], are described in more detail. The study combines remotely sensed cloud properties and emission data to trace the impact of changed air pollution on cloud optical properties over a large part of Europe.

[6] Since knowledge of the temporal and spatial variability of the aerosol concentration is a basic requirement for the interpretation of cloud optical properties, we first give an overview about pollution in East Germany and Poland within section 2, while the variability of cloud reflectance derived from satellite measurements is described in section 3. The results are then discussed in section 4.

2. Air Pollution in Poland and East Germany

[7] During the last two decades, enormous amounts of air pollutants, both particulate matter and the aerosol precursor gases sulphur dioxide (SO_2) and nitrogen oxides (NO_x) have been emitted mostly into the atmospheric boundary layer, but during the winter and nighttime they have also into the free troposphere from high power plant stacks over Europe.

[8] Before 1989 the economical buildup of Central and Eastern European countries (CEEC) was governed by a continuous growth of heavy industry branches like metallurgy, shipyards, military production complexes, and power plants. These activities demanded a large energy supply and were connected with wasteful energy use mainly from hard coal or lignite. As a result the maximum atmospheric pollution load was observed during the 1980s.

[9] From 1989 onward, radical changes in politics and the economy reshaped all industry branches, but especially those responsible for discharge of atmospheric pollutants. Since the policies for a transition undertaken by individual countries depended on complex sociological and economic conditions, they differed and still differ in speed and efficiency. In general, sudden changes took place in eastern Germany, but they were of a gradual nature in other CEEC. In the case of Poland, the largest country within the CEEC, the transition incorporated both the transfer of large, mostly inefficient companies into the market economy and the restoration of small, technology-oriented market activities. Such a transition for large industry branches like metallurgy or coal mining required complex multistage implementations. The growth of more energy-efficient market activities since 1990 resulted in the reduction of atmospheric pollution.

[10] Extremely high loads of particulate and gaseous atmospheric pollution in Europe originated from specific industry areas in Poland and eastern Germany. Among the pollutants with a potentially strong impact on the indirect aerosol effect are particulate matter (PM), sulphur dioxide (SO_2), nitrogen oxides (NO_x), and ammonia (NH_3). Emission of anthropogenic particulate matter, often called primary particulate matter (PPM), stems predominantly from public electric power, district heating, industrial combustion, commercial and residential combustion, road transport, emissions from industrial processes, and agriculture. The source category of inorganic PPM has as a primary contributor solid fuel combustion at large point sources, e.g., the cement, iron, and steel industries. Organic compounds and black carbon (BC) mainly originate from mobile sources, small combustion, and petroleum extraction and refining.

[11] Emission inventories have been compiled not only for total PPM [*Berdowski et al.*, 1997] but also for black carbon (BC) [*Cooke and Wilson*, 1996; *Liousse et al.*, 1996], which is mainly elemental and to a minor part organic carbon, for heavy metals, e.g., lead and cadmium, and for persistent organic pollutants [*Umweltbundesamt*, 1994a]. While the location of main source regions, especially point sources, is well known, information about the interannual variability of emissions in Europe during the last 20 years is largely lacking. *Cooke and Wilson* [1996] estimated the BC emission of Western Europe to be $\sim$1 Tg C yr^{-1}.

[12] For Germany, annual total PPM emissions were estimated by *Umweltbundesamt* [1994b]. While for the western part the annual emissions amounted to 0.4–0.6 Tg yr^{-1} during 1985–1989, the values for the much smaller eastern part were 4 times higher, reaching 2.2–2.5 Tg yr^{-1} PPM. The emissions in East Germany, the former German Democratic Republic (GDR), originated from large lignite power plants, which accounted for approximately 50% of total emission. More than 300 large combustion plants contributed to the PPM emissions, and stacks higher than 100 m were nearly ubiquitous. The emission data show a clearly decreasing trend for western and eastern parts of Germany since the middle and late 1980s, respectively.

[13] Besides direct emission of PPM, the formation of secondary inorganic aerosol (SIA) and biogenic secondary organic aerosol (BSOA) also contribute to atmospheric aerosol mass. While BSOA is seen as a minor fraction of lower than 5% of the total particulate matter, SIA is the most important contributor in Central Europe with 50–70% [*European Monitoring and Evaluation Programme* (*EMEP*), 2000]. The emissions of the precursor gases SO_2, NO_x, and NH_3 contributing to SIA are the best known of all anthropogenic emissions since the United Nations Economic Commission for Europe initiated the European Monitoring and Evaluation Programme (EMEP) already in 1979. The EMEP emission database includes annual totals of the above species since 1980. The major part of this database contains official emissions submitted by the European countries [*Vestreng and Storen*, 2000]. The highest precursor gas emissions occurred in the 1980s. The emission estimates published by the Meteorological Synthesizing Centre West (MSC-W) of EMEP [see *Vestreng and Storen*, 2000] amount to 53 Tg SO_2 in 1985 for all of Europe. During this time, important contributors from Central Europe were Germany and Poland. In addition, emissions originating from the United Kingdom, France, Netherlands, Czech Republic, and Ukraine contributed considerably to air pollution in Germany and Poland because of long-range transport. Within the period between 1985 and 1989 in most of the European countries the SO_2 emissions decreased slightly by $\sim$10%.

[14] In 1989 the situation changed [*Mylona*, 1999]. Almost immediately after the collapse of the East Bloc, a significant decrease with respect to atmospheric pollution was observed in East Germany, while the changes in other

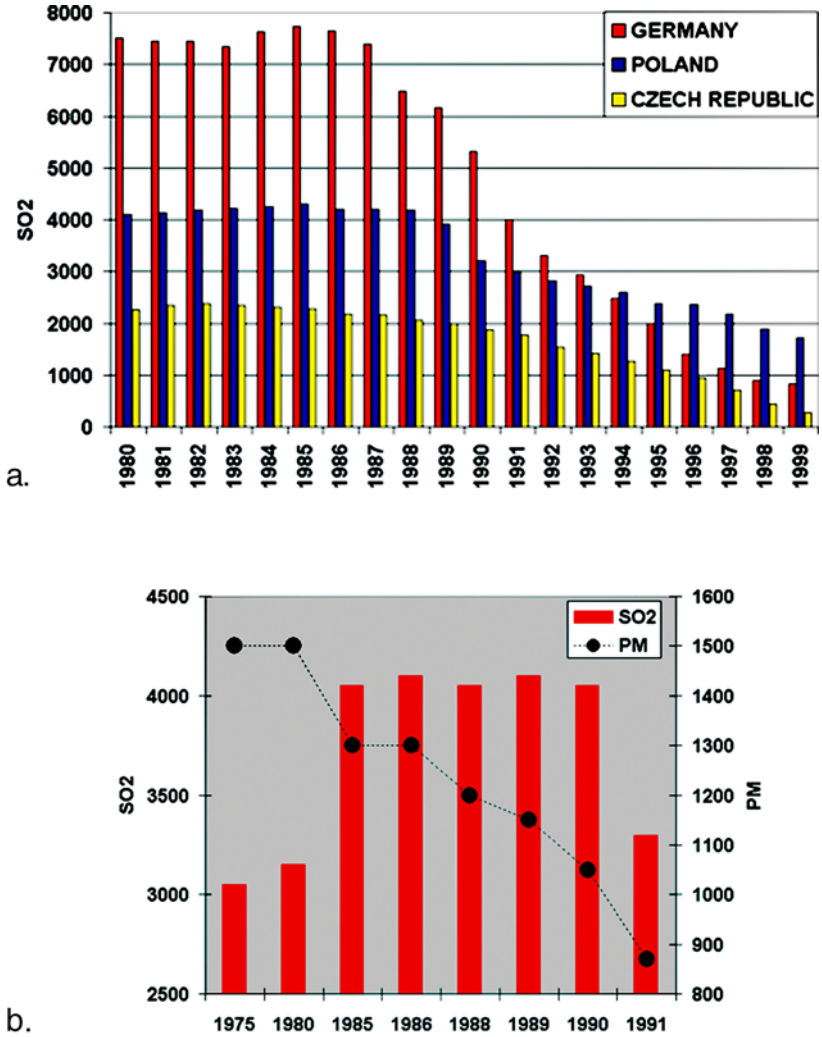

Figure 1. (a) Annual sulphur dioxide (SO_2) emissions from Germany (including the former GDR), Poland, and the Czech Republic, in kilotons for the period 1980–1999 according to the EMEP database [*Mylona*, 1999]. (b) Annual emissions of particulate matter (PM) and sulphur dioxide (SO_2) for power plants in the area of the former GDR, in kilotons. Data are from the German Environmental Agency [*Umweltbundesamt*, 1994b]. (c and d) Model-predicted monthly average sulphur dioxide concentration in ambient air over Europe in 1980 for January (Figure 1c) and November (Figure 1d) (units are $\mu g\ S\ m^{-3}$).

CEEC, including Poland, were more gradual (see Figure 1a). The strong decrease in atmospheric pollution in the former German Democratic Republic (GDR) was related to massive reduction of high stack emissions due to radically closed or modernized industry. In Poland the first signs of pollution decrease were seen for low-level emissions, mostly for residential combustion, which was followed by gradual reduction of emissions from public electric power plants, district heating, and industrial combustion. Significant reduction in atmospheric pollution in both countries was enacted for high stack emissions from industry by deploying exhaust filtration and desulphurization or (additionally in Germany) denoxification systems or modernization of technology by industry. The resulting strong decrease of the sulphur emission in Europe by approximately 50%, from 49 Tg in 1988 to 26 Tg in 1998, has been reported by EMEP [*Vestreng and Storen*, 2000]. In contrast to SO_2 the emission database reflects only a weak decrease of 10–20% for NO_x and NH_3 since 1990 for all of Europe.

[15] The decrease of emissions was confirmed by in situ measurements in main source areas of pollution. For example, in the city of Krakow a significant reduction of atmospheric pollution was observed from 1994 to 1998, when the emission of particulate matter and gases from industry and electric power plants decreased by ~50% [*Turzański and Paula-Wilga*, 1999]. In the Katowice area (Upper Silesia), where the transformation of industry was massive, the concentration of particulate matter with a diameter smaller than 10 μm (PM_{10}) decreased 2.3 times from 1989 to 1996 and turned into a steady annual decrease by a factor of 1.3–1.4 from 1993 to 1996 [*Pastuszka*, 1997]. In the north of Poland, in the urbanized region of Gdynia, close to the Gulf of Gdańsk, known for shipyard and transportation activities, a reduction of particulate matter

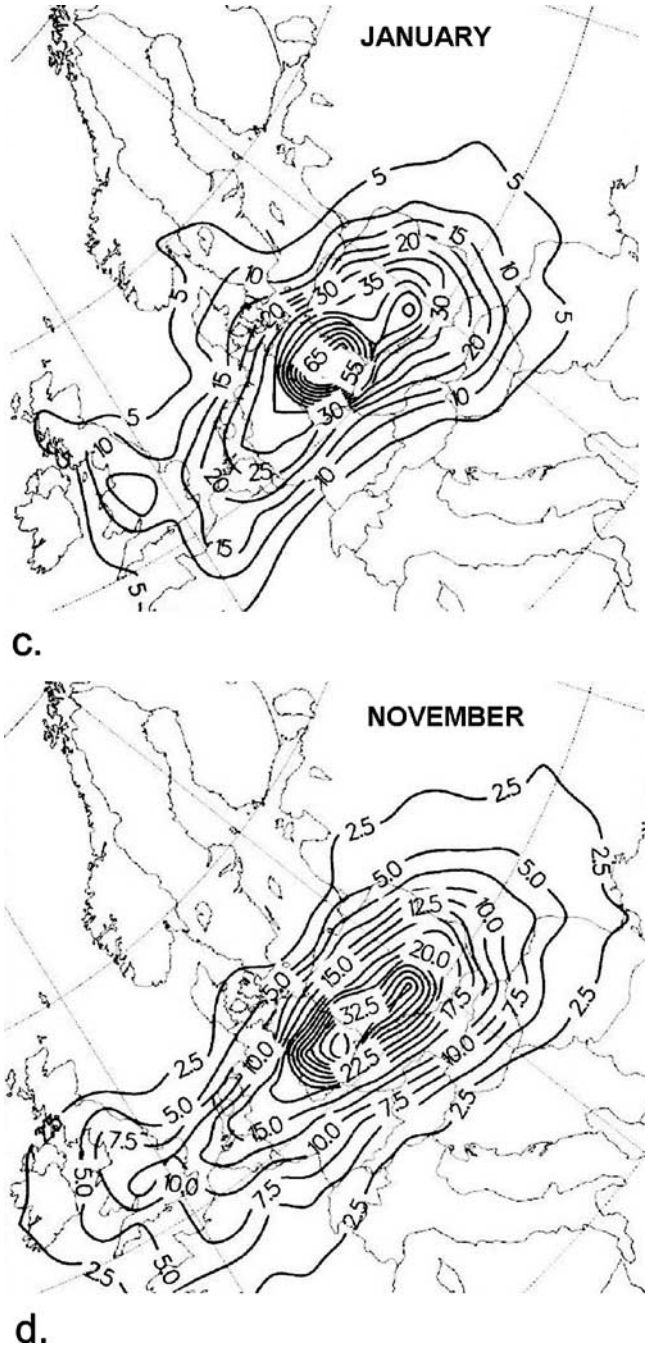

Figure 1. (continued)

in air has been observed since 1972. There the total particulate matter (PM) load into air showed an annual reduction of 15%. Since 1991, about a 30% reduction of total annual PM was observed over the northwest region of Poland (J. Woroń, EMEP representative for Poland, Institute for Meteorology and Water Management, Gdynia, Poland, personal communication, 2000). A reduction twice as high in similar maritime regions in northwest Poland indicates that the pollution that previously originated over East Germany has significantly impacted PM concentrations over northwest Poland, as southwesterly winds dominate in that region.

2.1. Krakow and Katowice

[16] In Poland, especially in the urbanized Krakow-Katowice region, both gaseous and aerosol pollution, but in particular sulphate and carbonaceous aerosols, stabilized at a very high level. The Krakow-Katowice area was regarded as having one of the highest atmospheric pollution levels of all cities in Poland. In 1997, for example, the city of Krakow was rated as the third highest in particulate matter (PM) concentration, with an annual emission of 10,900 t. For the same year the annual emission of polluting gases was 103,400 t, including 26,900 t for SO_2 alone [*Turzański and Paula-Wilga*, 1999]. Within the city area, extending 30 km west to east and 15 km north to south, are located 30 industry-related major atmospheric pollution point sources. These include the largest Polish metallurgy plant (Huta Sendzimira), situated ~15 km to the east, and the large coal-fired electric power plant Skawina, located only 15 km southwest of the city center.

[17] In Krakow, a significant decrease in the atmospheric pollution trend has been noticed after ~2 years of transition. The gradual modernization of industry and, in particular, a significant reduction of coal combustion plants including metallurgy industries, accompanied by the growth of a new, more energy-efficient market economy, resulted in an extended transition period with respect to atmospheric pollution. In addition, the emissions from individual households showed a decrease since 1991 [*Turzański and Paula-Wilga*, 1999]. That process has been stimulated by the reduction of coal combustion, as more oil and natural gas are used nowadays for heating. This caused a major reduction of near-surface atmospheric pollution and has led to improved air quality in the Krakow-Katowice urbanized areas.

[18] In the Krakow area the air quality is strongly influenced by calm conditions that are frequent over the low-lying river valleys of the Wisła, Rudawa, Wilga, Białucha, and Dłubnia, which are located within the city of Krakow. These conditions favor accumulation of air pollution and the formation of smog, especially during periods with temperature inversions, existing 36–42% of the time [*Turzański and Paula-Wilga*, 1999].

[19] The city of Katowice, located only ~50 km from Krakow in the center of Upper Silesia, is the largest highly industrialized area in Poland. Within that area, hundreds of large and small heavy industry plants are located. The trend in atmospheric pollution is difficult to estimate. The averaged data on the concentrations of particulate matter with a diameter lower than 2.5 μm ($PM_{2.5}$) and PM_{10} were given as 138 and 185 μg m^{-3}, respectively, for 1990 [*Pastuszka*, 1997]. The values have decreased to ~60 μg m^{-3} toward the end of the 1990s [*Pastuszka*, 1997; *Turzański and Paula-Wilga*, 1999].

[20] During the early 1980s a slightly increasing tendency of the total load of particulate matter in the atmospheric boundary layer was replaced by a slight decrease starting in 1986. From 1991 to 1993 an extremely fast PM concentration reduction of 60 μg m^{-3} was observed [*Pastuszka*, 1997; *Turzański and Paula-Wilga*, 1999]. Afterward, the reductions of both particulate and gaseous pollution continued, reaching 60% from 1994 to 1998 [*Turzański and Paula-*

Wilga, 1999]. It has to be pointed out that these decreasing emissions are in disagreement with a publication by *Berdowski et al.* [1997] that speaks about a slight increase of PM_{10} and $PM_{2.5}$ emissions for all of Poland, from 93,000 to 100,000 t per year for the 1990–1993 period.

2.2. Halle, Leipzig, and Cottbus

[21] During the 1980s, another area of very high atmospheric pollution was East Germany. There a large part of the total gaseous and particulate emission was emitted from elevated stacks of lignite combustion plants, accounting for ~50% of the PM emissions. For gaseous emissions the contribution of power plants was even higher, for example, reaching more than 75% for SO_2. Since the emission height of many point sources lay above 100 m, the formation of secondary aerosols has been favored.

[22] The main emission centers of particulate and gaseous pollutants in the GDR were located around the cities of Halle, Leipzig, and Cottbus. In 1989, more than 200 of 460 point sources were situated in and around these cities.

[23] The PM emissions in the former GDR decreased nearly continuously from the beginning of the 1980s [*Umweltbundesamt*, 1994b], when they had reached ~2.6 Tg. The decline amounted to ~1 Tg for the source categories of power plants and industry and ~0.7 Tg only for the power plants (see Figure 1b). However, there was an interruption of the continuous downward trend in the PM emissions during the 1980s. Because of a considerable cut in the supply of oil from the Soviet Union in 1982 a renaissance of lignite took place. The consequence was a slight increase of less than 0.1 Tg PM emission until 1986. After 1986 the decrease of the PM emissions was the most pronounced, and it was due to filtration of PM in the large stacks.

[24] The SO_2 emissions of the power plants show a different behavior (see Figure 1b). In the beginning of the 1980s the emissions were ~3.1 Tg yr^{-1}, climbing to ~4.1 Tg yr^{-1} [*Umweltbundesamt*, 1994b]. This was a clear exception as compared to the slight decreases during the 1980s in western Central Europe.

[25] The strong contribution of elevated point sources around Halle, Leipzig, and Cottbus resulted in pronounced spatial differences in PM concentrations in air. For example, in Cottbus, enormous amounts of PM were emitted by the industrial complex "Gaskombinat Schwarze Pumpe." The emission of individual point sources there reached at least 10,000 t yr^{-1}. In the region Halle-Leipzig, quite a number of point sources were located at the chemical plants "Chemie AG Bitterfeld-Wolfen," but in Schkopau (Halle), "Chemische Werke Buna" was also a major emission area.

[26] Consequently, the air concentrations of pollutants showed a pronounced maximum in the former GDR accompanied by spatial heterogeneity in Central Europe in general. Our model estimates (for model details, see *Eliassen and Saltbones* [1983] and *Krüger and Tuovinen* [1997]), based on emission data for 1980 [*Meinl et al.*, 1989], confirm a strong monthly variability due to distinct removal by dry and wet deposition processes. Also, increased air concentrations occur predominantly eastward of the major power plant emissions in the former GDR and in Poland (see Figures 1c and 1d). A few years later, during the late 1980s, the measured PM and SO_2 concentration peaks show values even higher than 150 μg m^{-3} around Halle, Leipzig, and Cottbus, while the concentrations in rural areas were much lower, by ~50 μg m^{-3} [*Umweltbundesamt*, 1994b].

[27] In the beginning of the 1990s, PM and SO_2 concentrations rapidly declined because of massive emission reductions. The annual mean concentration values for SO_2 were lower by ~50% in rural areas and by ~70% in the cities as compared to peak values in 1985. The PM concentrations showed a similar strong decrease, which again, as for SO_2, was dependent on the region [*Umweltbundesamt*, 1994b].

[28] We expected that such strong emission reductions in both PM and SO_2 should have major consequences for optical properties of clouds. Therefore we investigated changes in cloud reflectance and its variability as continuously observed from space since the early 1980s over the former GDR and the surrounding areas of Central Europe.

3. Variability of Cloud Reflectance

[29] In order to study the variability of cloud reflectance we evaluated the reprocessed global National Oceanic and Atmospheric Administration (NOAA)/NASA Pathfinder data set from the advanced very high resolution radiometer (AVHRR) on board the afternoon NOAA series satellites (NOAA 7, 9, 11, and 14) [*James and Kalluri*, 1994]. The full five-channel AVHRR multispectral information was used for the detection of different cloud types. For cloud classification we applied the NOAA/National Environmental Satellite Data and Information Service algorithm [*Stowe et al.*, 1991].

[30] Since the optical properties of lower clouds are expected to be influenced more strongly by pollution than those of high clouds, our investigations were restricted to low- and medium-level clouds. After cloud classification the near-infrared channel 2 reflectance was further evaluated as it is nearly insensitive to Rayleigh scattering and has no strong contribution from aerosols above the low clouds.

[31] The idea was to compare time periods of distinct emissions of PM and SO_2. Therefore two episodes during the 1980s, from 1981 to 1984 and from 1985 and 1989, and one during the 1990s, from 1996 to 1999 (denoted as 8184, 8589, and 9699, respectively), were chosen.

[32] Because the height of the atmospheric boundary layer and solar radiation intensity itself have an influence on the concentration of pollutants, two seasons, namely, the winter months (January, February, November, and December, denoted as JFND8184, JFND8589, and JFND9699) and the summer months (May, June, July, and August, denoted as MJJA8184, MJJA8589, and MJJA9699) were evaluated separately.

[33] Since we have found the indirect aerosol effect near the strong emission sources of PM and SO_2 [*Krüger and Graßl*, 2002], the area of interest was again a large part of Central Europe including smaller parts of Western and Eastern Europe (longitude −5°W to 31°E, latitude 48°–60°N). There the influence from the former GDR and Poland, regions of extremely high emissions of primary particles as well as precursor gases during the 1980s, is dominant.

[34] Now we investigated the variability of cloud reflectance in more detail over the well-known areas of strong air

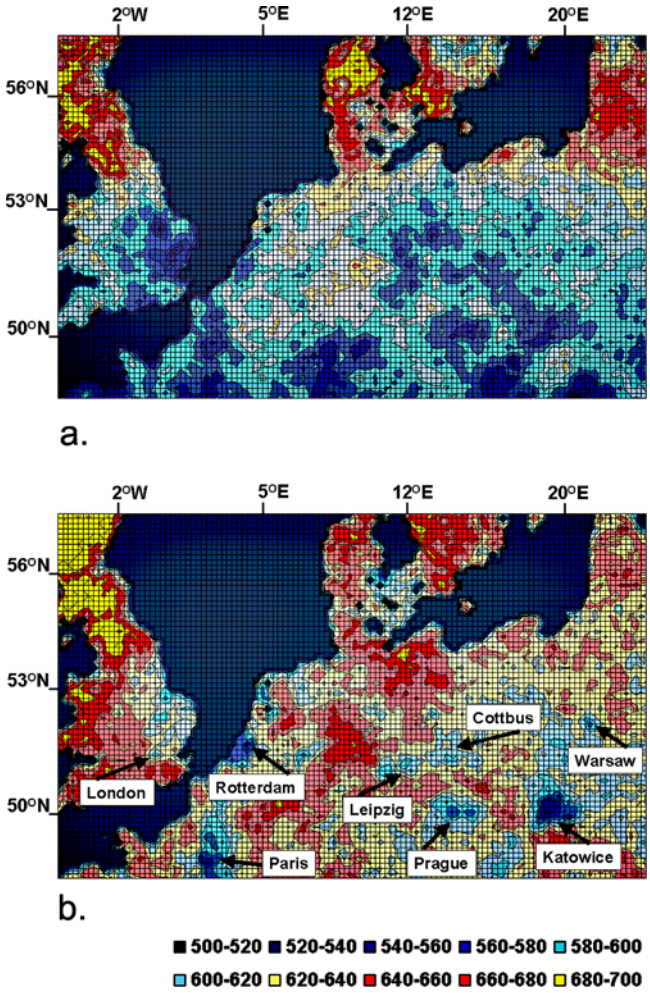

Figure 2. Mean cloud reflectance of low- and medium-level clouds derived from AVHRR channel 2 data over parts of Europe, given in thousands. Data are shown from 5.0°W to 24.0°E longitude and 48.5° to 57.5°N latitude for the winter periods (a) November and December and (b) January and February from 1985 to 1989 (excluding data from 1987). The grid size is 0.25° longitude and 0.125° latitude. The area covers parts of the United Kingdom, Denmark, Sweden, France, Benelux, Germany, Poland, Czech Republic, the Baltic countries, and Ukraine. The North Sea and the Baltic Sea are in black. Strongly polluted areas are indicated.

pollution in Europe where an increased variability had been detected during winter in source regions [*Krüger and Graßl*, 2002]. These areas, in addition, were accompanied by much lower mean reflectance. However, the spatial heterogeneity of the wintertime cloud reflectance over Europe is also remarkable. There is a clear negative gradient of cloud reflectance from Great Britain, Scandinavia, and the former Soviet Union to densely populated industrial regions of Europe, with up to 10% lowered values over strongly polluted regions (see Figures 2a and 2b). The areas of minimum mean cloud reflectance with values even lower than 58% for JFND8589 are located around London, Paris, Rotterdam, Leipzig, Prague, Katowice, Krakow, and Warsaw. The reflectance decrease from "remote" clouds to clouds over source regions is due to the impact of black carbon (BC) emissions originating mainly from power plants, small combustion, and mobile sources. In source regions the single-scattering albedo of water clouds is therefore lower.

[35] Since BC particles are hydrophobic immediately after emission and chemically inert [*Crutzen et al.*, 1984], the lower reflectance of water clouds can be explained by the high amount of absorbing particles in source regions, which favors the physical transformation of black carbon into a hydrophilic form through coagulation with, for example, sulphate or nitrate particles. The condensation process close to source regions is based on internally mixed aerosol with the consequence of an increased portion of BC inside cloud droplets. An additional explanation for the significantly increased absorption might be that low clouds in source regions contain a higher portion of BC particles in the interstitial aerosol. Since the absorption of solar radiation in clouds is thus increased, we call this process the absorption part of the first indirect aerosol effect.

[36] Besides the feature of spatial heterogeneity, there are pronounced differences in the mean reflectance of the total area for the individual episodes. As compared to the periods 1981–1984 and 1996–1999, the mean reflectances for winter and summer are generally increased during the period 1985–1989 (Table 1), which points to the obvious connection to peak values of precursor emissions during the late 1980s. Since strongly increased formation of secondary aerosols took place then, we attribute the increase of reflectance to the radius effect as part of the first indirect aerosol effect [*Krüger and Graßl*, 2002]. The characteristics are quite pronounced even after subdivision into the main emission areas in Germany and Poland, which are the regions around Halle-Leipzig-Cottbus and Krakow-Katowice.

[37] In contrast to mean reflectance the trend of variability shows a different behavior. There is a continuous decrease of variability from JFND8184 to JFND9699. The tendency since the beginning of the 1980s is in good agreement with the continuous reduction of total PM emission in Europe. On the basis of this finding, we argue that emissions of PM are a major factor influencing the variability of cloud reflectance.

[38] In general, the variability of cloud reflectance is smaller for clouds in remote regions, e.g., over the west

Table 1. Mean Cloud Reflectance Derived From AVHRR Channel 2 Data Over Parts of Europe (−5.0° to 24.0° Longitude and 48.5°–57.5°N Latitude) and the Areas Centered Around Halle, Leipzig, and Cottbus (10.0°–15.3° Longitude and 50.8°–52.3°N Latitude) and Around Krakow and Katowice (16.5°–22.3° Longitude and 49.5°–51.5°N Latitude) for the Winter Period January, February, November, and December From 1981 to 1984, 1985 to 1989 (Excluding Data From 1987 Because of Incomplete Data), and 1996 to 1999[a]

	1981–1984	1985–1989	1996–1999
Total Area	60.8 (18.3)	61.5 (17.5)	58.7 (17.4)
Halle-Leipzig	58.5 (20.3)	60.7 (17.7)	58.4 (17.1)
Krakow-Katowice	58.8 (19.3)	59.9 (18.2)	57.1 (18.1)

[a]Mean cloud reflectance is given in percent. The standard deviation is given in parentheses.

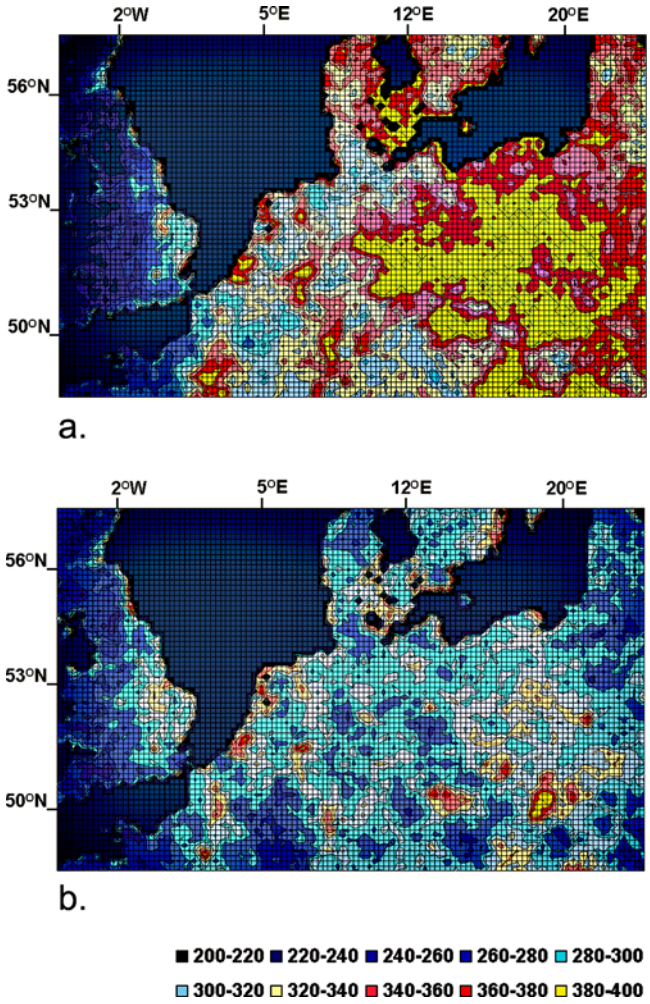

Figure 3. Mean coefficient of variation of cloud reflectance derived from AVHRR channel 2 data over parts of Europe, given in thousands; area is as in Figure 2, but for the four months January, February, November, and December from (a) 1981 to 1984 and (b) 1996 to 1999.

United Kingdom. However, over London and the industrial areas near the British east coast the variability already increases slightly.

[39] Over the European continent, cloud reflectance variability shows highest values in the source regions of PM mainly in the eastern part of our test area. It is obvious that the strongest variability occurred during JFND8184 in Germany and Poland (Figure 3a). The impressive plume of high variability over nearly all regions of the former GDR and Poland corresponds well with the higher degree of pollution extending mainly eastward from the major source regions (see Figures 1c and 1d).

[40] For JFND8589 this feature already declined [see *Krüger and Graßl*, 2002]. During JFND9699 (Figure 3b), only a slightly increased variability, which is limited to the well-known emission regions of PM, is still to be seen. For the Halle-Leipzig-Cottbus and the Kracow-Katowice areas, the hot spots of pollution in Germany and Poland, the general tendency toward lower cloud reflectance is well confirmed. However, as compared to Krakow-Katowice, the Halle-Leipzig and Cottbus regions show a much stronger decrease in variability from the late 1980s to the late 1990s, in agreement with the stronger emission reduction in eastern Germany. In both areas of the former GDR the disappearance of high variability was accompanied by a pronounced change in PM concentrations. Hence our above hypothesis concerning a general dependency of cloud reflectance on the PM concentration in the boundary layer is well supported.

[41] More characteristics of cloud reflectance variability can be found by analyzing the frequency distributions of cloud reflectance. Also, as Figure 2 indicates, a further subdivision of the episodes is useful for analyzing the influence of increased concentrations of pollutants. Therefore we divided the data into episodes of two months, November–December (ND) and January–February (JF). Especially for the low planetary boundary layer heights in full winter, some remarkable details about the aerosol influence on cloud optical characteristics become visible.

[42] We started to look again at the mean reflectance in our area. The intention was to eventually detect characteristics of the indirect aerosol effect for different cloud optical thickness during early and late winter. However, for this question, the change of mean reflectance for JF and ND shows no tendency and therefore does not allow straightforward conclusions.

[43] However, if we compare the change for the individual episodes JF and ND with the emissions of SO_2 and PM, interesting similarities become visible (see Table 2). We see a remarkable dependence of the JF reflectance on SO_2 emissions. The maximum value of 63.1% for JF8589 was reached during the time of strongest SO_2 emissions. For the two other episodes, JF8184 and JF9699, the reflectance was more than 2.5% lower. On the other hand, the reduction of the PM emissions from 1981 to 1999 is accompanied by an even stronger decrease in reflectance from 62.4% for ND8184 to 58.6% for the ND9699 episode. These results already show that a high amount of primary particles during ND8184 as well as enhanced formation of secondary aerosols during JF8589 were leading to an increased radius effect.

[44] A closer look into the variability of cloud reflectance confirms that the strong emission of PM is the main reason for the high variability during JF8184 as well as ND8184. A dependency of variability for the JF episodes on enhanced formation of secondary aerosols during 8589 is not seen. This indicates the presence of at least one additional process influencing the variability during JF beside the radius effect.

Table 2. Mean Cloud Reflectance Derived From AVHRR Channel 2 Data Over Parts of Europe (−5.0° to 24.0° Longitude and 48.5° to 57.5°N Latitude) for the Winter Periods ND, JF, and JFND and for Summer Period MJJA From 1981 to 1984, 1985 to 1989 (Excluding Data From 1987), and 1996 to 1999[a]

	1981–1984	1985–1989	1996–1999
ND	62.4 (19.0)	59.8 (18.1)	58.1 (18.7)
JF	59.4 (17.6)	63.4 (16.8)	59.2 (16.1)
JFND	60.8 (18.3)	61.5 (17.5)	58.7 (17.4)
MJJA	64.9 (12.1)	65.7 (12.5)	63.6 (11.3)

[a]Mean cloud reflectance is given in percent. The standard deviation is given in parentheses. ND, November and December; JF, January and February; JFND, January, February, November, and December; MJJA, May, June, July, and August.

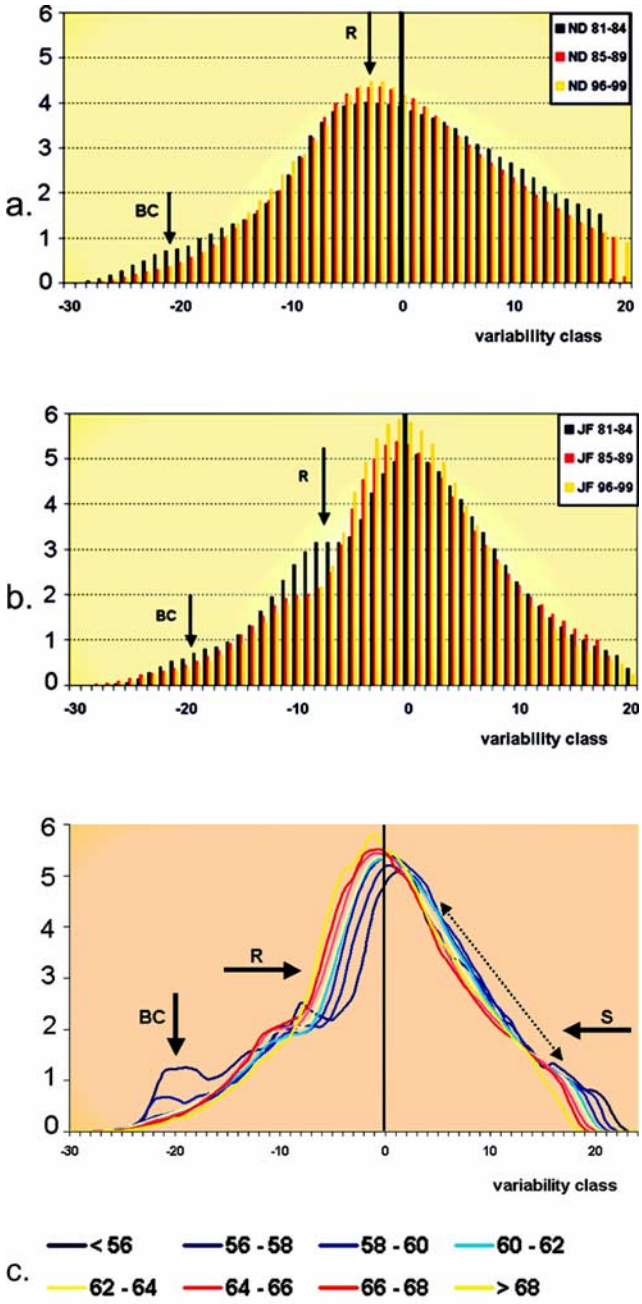

Figure 4. (a and b) Frequency distribution of the deviation from mean cloud reflectance that is shown in Table 2 (in percent per variability class interval of 2% width) for November and December (ND) (Figure 4a) and January and February (JF) (Figure 4b) during 4-year periods (1981–1984, 1985–1989, and 1996–1999), excluding 1987. The black carbon peak (BC) and the radius effect (R) are indicated. (c) Frequency distribution of the deviation from mean cloud reflectance for JF8589 as depicted in Table 2 (in percent per variability class interval of 2% width). Colors refer to different cloud reflectance classes for the episode JFND8589 [see *Krüger and Graßl*, 2002] in percent (source regions, blue; more remote, red and yellow, as in Figure 2). The main characteristics of the first indirect aerosol effect are indicated (R, radius effect; S, saturation effect through aerosol absorption). The black carbon peak (BC) is due to the frequency distribution in source regions of air pollution. The additional process responsible is the absorption effect described above, which can strongly reduce the cloud reflectance for sufficiently optically thick clouds.

[45] The frequency distributions in Figures 4a–4c show more details regarding the different indirect aerosol effects. The distributions are generally much broader in ND as compared to JF. The shape for ND (Figure 4a) is positively skewed, which already indicates the modification of the normal distribution by pollution. The frequency distribution is broadest during ND8184, pointing to a major impact of PM emissions on the variability. The maximum in the negative branch during ND can be well explained by the radius effect, which rather increases the reflectance of optically thinner clouds, i.e., clouds with lower reflectance. However, the increased frequency for optically thick clouds in ND8184, seen in the positive branch, is also a clear indication of an increased cloud optical depth.

[46] During JF the influence of the radius effect becomes more evident. This is seen from the frequency distribution (Figure 4b) at the range of −20% deviation from the mean. Since the reflectance at this point is ∼40%, the optical thickness should be comparably low at ∼20. For layer clouds of this reflectance class, radiative transfer calculations give the most pronounced increase in cloud reflectance because of the radius effect [*Graßl*, 1978]. In Figure 4b at −20% reflectance the radius effect is seen in a clear shift to higher values, which modifies the shape of the distribution considerably.

[47] Further confirmation of our interpretation can be found by looking at the frequency distributions for areas of different degree of local pollution, i.e., differently lowered mean JFND reflectance (Figure 4c). As discussed above, the spatial heterogeneity of the mean reflectance is considered as an indicator for the BC content in the clouds (see Figure 2). The lower mean reflectance in main pollution areas in Figure 2 can be explained by a higher BC content, i.e., the absorption effect. Therefore source regions of pollution and more remote regions can be identified by subdivision into classes of different mean reflectance.

[48] If we compare now the frequency distributions for these classes of different mean JFND reflectance [see *Krüger and Graßl*, 2002], more details of the indirect aerosol effect become visible (Figure 4c). First, again for optically thinner clouds starting at about −20%, there is a clear shift toward higher reflectance for polluted areas, while for remote clouds no shift at all is seen. This subdivision of clouds shows clearly: The shift of the frequency distribution represents the radius effect, which generally depends on the degree of pollution. The radius effect is enhanced in more highly polluted regions.

[49] Another characteristic of the absorption effect is visible in the range at about +30% in Figure 4c, which represents optically thick clouds. At +30% all curves are converging, indicating another shift in the other direction for the positive branch of the frequency distribution. This shift is also known from theory. The shift, which is stronger in polluted regions, is much less pronounced than the shift by the radius effect for the optically thin clouds is. The change, now for the optically thick clouds, again clearly depends on the degree of the pollution. This second shift is mainly induced by the saturation effect of the cloud reflectance, which appears for clouds that are sufficiently optically thick.

The absorption effect, which works against the radius effect, is responsible for this behavior of the frequency distributions. If we consider the reflectance and other optical properties of the cloud layer to be functions of only optical thickness and single-scattering albedo, it becomes obvious that for a fixed single-scattering albedo the rate of increase of reflectance decreases with increasing optical thickness. Just this effect is seen in our results for the positive branch between +20% and +30% deviation from mean with a reflectance in the range of nearly 80–90% (see Figure 4c).

[50] It should be noted that the shifts in frequency distributions for JF9699 and JF8184 show similar characteristics as for JF8589.

[51] In the case of very highly reflecting optically thick clouds there is negligible anthropogenic influence. This can be explained by optically thick clouds possibly in combination with an additional cloud layer above, i.e., cumulonimbus combined with a thick cirrus layer.

[52] For very low reflectance in source regions of pollution, i.e., for strongly polluted areas with mean reflectances below 58% during winter, the frequency distributions include a secondary peak (see Figure 4c). The distributions show this peak at −40%, with a cloud reflectance that is below 25%. These remarkably low reflectance values most likely indicate clouds, i.e., subpixel cloudiness, within thick haze layers containing extremely high amounts of BC. The circumstance that the secondary peak disappears for the late 1990s supports the fact that brown haze occurred during the 1980s in Europe. Therefore we tentatively name this anthropogenic influence in the frequency distribution the black carbon peak.

[53] The black carbon peak is most pronounced during 1981–1984 for ND and JF, but it is also pronounced for JF8589. In the frequency distributions for ND8589, ND9699, and JF9699 such a pronounced secondary peak induced by haze does not become visible. The occurrence of haze confirms the high degree of pollution during the 1980s.

[54] Besides the secondary peak, called the black carbon peak, another point now becomes clear: Near the center the frequency distributions are generally more narrow in polluted regions. This is the result of a stronger radius effect for optically thinner clouds and a stronger absorption effect for optically thicker clouds working in opposite directions.

[55] The frequency distributions for summer are much narrower than those for winter. The mean standard deviation for the four summer months (MJJA) ranges from 11.3 to 12.5% (see Table 2). As in winter the values for Halle-Leipzig-Cottbus and Crakow-Katowice are increased as compared to the mean of the total area. However, during summer, in contrast to winter, variability follows the amount of SO_2 emission. The variability increases with increasing reflectance, which means that the SO_2 emission has a major influence on both the mean reflectance and the variability.

4. Discussion and Conclusions

[56] Our results show the radius effect (cloud albedo increase with pollution increase) over Central Europe in a region with a high density of power plants and traffic. This conclusion is derived through analysis of cloud reflectance frequency distributions from long-term satellite measurements.

[57] Unfortunately, a comparison of our results with the those of the International Satellite Cloud Climatology Project (ISCCP) is not advisable because of, first, the quite different spatial resolutions of the data sets. Second, a direct comparison with the ISCCP statistics http://isccp.giss.nasa.gov) is hampered by the distinct procedures for cloud classification.

[58] However, earlier studies dealing with satellite data and with in situ measurements confirm the strong influence of the elevated point sources on cloud albedo. There is, first, the work by *Rosenfeld* [2000], who derived smaller droplets within the dispersion plume of point sources from individual satellite scenes. The radius effect was detected for power plants as well as for lead smelters and oil refineries. Further, there are airborne in situ measurements made downwind of a coal-fired power plant near to Dresden in eastern Germany [*Keil et al.*, 2002]. The analysis of aerosol, microphysical, and solar radiative parameters within the dispersion plume generally confirms an albedo increase. However, despite enhanced aerosol particle and cloud droplet number concentrations, it was not possible to infer a decrease in effective cloud droplet radius by in situ measurements, which could be caused by additional water vapor emitted by the elevated stacks.

[59] In our study, a very large amount of data yielded a clearly modified shape of the frequency distribution in a strongly polluted region, which is well explained by the radius effect for optically thinner clouds. This long-term change during the past decades induced by pollution can be reconstructed in more detail as discussed below.

[60] Generally, the indirect aerosol effects have a strong influence on the variability of cloud reflectance. The variability increases when both less polluted and strongly polluted clouds are contributing. The higher variability can be achieved by a high BC content lowering the reflectance of strongly polluted clouds. However, effective secondary aerosol formation, leading to increased reflectance in the absence of a dominating absorbing component, can also be the reason. Besides, our data show that the influence of air pollution on cloud reflectance mainly depends on height and stability of the boundary layer. Additionally, the height of the cloud base and cloud top may have an influence. Explanation of our results can be made by considering the factors above.

[61] During ND the European boundary layer is more unstable and humid. Thus the impact of pollution on cloud formation and reflectance is more effective. Enhanced mixing, in particular, establishes the efficient vertical transport of particles into the cloud level. It can be assumed that as compared to JF, clouds, e.g., cumulus clouds, in ND have higher vertical extension, have a higher liquid water path, are optically thicker, and have higher vertical velocities. For cumulus clouds the inflow of pollutants is strong at the cloud base. However, the wet deposition processes, i.e., in-cloud and below-cloud scavenging, are effective in removing aerosols. Therefore, for cumulus clouds, a weaker indirect aerosol effect as compared to stratus clouds should be expected under the conditions of a higher PM load in the boundary layer.

[62] In order to make it visible we separated our data into stratus and cumulus cases by use of cloud observations in the strongly polluted area of Halle-Leipzig. Our hypothesis

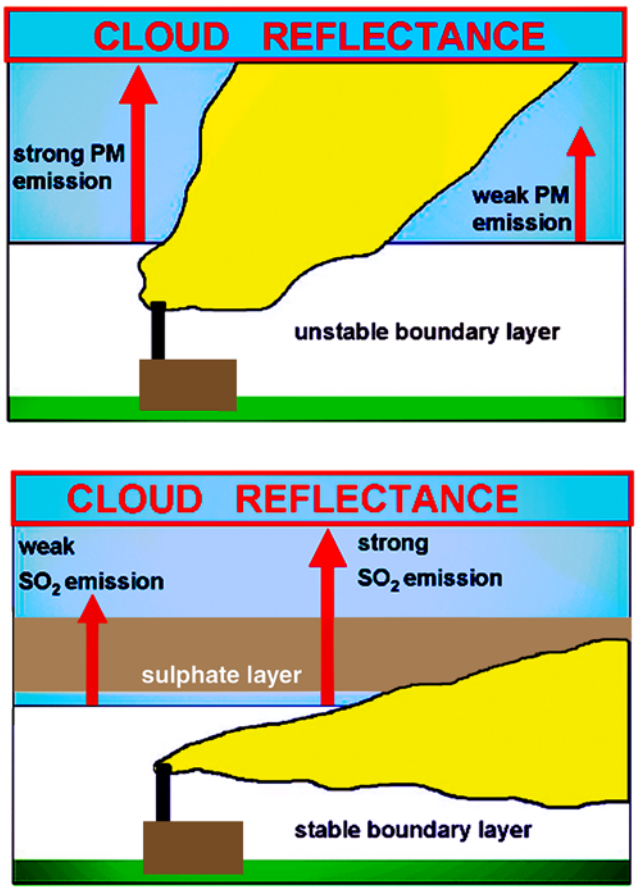

Figure 5. Schematic illustrating the different mechanisms of the so-called first indirect aerosol effect, i.e., the radius and the absorption effects, in unstable and stable boundary layers (plume of air pollutants originating from elevated sources in yellow, cloud layer in blue, and sulphate layer in brown). In the unstable boundary layer, aerosol particles originating from the surface can directly reach the cloud level by turbulence. The radius effect is working efficiently for strong primary particle emission. In stable boundary layers the dry deposition process prevents a strong effect by primary particles while the secondary aerosol formation becomes the major process. Under these conditions the formation of sulphate layers is pronounced. The development of haze layers is favored during weather situations with weak gradients, with low wind speed, and in absence of strong turbulence. The aerosol particle number can be enhanced by sulphate formation via the aqueous phase. An alternative process is the condensation of gaseous sulphuric acid on microparticles. Consequently, the cloud reflectance is increased by the radius effect during strong emissions of aerosol precursor gases.

is confirmed: The reflectance of stratus clouds for ND8184 is increased by more than 13%, while cumulus clouds show a much lower increase of 4% as compared to JF8184 (see Figure 5 and Table 3). This indicates the much more pronounced self-cleaning capacity of the atmosphere by cumulus clouds near the sources of pollution if wet deposition is active in unstable boundary layers.

[63] During the winters of the late 1980s the occurrence of enhanced indirect effects is shifted to JF. Now, in the case of more stable atmosphere, both cloud types stratus and cumulus are affected by haze layers. This is seen by comparing the data for cumulus and stratus clouds during the SO_2-rich emission episode of 1985–1989 (Table 3; also Figure 5) in much colder atmospheres. In contrast to ND the stable conditions are more frequent during the late winter months JF. This results in lower boundary layer heights and a clearly reduced vertical transport of particles. Despite the low mean cloud base, in many cases an increased dry deposition prevents the transmission of aerosol particles into the cloud layer. If cold cumulus clouds occur, the liquid water content is approximately several times lower than that for the more extended cumulus in the warmer months ND. Just this, referring to a low optical thickness, is the precondition for the enhanced radius effect. In addition, several shorter life-cycles of cold shallow cumuli might be rather effective in accelerating the aging of aerosols.

[64] Therefore our data show strong indirect aerosol effects during JF occurring for both layer clouds as well as cumulus clouds. Since the majority of cloudy atmospheres in late winter (JF) are accompanied by more stable stratification, a major influence of directly emitted larger particles can be excluded. Indeed, as Table 2 shows, a pronounced radius effect in JF is not seen for the episode 1981–1984. However, a maximum indirect aerosol effect takes place for the strongest precursor gas emissions from high stacks of power plants in the former GDR, pointing to the major influence of secondary aerosol formation.

[65] The coincidence with the high frequency of haze occurrence during JF8589 supports this explanation. In combination with a declining wet deposition in late winter, pollution also tends to accumulate within the boundary layer during the low mixing heights. Under these conditions, directly emitted fine BC particles from elevated stacks can contribute as the absorbing component. Furthermore, calm weather situations during late winter favor the aging of aerosols and lead, consequently, to more hydrophobic particles.

[66] The haze layers we detect are most likely sulphate dust layers, which occur in the absence of strong turbulence. Generally, the enhancement of aerosol particle number

Table 3. Mean Cloud Reflectance Derived From AVHRR Channel 2 Data for Days With Cloud Observations of Low Stratus or Cumulus Over the Area Around Halle and Leipzig (10.0°–15.3° Longitude and 50.8°–52.3°N Latitude) for the Winter Periods JF and ND From 1981 to 1984, 1985 to 1989 (Excluding Data From 1987), and 1996 to 1999[a]

	1981–1984	1985–1989	1996–1999
Stratus ND	70.9 (21.3)	57.8 (16.8)	58.2 (17.9)
Stratus JF	57.5 (20.3)	65.0 (14.9)	58.3 (11.1)
Cumulus ND	59.8 (19.9)	59.0 (18.2)	54.3 (17.9)
Cumulus JF	55.8 (20.5)	62.6 (17.9)	57.1 (16.0)

[a]Mean cloud reflectance is given in percent. The standard deviation is given in parentheses. ND, November and December; JF, January and February.

might be the result of sulphate formation via the aqueous phase. However, the condensation of gaseous sulphuric acid on microparticles should also be considered. In ND, however, a larger part of the pollutants is wet deposited, and fewer haze layers are resulting at the cloud level since the condensation nuclei are well mixed in the boundary layer. The haze layers above well explain the satellite measurements, which show a pronounced radius effect dominating the absorption effect, as seen by the highest reflectance and the moderate variability for episode JF8589.

[67] We conclude that strong pollution as seen for JF8589 generally tends to narrow the frequency distribution of cloud reflectance. However, the stability of the atmosphere determines the magnitude of particle transfer into the cloud level, and therefore the variability of cloud reflectance is increased because of the variability of the turbulence. The latter effect leads to a slightly higher standard deviation during the early 1980s as compared to the late 1980s. On the other hand, a higher difference between the mean JF and mean ND reflectance explains a higher JFND variability. As discussed above, a higher difference in cloud reflectance (Table 2) is mainly due to the increase of pollution during ND8184 and JF8589. While the variability increase for ND8184 is due to increased PM emissions, higher SO_2 emissions are the main cause during JF8589. If we compare this with the lower mean reflectance induced by higher BC content in aerosol during the early 1980s, then the much higher coefficient of variation for JFND8184 (Figure 3a) is well explained.

[68] During summer, the SO_2 emissions and thus the secondary aerosols largely determine the indirect aerosol effect, with dominance of sulphate particles. Experiments confirm that the contribution of BC to total particulate matter in remote areas, i.e., the Baltic Sea, is found to be nearly 2 times lower than it is in winter [*Kusmierczyk-Michulec et al.*, 2001]. The secondary aerosol formation can take place in the higher part of the boundary layer, while the higher PM concentrations occur much nearer to the surface. The consequence is that BC is much less efficiently incorporated into clouds. Because of the low BC content the variability of cloud reflectance is only slightly increased because of a limited absorption effect.

[69] We conclude that our study reveals a clear indication of impacts of air pollution on cloud reflectance over parts of Europe during the recent two decades. In summary, our results show the following: (1) The emissions of PM, including BC, and aerosol precursor gases have a pronounced influence on the cloud reflectance and its variability. (2) The cloud reflectance and its variability are determined by the radius effect, the absorption effect, and the saturation effect due to absorbing aerosols. (3) The so-called first indirect aerosol effect, i.e., the effect of a smaller droplet radius and stronger absorption, can be established via different pathways: under more unstable conditions by primary particle emission and in stable boundary layers through secondary aerosol formation. (4) The BC content is the major factor influencing the variability as seen by strong shifts of the frequency distributions to lower reflectance in polluted regions during winter. (5) A high concentration of secondary aerosols leads to a strong radius effect and shifts the frequency distributions to higher reflectance during summer, as well as during winter under stable boundary layers. (6) Haze layers occurring in winter confirm the high degree of pollution during the 1980s but have only a marginal influence on the overall variability.

[70] Besides this, our results still show a radius effect during the winters of the late 1990s. While haze is absent, the frequency distributions indicate a slight increase of variability from ND8589 to ND9699. This could be due to increasing emissions of fine particles with a strong absorbing component.

[71] Since the idea of this study was to detect the characteristics of indirect aerosol effects for widely suppressed interannual variability, further studies, including an evaluation of higher-resolution ISCCP data, are needed in order to estimate the climate forcing induced by anthropogenic aerosols.

References

Berdowski, J. J. M., W. Mulder, C. Veldt, A. J. H. Visschedijk, and P. Y. J. Zandveld (1997), Particulate matter emissions (PM_{10}-$PM_{2.5}$-$PM_{0.1}$) in Europe in 1990 and 1993, *Rep. TNO-MEP-R 96/472*, 90 pp., Neth. Organ. for Appl. Sci. Res., The Hague.

Cooke, W. F., and J. J. N. Wilson (1996), A global black carbon aerosol model, *J. Geophys. Res.*, *101*(D14), 19,395–19,409.

Crutzen, P., I. Galbally, and C. Bruhl (1984), Atmospheric effects from post nuclear fires, *Clim. Change*, *6*, 323–364.

Eliassen, A., and J. Saltbones (1983), Modelling of long-range transport of sulphur over Europe: A two year model run and some model experiments, *Atmos. Environ.*, *9*, 425–429.

European Monitoring and Evaluation Programme (EMEP) (2000), Status report with respect to measurements, modelling and emissions of particulate matter in EMEP: An integrated approach: Joint CCC and MSC-W report 2000, *EMEP MSC-W Note 5/00*, Meteorol. Syn. Cent. West, Norw. Meteorol. Inst., Oslo, Aug.

Graßl, H. (1978), Strahlung in getrübten Atmosphären und in Wolken, *Hamburger Geophys. Einzelschr. 37*, Univ. Hamburg, Hamburg, Germany.

Intergovernmental Panel on Climate Change (IPCC) (2001), *Climate Change: The Scientific Basis*, *Contribution of Working Group I to the Third Assessment Report of the Intergovernmental Panel on Climate Change*, edited by J. T. Houghton et al., 881 pp., Cambridge Univ. Press, New York.

James, M. E., and S. N. V. Kalluri (1994), The Pathfinder AVHRR land data set: An improved coarse resolution data set for terrestrial monitoring, *Int. J. Remote Sens.*, *15*(17), 3347–3363.

Keil, A., M. Wendisch, and J. Heintzenberg (2002), A case study on microphysical and radiative properties of power-plant-originated clouds, *Atmos. Res.*, *63*, 291–301.

Krüger, O., and H. Graßl (2002), The indirect aerosol effect over Europe, *Geophys. Res. Lett.*, *29*(19), 1925, doi:10.1029/2001GL014081.

Krüger, O., and J.-P. Tuovinen (1997), The effect of variable sub-grid deposition factors on the results of the Lagrangian long-range transport model of EMEP, *Atmos. Environ.*, *31*, 4199–4209.

Kusmierczyk-Michulec, J., M. Schulz, S. Ruellan, O. Krüger, E. Plate, R. Marks, G. de Leeuw, and H. Cachier (2001), Aerosol composition and related optical properties in the marine boundary layer over the Baltic Sea, *J. Aerosol Sci.*, *32*, 933–955.

Liousse, C., J. E. Penner, C. Chuang, J. J. Walton, H. Eddleman, and H. Cachier (1996), A global three-dimensional model study of carbonaceous aerosols, *J. Geophys. Res.*, *101*(D14), 19,411–19,432.

Meinl, H., P. Builtjes, W. Klug, and R. Stern (1989), Photochemical Oxidant and Acid Deposition Model Application Within the Framework of Control Strategy Development (PHOXA) summary report, Umweltbundesamt Fed. Repub. of Ger., Berlin, July.

Mylona, S. (1999), EMEP emission data: Status report 1999, *EMEP/MSC-W Note 1/99*, Meteorol. Syn. Cent. West, Norw. Meteorol. Inst., Oslo, July.

Pastuszka, J. S. (1997), Study of PM-10 and PM-2.5 concentrations in southern Poland, *J. Aerosol Sci.*, *28*, Suppl. 1, S227–S228.

Rosenfeld, D. (2000), Suppression of rain and snow by urban and industrial air pollution, *Science*, *287*, 1793–1796.

Stowe, L. L., E. P. McLain, R. Carey, P. Pellegrino, G. G. Gutman, P. Davis, C. Long, and S. Hart (1991), Global distribution of cloud cover derived

from NOAA/AVHRR operational satellite data, *Adv. Space Res.*, *11*(3), 51–54.

Turzański, K. P., and J. Paula-Wilga (Eds.) (1999), Raport o stanie œrodowiska naturalnego miasta Krakowa w latach 1994–1998, 146 pp., City of Krakow, Krakow, Poland.

Twomey, S. (1977), The influence of pollution on the shortwave albedo of clouds, *J. Atmos. Sci.*, *34*, 1149–1152.

Umweltbundesamt (1994a), The European atmospheric emission inventory of heavy metals and persistent organic pollutants for 1990, Berlin.

Umweltbundesamt (1994b), Daten zur Umwelt, 1992/3, Berlin.

Vestreng, V., and E. Storen (2000), Analysis of UNECE/EMEP emission data: MSC-W status report 2000, *EMEP MSC-W Note 1/00*, Meteorol. Syn. Cent. West, Norw. Meteorol. Inst., Oslo, July.

H. Graßl and O. Krüger, Meteorological Institute, University of Hamburg, Bundesstrasse 55, D-20146 Hamburg, Germany. (grassl@dkrz.de; olaf.krueger@dkrz.de)

R. Marks, Institute of Marine Sciences, University of Szczecin, ul. Waska 13, 71-415 Szczecin, Poland. (marks@sus.univ.szczecin.pl)

Paper IV

Pollution Lifts Clouds:
A Further Indirect Aerosol Effect

Olaf Krüger[a,c], Abhay Devasthale[a,b], Hartmut Graßl[a,c]

a Meteorological Institute, University of Hamburg
b International Max Planck Research School
c Max Planck Institute for Meteorology
Bundesstr. 53, 20146 Hamburg, Germany

The anthropogenic release of chemicals into the atmosphere has already changed climate during the past century. A large part of the observed warming at the surface can be attributed to changes in atmospheric composition[1].
In contrast to the rather good knowledge about greenhouse gas trends, the tropospheric aerosol particle trends and their resulting effects on climate remain one of the great uncertainties[2,3,4]. An important question related to aerosol effects is: Can these aerosol particles, originating from burning of fossil fuels and biomass or secondary particles formed in the atmosphere affect the dynamics of convective clouds? If so, air pollution could be related to extreme precipitation events[5].
Here, we present first evidence that an increase in aerosol particle number concentration lifts cloud top height. Our analysis of satellite measurements reveals an indirect aerosol effect in the thermal infrared spectral range. The radiative forcing in the thermal infrared overrides the solar one.

Since the interaction of electromagnetic radiation with gases, aerosols and hydrometeors is described through the wavelength dependent scattering and absorption, satellites are able to observe polluted clouds[6,7,8]. Therefore, any long-term change in cloud optics, i.e. the fraction of incident solar radiation backscattered by clouds, is a suitable indicator of pollution effects on clouds[9,10]. Effects of these processes, termed indirect aerosol effects, have been detected on regional scale over Europe and China, where pollution changes have led to changes in cloud droplet scattering and cloud absorption[8,11,12].
Three general cases of perturbation were involved: Firstly, the abundance of only weakly absorbing anthropogenic aerosol particles. A prominent example is the sulphur rich case in Europe during the late 1980s, where aerosol precursor gas emissions dominated the aerosol system and lead to increased aerosol and cloud droplet number concentrations. In that case[12] the cloud albedo was significantly increased by up to 10%.
Secondly, if soot particles are emitted simultaneously, then optically thin clouds still show an albedo increase. Therefore kind of a paradox can be observed: As long as the vertical extent of clouds, or more precisely, cloud optical thickness is small the albedo is increased. For optically thicker clouds the enhanced absorption will be dominant and they appear darker

than unpolluted clouds. The latter effect was detected for clouds close to European industrial centres during winter[12].
In the third case absorbing aerosol is dominant. The black carbon rich case, accompanied by generally reduced cloud albedo, is observed during winter over the Red Basin in China[11].
The identification of cloud albedo changes as a consequence of pollution changes over Europe and China motivated us to further investigate, whether the anthropogenic aerosol particles would even change cloud dynamics. Southern China during the summer monsoon seems a perfect natural laboratory to jointly study the influence of soot and sulphate particles on cloud dynamics.
Our hypothesis was: If there is an influence on cloud dynamics it should be detectable in areas of strongest cloud albedo changes. Because a change in cloud dynamics will always be accompanied by a change in cloud brightness temperature the science question changed to:

Does brightness temperature of cloud tops change in strongly polluted regions ?

The question makes it evident: If an influence of air pollution on cloud dynamics could be found then thermal radiation is also involved in indirect aerosol forcing. To answer the question we analyzed satellite data in regions, which underwent very strong changes in air pollution.
Among those regions is southern China, especially the Red Basin. This area is already under discussion with respect to an aerosol influence on extreme precipitation[13].
From the late 1980s to the late 1990s absorbing aerosols reduced the local planetary albedo (LPA) over China north of 28^0 N by more than 5%. Amazingly, the picture during the summer monsoon reverses: South of 28^0 N there is a conspicuous increase of LPA by more than 5%.
Indeed, our analysis reveals (Fig. 1): In the southern part of the most polluted region of South East Asia cloud top temperatures were falling, i.e. cloud top height is rising, from the late 1980s to the late 1990s. Cloud brightness temperature from the late 1980s to the late 1990s decreased by values sometimes higher than 10K. The maximum decrease in cloud brightness temperature exactly corresponds to the areas with maximum LPA increase. South of 28^0 N the coverage of convective clouds clearly enhances. However, despite the frequent lifting of cloud tops in the South, i.e. in the polluted regions of Nanning, Hong Kong and the Pearl River Delta, there is an increase of 2K over the cities in the Red Basin. These opposite changes of mean cloud top height raise another question:

Does soot reduce the pollution effect on cloud brightness temperature ?

Since absorbing aerosols are found to reduce scattered cloudiness[14,15] (inhomogeneous cloudiness including partly cloud covered pixels) further insight into the processes can be obtained by separating into scattered cloudiness and the remaining homogeneous part, excluding cirrus.
The subdivision confirms contrary indirect aerosol effects (Fig. 2): While the strongest brightness temperature decrease of up to 12K for homogeneous cloud cover occurs near to the cities Nanning, Guangzhou,

Guilin, Xiamen, Fuzhou, Changsha, Nanchang, Wuhan, Chongquing, Chengdu and Nanchong, brightness temperature for scattered cloudiness show the opposite tendency: In regions where homogeneous cloudiness has a maximum increase in cloud top height, the height of scattered clouds is lowered most, as seen for clouds within and close to the Red Basin, where a high black carbon concentration strongly reduces cloud albedo, enhances solar heating in the brown haze layer and thus stabilizes the planetary boundary layer. Since scattered clouds cover does not change two processes seem to cancel each other: cloud lifetime enhancement by pollution and local heating by brown haze in the upper planetary boundary layer. This interpretation is in agreement with the findings during INDOEX[14] and in the Amazon region[15].

Our conclusion that pollution strengthens cloud dynamics is also confirmed by the analysis of cloud brightness temperature trends over Europe[16]: Cloud top height declined by more than 4K after the collapse of the East Block over the so-called black triangle and the strongly polluted part of Poland, where we had identified pronounced indirect aerosol effects in the solar part of the spectrum[12]. Both in Europe and China strongest changes occur for convective clouds in the urban environment.

What follows is an attempt to explain our results. Most likely increased aerosol number density at the cloud condensation level intensifies convection and hence enhances cloud top height. Once the number of condensation nuclei is strongly enhanced more small droplets form inhibiting drizzle formation. The characteristics of such clouds are an increased cloud water concentration and a droplet spectrum shifted to smaller sizes. The suppression of the warm rain formation will prolong cloud lifetime and allow the development of more vigorous convection. Such clouds with a high number of super-cooled small droplets at temperatures well below 250K, will - when freezing sets in - enhance the vertical movement again by the additional release of heat during freezing. Under such conditions extreme events of precipitation might occur. Such powerful deep convective clouds might also penetrate the tropopause and inject polluted air (only less soluble compounds) into the stratosphere over China.

Our results imply that anthropogenic aerosols also perturb the terrestrial radiation budget. A very rough first guess of this forcing is derived from the Stefan Boltzmann law: If cloud top temperature decreases by 1K at 235K it would lead to an additional forcing of about +3W/m^2, i.e. the atmosphere-earth system looses locally 3W/m^2 less to space. As cloud top brightness temperatures decreased by sometimes more than 10K on regional scale over China the corresponding cloud forcing can surmount +30W/m^2. This first guess already shows that the changes in the thermal infrared radiation range are of the same order of magnitude as solar or short-wave cloud forcing resulting from an enhanced cloud albedo.

Radiative transfer calculations[17] confirm these first estimates. For a convective cloud with a base at 1km height and a cloud top at 8km the following radiation flux density changes were calculated: If the cloud top is lifted by 1km from 8 to 9km the net long-wave or thermal infrared flux density at the top of the atmosphere (TOA) is lowered by 15W/m^2. At the same time cloud optical depth in the solar radiation range is enhanced leading to slightly higher albedo, resulting in a net solar radiation flux

density change of -7W/m^2 at TOA. Hence the thermal infrared effect overrides the solar one, or – in other words – the cloud conundrum enters the thermal spectral range.

References and Notes

1. Houghton, J. T. *et al*. (eds) *Climate Change 2001: The Scientific Basis* (Cambridge Univ. Press, 2001).
2. Ramanathan, V., Crutzen, P.J., Kiehl, J.T., Rosenfeld, D., *Science*, 294, 2119 (2001).
3. Kaufman Y. J., Tanre D., and Boucher O., *Nature*, 419, 215 (2002).
4. Penner, J.E., *Nature*, 432, 962 (2004).
5. R. Schnur, Nature, 415, 484 (2002).
6. Rosenfeld, D., Science 287, 1793 (2000).
7. Breon F.M., Tanre D., and Generoso S., *Science*, 295, 834 (2002).
8. Krüger, O. and Graßl, H., *Geophysical Research Letters* 29, 19, 1925, doi:10.1029/2001GL014081 (2002).
9. Twomey, S., *Atmospheric Environment* 8, 1251 (1974).
10. Graßl, H., *Contributions to Atmospheric Physics* 48, 199 (1975).
11. Krüger, O. and Graßl, H., *Geophysical Research Letters* 31, doi:10.1029/2003GL019111 (2004).
12. Krüger, O., Marks, R. and Graßl, H. *Journal of Geophysical Research* 109, doi:10.1029/2004JD004625 (2004).
13. Menon, S., Hansen, J., Nazarenko, L., Luo, Y., *Science* 297, 2250 (2002).
14. Ackerman, A.S., Toon, O.B., Stevens, D.E., Heymsfield, A.J., Ramanathan, V., Welton, E.J., *Science* 288, 1042 (2000).
15. I. Koren, Kaufman, Y.J., Remer, L.A., Martins, J.V., *Science* 303, 1342 (2004).
16. Devasthale, A., Krüger, O., Graßl, H., submitted to *IEEE Geoscience and Remote Sensing Letters* (2005).
17. Key, J. and Schweiger, A.J., *Computers & Geosciences* 24, 443 (1998).

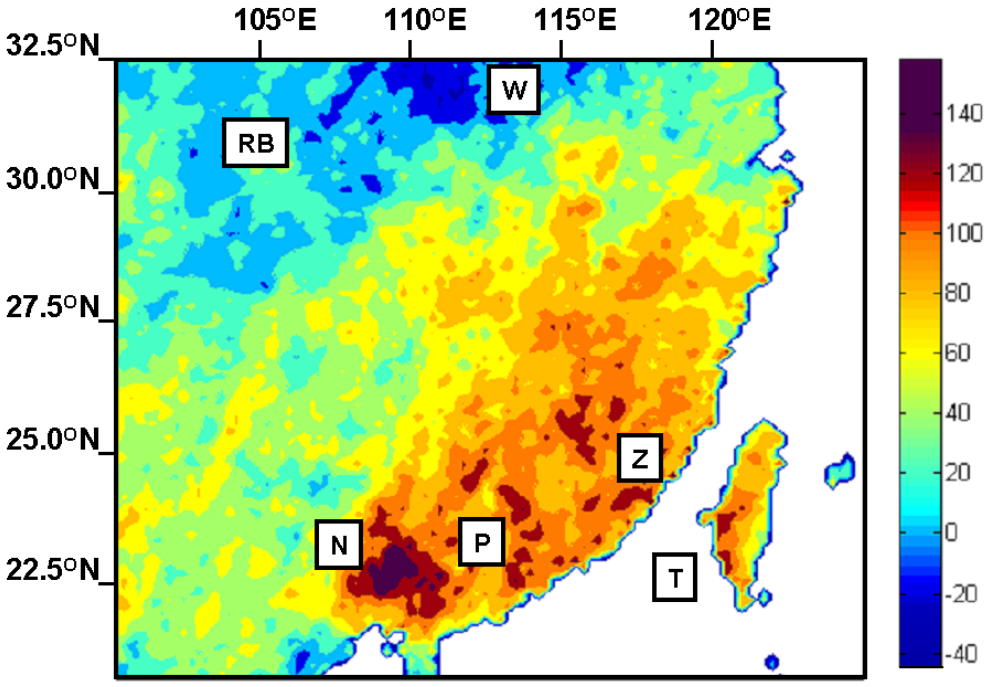

Figure 1.

Mean cloud top brightness temperature changes (for homogeneous plus scattered cloudiness) over southern China during the summer monsoon (June, July, August) from the late 1980s to the late 1990s observed from NOAA satellites in the thermal infrared spectral range at 12μm (AVHRR channel 5) [unit: 0.1 K]. The grid size is 0.250^0 in longitude and 0.125^0 in latitude. Mean cloud top height shows a strong increase dependent on aerosol absorption. While in the Red Basin (RB) and around Wuhan (W) at the Jangtze River the dominance of black carbon is lowering the height of scattered cloudiness through stabilization of the ABL, a lifting of >6K occurs for homogeneous cloudiness in the polluted regions Nanning (N), the Pearl River Delta (P), Zhangzhou (Z) and Taiwan (T).

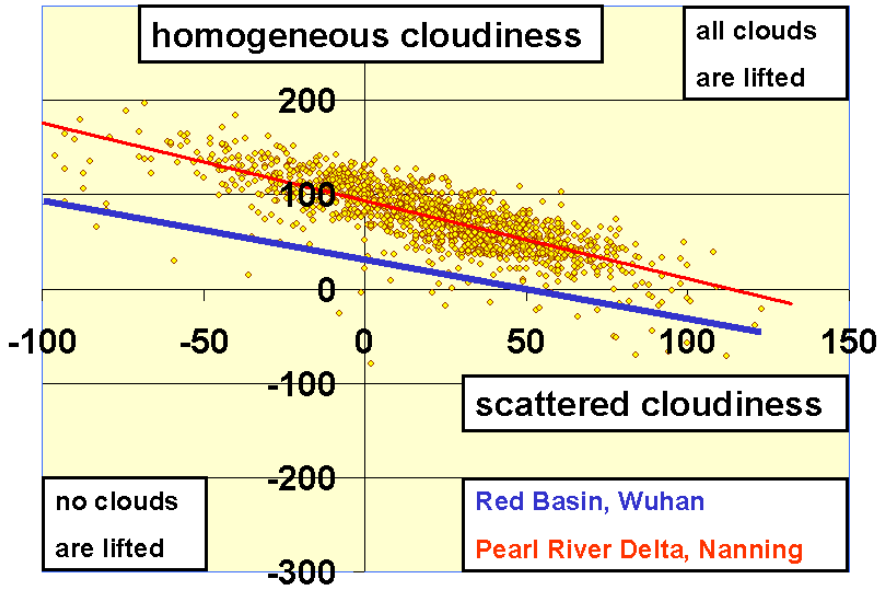

Figure 2.

Changes in brightness temperature [unit: 0.1 K] for homogeneous cloudiness compared to changes in scattered cloudiness. The scatter diagram shows the trend (decrease in brightness temperature is positive) for the southeastern part (from 20.0^0N to 26.0^0N and 100.0^0E to 125.0^0E), including Nanning and the Pearl River Delta region (the regression line in red); for the northwestern part (from 27.5^0N to 32.5^0N and 100.0^0E to 115.0^0E) including the Red Basin and Wuhan only the regression line in blue is given.

Publikationsreihe des MPI-M
„Berichte zur Erdsystemforschung“ , „*Reports on Earth System Science*“, ISSN 1614-1199
Sie enthält wissenschaftliche und technische Beiträge, inklusive Dissertationen.

Berichte zur Erdsystemforschung Nr.1 Juli 2004	**Simulation of Low-Frequency Climate Variability in the North Atlantic Ocean and the Arctic** Helmuth Haak
Berichte zur Erdsystemforschung Nr.2 Juli 2004	**Satellitenfernerkundung des Emissionsvermögens von Landoberflächen im Mikrowellenbereich** Claudia Wunram
Berichte zur Erdsystemforschung Nr.3 Juli 2004	**A Multi-Actor Dynamic Integrated Assessment Model (MADIAM)** Michael Weber
Berichte zur Erdsystemforschung Nr.4 November 2004	**The Impact of International Greenhouse Gas Emissions Reduction on Indonesia** Armi Susandi
Berichte zur Erdsystemforschung Nr.5 Januar 2005	**Proceedings of the first HyCARE meeting, Hamburg, 16-17 December 2004** Edited by Martin G. Schultz
Berichte zur Erdsystemforschung Nr.6 Januar 2005	**Mechanisms and Predictability of North Atlantic - European Climate** Holger Pohlmann
Berichte zur Erdsystemforschung Nr.7 November 2004	**Interannual and Decadal Variability in the Air-Sea Exchange of CO2 - a Model Study** Patrick Wetzel
Berichte zur Erdsystemforschung Nr.8 Dezember 2004	**Interannual Climate Variability in the Tropical Indian Ocean: A Study with a Hierarchy of Coupled General Circulation Models** Astrid Baquero Bernal
Berichte zur Erdsystemforschung Nr9 Februar 2005	**Towards the Assessment of the Aerosol Radiative Effects, A Global Modelling Approach** Philip Stier
Berichte zur Erdsystemforschung Nr.10 März 2005	**Validation of the hydrological cycle of ERA40** Stefan Hagemann, Klaus Arpe and Lennart Bengtsson
Berichte zur Erdsystemforschung Nr.11 Februar 2005	**Tropical Pacific/Atlantic Climate Variability and the Subtropical-Tropical Cells** Katja Lohmann
Berichte zur Erdsystemforschung Nr.12 Juli 2005	**Sea Ice Export through Fram Strait: Variability and Interactions with Climate**- Torben Königk
Berichte zur Erdsystemforschung Nr.13 August 2005	**Global oceanic heat and fresh water forcing datasets based on ERA-40 and ERA-15** Frank Röske
Berichte zur Erdsystemforschung Nr.14 August 2005	**The** HAM**burg** O**cean** C**arbon** C**ycle Model HAMOCC5.1 - Technical Description Release 1.1** Ernst Maier-Reimer, Iris Kriest, Joachim Segschneider, Patrick Wetzel
Berichte zur Erdsystemforschung Nr.15 Juli 2005	**Long-range Atmospheric Transport and Total Environmental Fate of Persistent Organic Pollutants - A Study using a General Circulation Model** Semeena Valiyaveetil Shamsudheen

Publikationsreihe des MPI-M
„Berichte zur Erdsystemforschung“ , „*Reports on Earth System Science*“, ISSN 1614-1199
Sie enthält wissenschaftliche und technische Beiträge, inklusive Dissertationen.

Berichte zur Erdsystemforschung Nr.16 Oktober 2005	**Aerosol Indirect Effect in the Thermal Spectral Range as Seen from Satellites** Abhay Devasthale
Berichte zur Erdsystemforschung Nr.17 Dezember 2005	**Interactions between Climate and Land Cover Changes** Xuefeng Cui
Berichte zur Erdsystemforschung Nr.18 Januar 2006	**Rauchpartikel in der Atmosphäre: Modellstudien am Beispiel indonesischer Brände** Bärbel Langmann
Berichte zur Erdsystemforschung Nr.19 Februar 2006	**DMS cycle in the ocean-atmosphere system and its response to anthropogenic perturbations** Silvia Kloster
Berichte zur Erdsystemforschung Nr.20 Februar 2006	**Held-Suarez Test with ECHAM5** Hui Wan, Marco A. Giorgetta, Luca Bonaventura
Berichte zur Erdsystemforschung Nr.21 Februar 2006	**Assessing the Agricultural System and the Carbon Cycle under Climate Change in Europe using a Dynamic Global Vegetation Model** Luca Criscuolo
Berichte zur Erdsystemforschung Nr.22 März 2006	**More accurate areal preciption over land and sea, APOLAS Abschlussbericht** K. Bumke, M. Clemens, H. Graßl, S. Pang, G. Peters, J.E.E. Seltmann, T. Siebenborn, A. Wagner
Berichte zur Erdsystemforschung Nr.23 März 2006	**Modeling cold cloud processes with the regional climate model REMO** Susanne Pfeifer
Berichte zur Erdsystemforschung Nr.24 Mai 2006	**Regional Modeling of Inorganic and Organic Aerosol Distribution and Climate Impact over Europe** Elina Marmer
Berichte zur Erdsystemforschung Nr.25 Mai 2006	**Proceedings of the 2nd HyCARE meeting, Laxenburg, Austria, 19-20 Dec 2005** Edited by Martin G. Schultz and Malte Schwoon
Berichte zur Erdsystemforschung Nr.26 Juni 2006	**The global agricultural land-use model KLUM – A coupling tool for integrated assessment** Kerstin Ellen Ronneberger
Berichte zur Erdsystemforschung Nr.27 Juli 2006	**Long-term interactions between vegetation and climate -- Model simulations for past and future** Guillaume Schurgers
Berichte zur Erdsystemforschung Nr.28 Juli 2006	**Global Wildland Fire Emission Modeling for Atmospheric Chemistry Studies** Judith Johanna Hoelzemann
Berichte zur Erdsystemforschung Nr.29 November 2006	**CO_2 fluxes and concentration patterns over Eurosiberia: A study using terrestrial biosphere models and the regional atmosphere model REMO** Caroline Narayan

Publikationsreihe des MPI-M
„Berichte zur Erdsystemforschung“ , „*Reports on Earth System Science*“, ISSN 1614-1199
Sie enthält wissenschaftliche und technische Beiträge, inklusive Dissertationen.

Berichte zur Erdsystemforschung Nr.30 November 2006	**Long-term interactions between ice sheets and climate under anthropogenic greenhouse forcing Simulations with two complex Earth System Models** Miren Vizcaino
Berichte zur Erdsystemforschung Nr.31 November 2006	**Effect of Daily Surface Flux Anomalies on the Time-Mean Oceanic Circulation** Balan Sarojini Beena
Berichte zur Erdsystemforschung Nr.32 November 2006	**Managing the Transition to Hydrogen and Fuel Cell Vehicles – Insights from Agent-based and Evolutionary Models –** Malte Schwoon
Berichte zur Erdsystemforschung Nr.33 November 2006	**Modeling the economic impacts of changes in thermohaline circulation with an emphasis on the Barents Sea fisheries** Peter Michael Link



ISSN 1614-1199